



Università degli Studi di Napoli  
Federico II

# Development of biomechanical-based analysis tools for the evaluation of infringements and performance in race-walking

Advisors:

Prof. Giuseppe Di Gironimo

Prof. Antonio Lanzotti

Candidate:

Teodorico CAPORASO

# Index

Index of Figures .....	IV
Index of Tables .....	IX
Abstract .....	1
Introduction.....	3
CHAPTER 1: ENGINEERING IN RACE-WALKING .....	5
1.1    The role of engineering in sport.....	7
1.1.1    The impact of technologies in sports .....	8
1.1.2    Sports engineering applications @ IDEAS Lab .....	10
1.2    Race-walking: history and rules .....	13
1.3    Infringements and performance in race-walking.....	18
1.4    Race-Walking stakeholders .....	28
1.5    Technology in Race-walking .....	30
CHAPTER 2: USER-CENTERED DESIGN FOR RACE-WALKING ANALYSIS TOOLS.....	43
2.1    Kansei Engineering .....	45
2.2    Definition domain.....	47
2.3    Span the Semantic and Properties Space .....	48
2.4    Selection of the Optimal System Architecture.....	53
CHAPTER 3: BIOMECHANICAL-BASED METHOD FOR ASSESSMENT OF INFRINGEMENTS AND PERFORMANCE IN RACE-WALKING.....	57
3.1    Inertial data processing.....	59
3.1.1    Signal Filtering .....	59
3.1.2    Detection of temporal gait event for the assessment of LOGC.....	60

3.2	Step Classification .....	63
3.2.1	Binary classification .....	63
3.2.2	Three-level classification .....	63
3.2.3	Fuzzy classification .....	65
3.2.4	Estimation of judge’s field of view – Step sequence classification.....	66
3.3	Performance indices assessment .....	68
3.4	Development of a customized strategy for élite race-walkers: radar chart representation.....	69
CHAPTER 4: EXPERIMENTAL VALIDATION OF INDICES FOR EVALUATING INFRINGEMENTS AND PERFORMANCE IN RACE WALKING SCENARIOS .....		
4.1	Laboratory tests .....	74
4.1.1	Participants.....	74
4.1.2	Devices and Experimental Settings .....	75
4.1.3	Experimental Protocol.....	77
4.1.4	Data analysis.....	79
4.1.5	Results and discussion.....	80
4.2	Field test .....	85
4.2.1	Field test: EP assessment .....	86
4.2.1.1	Experimental set-up.....	86
4.2.1.2	Experimental protocol .....	87
4.2.1.3	Results and discussion .....	88
4.2.2	Field test: experiments with elite athletes .....	91
4.2.2.1	Participants .....	91
4.2.2.2	Experimental protocol .....	92

4.2.2.3	Comparison and Evaluation: Data analysis.....	93
4.2.2.3.1	Binary step classification: Results and Discussion.....	97
Athlete 1	.....	97
Athlete 2	.....	101
Key outputs Binary classification	.....	105
4.2.2.3.2	Three level step classification: Results and Discussion .....	106
4.2.2.3.3	Fuzzy classification: Results and Discussion.....	108
4.2.3	Radar chart representation of infringements and performances for nine èlite athletes	109
CHAPTER 5:	TOWARDS THE EXPERIMENTAL PROOF-OF-CONCEPT OF A CUSTOM SYSTEM FOR EVALUATION OF INFRINGEMENTS AND PERFORMANCE IN RACE-WALKING .....	115
5.1	Proof of Concept: Measurement Unit.....	117
5.1.1	Inertial sensor platform.....	117
5.1.2	Inertial sensor packaging.....	118
5.2	Proof of Concept: Control Unit .....	121
5.2.1	Development of IART: a mobile app for evaluation of infringements and performance in race-walking .....	121
Conclusions.....		125
Acknowledgments.....		127
Appendix A .....		129
Questionnaire “Support device to control the loss of contact with the ground-level in the race-walking” .....		129
References.....		132

# Index of Figures

Figure 1 The flow chart of the case-study approach .....	6
Figure 2 First page of a newspaper and pictures of pedestrian race at the end of 18 <sup>th</sup> in England.....	13
Figure 3 Mean velocity of world records for the men’s 20km race-walking. ....	16
Figure 4 Mean velocity of world records for the men’s 50km race-walking.....	17
Figure 5 Highlights of a race-walking cycle: 1) the heel-strike event, 2) the mid-stance event, 3) the start of the propulsive action, 4) the toe-off event.....	18
Figure 6 Frontal plane in virtual view of a race-walker.....	19
Figure 7 Knee-flexion extension during the stance phase and related warning for bent knee .....	20
Figure 8 Temporal gait events: A) the toe-off and C) the heel-strike; B) shows a LOGC.....	21
Figure 9 A picture of the men’s 20 km race-walking in the last Olympic Games (Rio de Janeiro 2016 - FIDAL - G. Colombo) .....	23
Figure 10 Biomechanical warnings for the judging of infringements in race-walking .....	24
Figure 11 In a) a bent knee (with a flexion of knee before the vertical upright position); c) a LOGC picture. In b) the symbols associated with the two infringements (“<” bent knee and “-” LOGC) .....	25
Figure 12 In a) a race-walker received a yellow paddle; b) a picture of the electronic board with the red cards associated to the different race-walkers; c) a disqualification in competition of a race-walker .....	25
Figure 13 Percentage of red card for LOGC related to men’s 20 km, women’s 20 km and men’s 50 km and an overall during the last three edition of World IAAF Championship (Moscow 2013, Beijing 2015 and London 2017) and last edition of Summer Olympic Games (Rio de Janeiro 2016) and an overall of the four competition.....	26

Figure 14 Race-walking stakeholders.....	29
Figure 15 Pie chart of the race-walking studies participants divided into seven different range.....	38
Figure 16 Pie chart of the race-walking studies scenario. In the legend: LTO represents Laboratory Track Overground; LT represents Laboratory Treadmill; LO represents Laboratory Overground; RC represents Road Competition; TT represents Track Test; RT represents Road Test.....	38
Figure 17 Bar graph about sample frequencies of the equipment in race-walking studies. In blue the bars related to all the papers; in red the bars related to papers in real scenario.....	39
Figure 18 Bar graph about type of equipment in race-walking studies. On the x label V represents High Speed Camera video(s); P represents force platform(s); S represents Inertial Sensor(s); C represents infrared camera(s); IP represents Insole Pressure System; O represents Optojump. In blue the bars related to all the papers; in red the bars related to papers in real scenario .....	40
Figure 19 The flow chart of the Kansei Engineering approach .....	44
Figure 20 Chart of the effects (overall mean response with $\alpha = 0.05$ ) .....	55
Figure 21 Main effects plot for the overall mean response and optimal level of the significant A factor .....	55
Figure 22 Picture of a possible real scenario: measurement unit placed at the end of athlete's column vertebra in communication with the control unit handled by judge. ....	56
Figure 23 Flow chart of the methodological approach for inertial data processing and analysis .....	58
Figure 24 The power spectrum for accelerations on the x-axis.....	59
Figure 25 The comparison between the vertical acceleration based on raw data and the one two-times filtered.....	59
Figure 26 The signal processing applied to inertial system data in laboratory test .....	60

Figure 27 The signal processing applied to inertial system data in laboratory test .....	61
Figure 28 The correlation between the CoM accelerations and gait temporal events (TOE: toe-off event; HSE: heel strike event) for assessing the LOGC (using the threshold value E). The time between two following HSE represents the Step time.....	62
Figure 29 Acceleration data, on the left: the vertical acceleration near the bottom point of the cycle; on the right: antero-Posterior acceleration near the maximum point of the cycle. ....	64
Figure 30 The novel step classification. On the abscissa axis the value of LOGC <sub>T</sub> expressed in ms. On the ordinate axis the different step classification. On the graph the legal steps are in “green”, doubt steps in “yellow”, illegal steps in “red”. The vertical dotted line represents the limit of human eyes (40 ms). ....	65
Figure 31 Inertial system membership function compared with the binary classification .....	66
Figure 32 Judge’s field of view design: A) Judge; B) Athlete; C) Area of observation for a field of view at $\beta$ ; D) Additional Area for field of view allowed through acceptable eye rotation ( $\gamma$ ). The x axis represents the athlete’s direction of progression, y axis is orthogonal to the athlete’s direction of progression .....	67
Figure 33 In the figure the red indices are related to the infringements, the black ones to the performance. The blue opacity area ( $\beta$ ) represents the synthetic index. ....	71
Figure 34 The methodological approach .....	74
Figure 35 The experimental setting of the ErgoS Lab: the A zone shows the control volume, the B zone shows eight integrated platforms of force, and the capital letter C indicates the ten infrared digital cameras. The bottom left corner of the B zone matches with the origin of the reference system. The x and z axes show the anteroposterior direction and the medio-lateral direction, respectively; and the y axis (not visible since leaving the plane) indicates the vertical direction. All distance are expressed in meters. ....	78
Figure 36 Main phases of a race-walking cycle during a laboratory test.....	79
Figure 37 A basic ROC graph showing three classifiers.....	83

Figure 38 The variation of the accuracy in function of the E (toe-off threshold) .....	84
Figure 39 Flow chart methodological approach field test .....	85
Figure 40 Data collection setting: 1) the laptop with software for acquisition of inertial data and the USB Bluetooth; 2) the webcam; 3) the high-speed camera; 4) the tablet .....	86
Figure 41 Main phases of a race-walking cycle during a field test .....	87
Figure 42 Scatter plot of Optimal Threshold vs cadence Step ( in red the area exclud by analysis).....	89
Figure 43 Normal probability plot of residuals (response OT).....	90
Figure 44 Two photo sequences with magnifying glass focus around the left foot (near the TOE) and right foot (near the HSE): a) Last imagine with visible ground contact of left foot; b) First imagine without last visible ground contact of left foot; c) Last imagine without visible ground contact of right foot; d) First imagine with visible ground contact of right foot. ....	95
Figure 45 Comparison between the two classifications (M: represent the inertial system; GT: the high speed camera system) on three levels. The vertical dotted line represents the limit of human eyes (40 ms).....	95
Figure 46 Membership functions for the video ground truth system .....	96
Figure 47 A basic ROC graph showing the two classifiers: (A) advanced, (P) previous .....	100
Figure 48 A basic ROC graph showing the two classifiers for the athlete 2: (A) advanced, (P) previous.....	105
Figure 49 Two precision-recall curves represent the performance levels of two classifiers A and P.....	108
Figure 50 Radar charts for the experimental tests. The red indices are related to the infringements, the black ones to the performance. The coloured lines graphically show the trend of the indices at different speeds (blue: 12.0 km/h, red:13.0 km/h, green:14.0 km/h, yellow:14.5 km/h). ....	111

Figure 51: Performance ( $\rho$ , $\gamma$ , $\mu$ ), infringement ( $\alpha$ , $\delta$ ) and overall ( $\beta$ ) indices at different speeds. ES, effect sizes according to Hedges' g .....	112
Figure 52Pie graph showing $\kappa$ indices .....	113
Figure 53 Architecture design proof of concept development .....	116
Figure 54 Rendering of the box case components: a) whole box b) upper part; c) lower part .....	118
Figure 55 Picture showing the several component of measurement unit: inertial sensor, case box upper and lower part, port cover, 4 screws and battery. ....	120
Figure 56 A screenshot of the IDE Android Studio.....	122
Figure 57 Flow diagram of app user interface .....	123

# Index of Tables

Table 1 Estimation of performance improvement index ( $\Delta$ Overall) and the equipment factor assessed for each discipline ( $\Delta$ Equipment) in a specific interval of time ( $\Delta$ Time).....	9
Table 2 Estimates of performance improvement index ( $\Delta$ Overall) in a specific interval of time ( $\Delta$ Time) for the main race-walking man race event. ....	16
Table 3 Flight Time data (mean $\pm$ SD) and total red cards (loss of contact) .....	23
Table 4 The biomechanical studies of race-walking in the last five years .....	31
Table 5 Kansei words based on the affinity diagram .....	49
Table 6 Mean scores of properties .....	51
Table 7 Design factors and their levels selected for the development of concepts.....	51
Table 8 Fractional factorial design of three factors defining four concepts.....	53
Table 9 Subjective ratings collected for each Kansei word and their overall mean .....	54
Table 10 Analysis of variance for the overall mean response ( $\alpha = 0.05$ ).....	54
Table 11 Mean and standard deviation related to age, stature, weight and experience of race-walkers .....	75
Table 12 Data sheet of the inertial system .....	76
Table 13 Data sheet of the dynamic system .....	76
Table 14 Data sheet of the kinematic system .....	77
Table 15 Descriptive statistics for LOGC data stratified for measuring system [ms].....	80
Table 16 Steps classification according to three different methods for LOGC evaluation.....	81
Table 17 Comparison of classification metrics.....	82
Table 18 LOGC data collected during trials with inertial system (previous model) and ground truth.....	88

Table 19 Summary parameters of the model .....	90
Table 20 LOGC inertial assessment with the advanced model.....	91
Table 21 Mean and standard deviation related to their personal best, age, stature and experience of race-walkers .....	92
Table 22 Planning of trials analyzed: the line in reds include the trial tests for the overview athletes' analysis; the column in blue the trials for the specific speed analysis. ....	93
Table 23 Steps' classification according to contingency table for the trials at 12.0 km/h, 12.9 km/h, 13.7 km/h and 14.6 km/h (previous model).....	97
Table 24 Steps' classification according to contingency table for the trials at 12.0 km/h, 12.9 km/h, 13.7 km/h and 14.6 km/h (advanced model) .....	98
Table 25 Statistics for the two models at different velocities (best values are underlined in each column).....	99
Table 26 Contingency table of step sequences based on previous (right) and advanced (left) model.....	99
Table 27 Statistics for the two models in sequence step evaluation (best values are underlined in each column). ....	100
Table 28 LOGC data collected during trials of Athlete 2 with inertial system (advanced and previous model) and ground truth.....	101
Table 29 Steps' classification according to contingency table for the trials at 11.9 km/h, 12.9 km/h, 13.8 km/h and 15.7 km/h (previous models) – Athlete 2 .....	102
Table 30 Steps' classification according to contingency table for the trials at 11.9 km/h, 12.9 km/h, 13.8 km/h and 15.7 km/h (advanced model) – Athlete 2 .....	103
Table 31 Statistics for the two models at different velocities (best values are underlined in each column) – Athlete 2 .....	104
Table 32 Contingency table of step sequences based on previous (right) and advanced (left) model – Athlete 2.....	104

Table 33 Statistics for the two models in sequence step evaluation (best values are underlined in each column). .....	105
Table 34 Step sequences classification according to three multi-class confusion matrices for P and A model .....	106
Table 35 Comparison between Statistics based on the multi-class confusion matrices (best column values are underlined).....	107
Table 36 Coordinates of the four points in the Precision Recall graph .....	108
Table 37 Performance index $\alpha$ of the two models previous (P) and advanced (A) .....	109
Table 38 Performance index $\alpha$ in the step sequences analysis .....	109
Table 39 Performance and infringements parameters data collected during trials (mean $\pm$ SD) .....	110
Table 40 Data sheet of the BWT901CL, WitMotion inertial platform .....	117
Table 41 Additional technical features of the inertial sensor with case.....	119

# Abstract

Nowadays, the sports engineering and technology play an important role (like coaching and medical care) both for the overall performance of the athlete (training and competition) and in making sports more entertaining and safe. In this technological scenario an interesting case study, with a strong requirement of technology both for the improvement of performance and for the support of the judgments, is represented by the race-walking. This is a long-distance discipline within the track and field program characterized by two possible infringements (“bent knee” and “Loss Of Ground Contact”) but at the same time the best chronometric performance is required.

In this context, in order to assist coaching, judging and audience, the study aims at developing an innovative biomechanical based methodology for the performance and infringements assessment in race-walking using a wearable inertial system. For this aim, an user-center design for the development of the architecture of the system was carried out. So, the positioning on the human body and functional requirements of the system were defined through a Kansei Engineering approach by using a significant sample of athletes, coaches and judges within the race-walking environment. The analysis of variance (ANOVA) supported decisions concerning the optimal system architecture. This consists of: (i) an inertial sensor positioned close to the centre-of-mass of the subject (on L5 vertebra); (ii) a control unit.

Starting from the inertial data, a biomechanical based approach for the assessment of main parameters for performance and infringements in race-walking was developed. Based on the assessment of the LOGC time, according to the race-walking competition rules, three different step classification methods were proposed. In addition, we developed a customized strategy for elite race-walkers that allows to obtain key biomechanical indices related to performance and infringements (and a synthetic overall index). Their representation on a radar graph allows an intuitive analysis. The methodology was validated both in laboratory and field condition using a commercial inertial sensor. The first one was

conducted at the ErgoS Lab part of the Fraunhofer Joint Labs IDEAS ([www.ideas.unina.it](http://www.ideas.unina.it)) and CESMA ([www.cesma.unina.it](http://www.cesma.unina.it)). It consists of a motion capture system, including force platform (680 Hz) and infrared digital cameras (340 Hz), which are more accurate than the inertial system (200 Hz). The proposed biomechanical based approach and step classifications were evaluated in field tests, using a high speed camera system (240Hz). These experimental tests were performed in a training scenario with nine international elite race-walkers. They performed four outdoor field tests at different velocities. Through statistical classification, it was found that the proposed methodology has achieved encouraging results in comparison with state-of-the-art approaches and could be a good tool to assist experts in step classification. The statistical analysis also confirms the quality and reliability of the proposed biomechanical indices as well as of their representation.

Finally, a prototype of a customized sensor for race-walking and a dedicated mobile app were developed. Starting from an inertial sensor platform integrated with a Bluetooth module, the mobile app with two possible settings (coach and judge) was developed. It offers an example of a useful and practical tool for field applications.

# Introduction

Recent history shows that, at various levels and in many disciplines, technological evolution has radically changed the way how sport is approached from the monitoring and training point of view; consequently, the performance of the athletes has improved. The use of technology for sport applications allows to collect a large amount of data by different tools. Video and tracking technology, wearable devices, fitness trackers, equipment design and clothing, as well as the novel materials introduced in the recent years, have strongly influenced the performance. The adoption of these new tools is useful to understand and evaluate the dynamic evolution of the general state of the athlete's physical condition. More recently, technologies have been tested also to help the judgment system in many sports.

This influence is also evident in the world of the race-walking. Race-walking is a long-distance discipline within the track and field program characterized by two possible infringements (bent knee and Loss Of Ground Contact) but at the same time the best chronometric performances are required. It is worth noticing that nowadays judges can rely only on their subjective observations (made by human eyes); to date, technology is not used to support the judging decisions. With the current method, there is a critical issue in race-walking competitions: the very short duration of the loss of ground contact events generates difficulties in a proper identification of a correct/incorrect gesture. This is a major problem since the looking for performance optimization might determine a good or bad final result. For example, increasing the step length even of a single centimeter can lead to a time improving of about 2 minutes at the end of 50 km, greater than the range between the first and the fourth at the Olympic games.

So, nowadays the context of the race-walking highlighted the need of an analysis tool for the monitoring of the performance and infringements, in order to assist coaching and judging. The present study aims at achieving this objective using a wearable inertial system. These custom tools could allow to assist coaching, judging and audience in race-walking. For this aim, the work involves the following objectives:

- to develop a user-center design for sport analysis tool in race-walking through a Kansei Engineering approach;
- to develop a biomechanical based approach for the assessment of the main parameters for infringements and performance in race-walking;
- to validate the methodology in laboratory and field condition using a commercial inertial sensor;
- to build a customized proof of concept for race-walking and a dedicated mobile app.

# CHAPTER 1:

# ENGINEERING IN RACE-WALKING

*In this first chapter, we present the role of engineering in sport with a particular focus on its influence in equipment improvements and performance analysis tools. Then, the case study of race-walking is introduced with an overview about its history and rules. After a short description of race-walking world with its main stakeholders, the role of technology in this particular sport is shown. Finally, a review of the last studies on race-walking biomechanics allows to understand the features of the current available technology with a focus on field tests. The flow chart in Figure 1 summarizes the approach used for our case-study.*

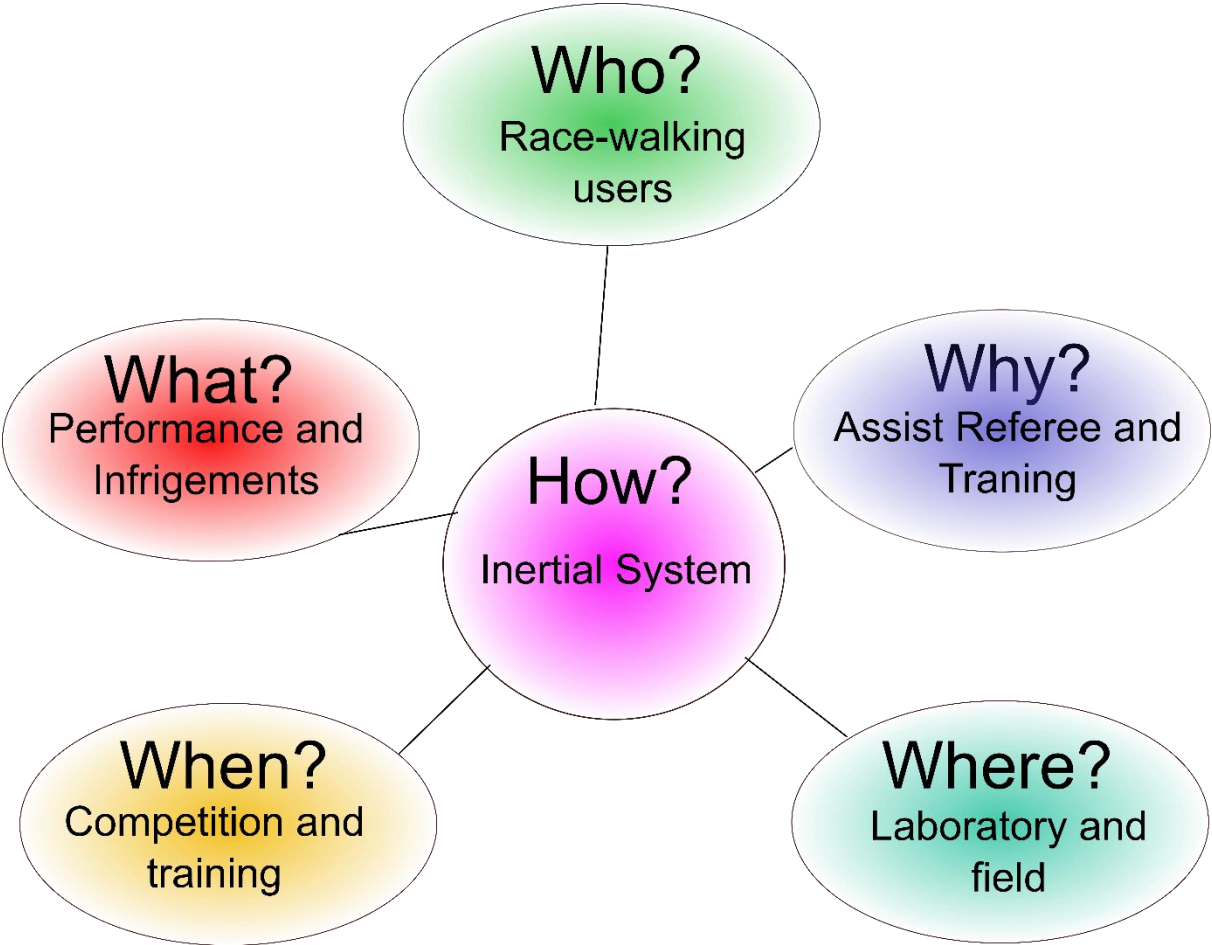


*Figure 1 The flow chart of the case-study approach*

## **1.1 The role of engineering in sport**

Although sport and engineering can appear different worlds, their interaction is increasingly marked. The engineering is involved in sport and it is part of the complex world around the athlete. It answers the requests of the best performance and protection of the athletes.

These motivations are at the basis of the birth of the “Sports Engineering”. It is a relatively young engineering discipline that links the gap between two distinctive fields: sport science and engineering. A possible definition of Sports engineering is: “the technical application of math and physics to solve sporting problems” and it “implies the design, development and research into external devices used by athletes, sports men and sports women, to enhance their performance” (Taha, 2013). On the other side the sport science is “a scientific process used to guide the practice of sport with the ultimate aim of improving sporting performance” (Bishop, 2008). It is evident a partial overlapping between the two discipline (as described by Haake (Haake S. , 1999)). They have the shared aim to improve the athlete’s performance, but they play a different role. In general, sports engineers develop a method, and then apply their skills to many different sporting fields. They are involved in designing and answering the athlete’s demands, besides measuring the performance of the athlete, the equipment itself, as well as their interaction. This information is precious for sports science expertise. Indeed, they use these data to have the best available evidence at the right time, in the right environment, for the right individual to improve the athlete’s performance (Bishop, 2008). The first steps of the engineering scientific study in the sport have led to a drive to build better, faster and stronger equipment and ultimately athletes as well. This has largely been driven by the rise of professional sport (and their associated budgets) together with national prestige in international competitions such as the Olympics. Moreover, in the Paralympic field sport engineering allows para-athletes to increase their participation in sport competition and their performance. Nowadays, sports engineering is a discipline that combines the fields of mechanical engineering, electronic and communications engineering, computational modelling and data analytics as well as biomechanics and sensors.

In detail, in the athlete's world sports engineering allows:

- to improve the design of equipment (and athlete's interaction) in order to increase the performance of the system (equipment plus athlete). For this aim, sports engineers use also the knowledge coming from basic discipline like aerodynamics (i.e. in sport like cycling, sailing, football, alpine skiing) and hydrodynamics (i.e. in sport like swimming, rowing, kayak) and materials science;
- to improve the design of equipment (and athlete's interaction) in order to increase the safety and reduce the risk of injuries of the athletes. For this aim, sports engineers use tools like: simulation models that allow to obtain good reproduction of the real situation (athlete's interactions and impacts) and to study behaviors of the different products, in order to define the best design and to choose the material with best proprieties;
- to develop tools for the measurement of athlete's performance (i.e. real time feedback system) in order to assess key performance indices (and race prediction pacing systems) useful to better understand and to improve the efficiency of the sport gesture. For this aim, the sports engineering uses the knowledge coming from the biomechanical and kinematics studies to develop protocol for data analysis and specific algorithms.
- to develop products and tools to increase the active engagement in sports for not able people. For this aim, sports engineers design adaptive products (i.e. wheelchair and handcycle) and they develop new methodologies of impairment classification to make them able to compete in sports (such as tests of impaired coordination for Paralympic classification (Connick, 2016)).

### **1.1.1 The impact of technologies in sports**

In this context, it is clear that the sports engineering and technology play an important role (like coaching and medical care) both for the overall performance of an athlete (training and competition) and in making sports more entertaining and safe.

As shown, the effects of sports engineering are related with sports equipment improvement but also with performance analysis tools. A quantitative evaluation of the evidence and the

magnitude of the technological effect on sport performance (in terms of sport equipment improvement) was showed by Haake (Haake S. J., 2009). In his research, he took into consideration four discipline of the Olympic games program: 100m, pole vault and javelin in track and field program, 1 hour on track in cycling program. Table 1 shows the results obtained.

*Table 1 Estimation of performance improvement index ( $\Delta$ Overall) and the equipment factor assessed for each discipline ( $\Delta$ Equipment) in a specific interval of time ( $\Delta$ Time).*

	100 m	Pole Vault	Javelin	1h Cycling
$\Delta$ Time [years]	108	94	76	111
$\Delta$ Overall	+24%	+86%	+95%	+221%
$\Delta$ Equipment	+4% (17%)	+30% (35%)	+30% (32%)	+100% (45%)

In a similar period of reference ( $\Delta$ Time) a large difference between each sport is shown. Cycling has seen the most important equipment improvement contribution, indeed Table 1 shows that the  $\Delta$ Equipment is 100% (in the one-hour cycling world record). It could be attributed to developments in bicycle aerodynamics (Lukes, 2005) and it is equal to the 45% of the overall improvement. In the track and field area, significant improvements (technological developments affected the index by about 30%) were seen with the introduction of new pole vaults (Burgess, 1996) and javelin (Hubbard, 1984) (although in the 1986 the change of center of mass location in the javelin significantly worsened performance). Finally, the analysis of the 100m sprint underlined that  $\Delta$ Equipment (due to improvement in aerodynamic clothing design (Chowdhury, 2009)) is just 4%, representing the 17% of the  $\Delta$ Overall equal to 24%. In this case, the improvement in the methodology of training represents a primary aspect in the overall increasing of the performance.

So, the weight of the improvement in the methodology of training is the key point in the performance increasing in long distance discipline (where, in relationship with the velocity, the aerodynamic clothing design is negligible). In this case the support of tools for the measurement of athlete's performance can play an important role for the training.

On the other side, the technological effect on sport is also evident in the support of the judgment. Several sports are already in full contact with the technology to assist the referee. Many systems are based on high speed camera systems. They allowed the development of tools like the Video Challenge in the volleyball that permits to determine if the ball has fallen down outside or inside the game area (Chen, 2011). In the tennis, since 2002 there is the technology of "Hawk-Eye" tennis ball tracking system. Starting from a high-speed camera system the ball is extracted on each frame and 2D 'tracklets' of the ball's motion are built up on the image plane. These tracklets are sent to the 3D Reconstitution module which constructs the tracklets into 3D tracks and determines the impact points between separate tracks (Owens, 2003). Other example of technological support is in the soccer, where since 2012 there is the "Goal-Line Technology". It provides a clear indication to the referee - typically on a special watch - whether the ball has fully crossed the line. In this case a technological solution based on electromagnetic field with a RFID (Radio-Frequency Identification) approach is also used (Psiuk, 2014).

In this technological scenario an interesting case study, where there is a strong requirement for technology both for the improvement of performance and for the support of the judgments, is represented by the race-walking.

### **1.1.2 Sports engineering applications @ IDEAS Lab**

The Joint Laboratory "Interactive DEsign And Simulation" (IDEAS, [www.ideas.unina.it](http://www.ideas.unina.it)) has been established by Fraunhofer IWU - Fraunhofer Institute for Machine Tools and Forming Technology in Chemnitz (Deutschland) and DII – Dept. of Industrial Engineering in Naples (Italy). The DII have also signed two scientific partnerships with:

- physicians specialized in Physical and Rehabilitation Medicine of the Multidisciplinary Department of Medicine for Surgery and Orthodontics of the University of Campania "L. Vanvitelli", in order to maximize the benefits of interdisciplinary research;
- Don Orione Rehabilitation Center of Ercolano (Naples), in order to increase our public and social engagement activities.

One of Joint Lab IDEAS is the Laboratory of Ergonomics and Sports (ErgoS Lab) at CESMA ([www.cesma.unina.it](http://www.cesma.unina.it)) - University of Naples Federico II. The ErgoS Lab is an advanced multifactorial laboratory for the analysis of human movement. The laboratory allows, in sports area, the use of different technologies. It gives the opportunity to have useful information and feedbacks to adjust and improve technique and performance. ErgoS Lab offers the possibility to simulate the movement with the standardization of training environment. In addition, the integration of motion capture system information with body pressure data offers useful measurements in ergonomic and comfort area. Posture and ergonomics evaluations permit to prevent occupational injury and illness also through a specific advanced design.

The laboratory is equipped with ten infrared and four colour digital cameras, eight tri-axial force platforms and six electromyography probes. A central workstation integrates, synchronizes and reworks the signals coming from the connected devices. A further stand-alone mobile system consisting of an inertial sensor synchronized with six EMG probes is used for outdoor measurements. A whole-body pressure mapping system made of resistive insoles for feet and two resistive mats for seat and backrest completes the lab equipment. Proper biomechanical analysis software allows to build up multifactorial protocols involving 3D kinematics and dynamics, muscle activity and pressure mapping. The laboratory is also equipped with an impact test apparatus, consisting of a vertical linear rail system allowing the adjustment of drop height.

Its main research themes are:

- Design of sport equipment (such as the improvement of the sports equipment performance carried out in the field of rowing (Caporaso T. G., 2018) (Caporaso T. P., 2018));
- Development and validation of protective device for impact safety in sports (for example, the improvement of the athlete safety in the field of soccer (Odenwald, 2016) (Lanzotti A. C., 2016) and the improvement of passive safety in sports and gymnastic equipment applications (Schwanitz, 2014) (Costabile G. A., 2013) (Costabile G. S., 2013)).

- Design of custom aids for health and sport based on biomechanics measurement systems for laboratory and outside laboratory use (such as design and developing of a biomechanics measurement system to acquire human body morphology) (Grazioso S. S., 2016) (Grazioso S. S., 2018) (Grazioso S. S., 2018);
- Development of performance analysis methods for use in élite sports performance and technique evaluation (Caporaso T. G., 2018);
- Development of custom metrics to measure human performance in partnership with coaches, trainers and physician useful to in the implementation of élite sport programs for able and disable people (for example developing customized methods for assessing motor tasks in people with intellectual disability) (Caporaso T. P., 2017) (Palomba A. C., 2018) .

Additional research items in sports area are in the following fields: swimming with the design of a packing system to use inertial sensor in swimming tests; and cycling for development of a multifactorial analysis protocol to carry out performance and posture indices useful to improve posture and reduce the risk of injuries (even using digital human modelling (Caporaso T. D., 2017)).

Finally, in this work will be presented an extended study on race-walking. This study covers different of the previously mentioned research items. Indeed, it is centred on the development of a biomechanics measurement system for real scenarios. It is based on user centred design and includes the development of performance analysis methods in élite sports. Finally, it allows to provide key performance indicators through a mobile app.

## 1.2 Race-walking: history and rules

Race-walking is a historical discipline born in Great Britain in the 16<sup>th</sup> century. The first race-walking events (called pedestrian race), took place at the end of the 18<sup>th</sup> in England and then even in the USA. These races were followed by press and people and race-walkers were very famous (see Figure 2). In the second part of the 19<sup>th</sup> century, race walking lost reliability to the public because of the lack of rules to identify the transition between walking and running (Schiffer, 2008).

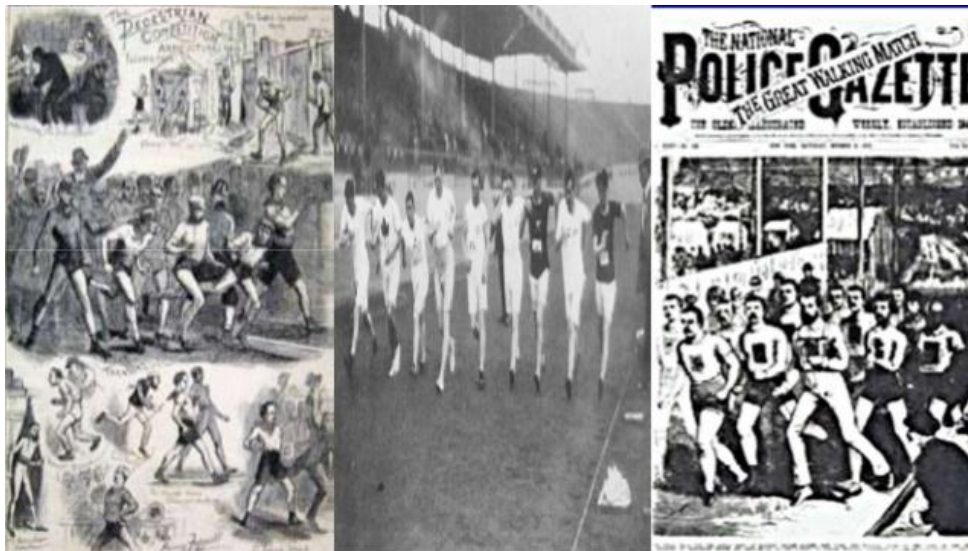


*Figure 2 First page of a newspaper and pictures of pedestrian race at the end of 18<sup>th</sup> in England*

In the scenario of the official sports events, it has always been included in the track and field program of the major international events. Indeed, race-walking became a permanent Olympic event in 1908 and has been included in the International Association of Athletics Federations (IAAF) World Championships. Although all the athletic disciplines have seen many changes over the time, the evolutions and the improvements of the race-walking have a unique history in the track and field world. In the scenario of official sports events, the central and critical point of race-walking's history is its rule (or definition).

The first "Rule of Race Walking" is dated 1877: "A succession of springs and the toes of one foot should not leave the ground till the heel of the other was down". The rule was changed many times: in the 1926 the first definition by IAAF stated: "Walking is a progression by

steps so taken that unbroken contact with the ground is maintained”; in the 1956 there was the introduction of comma about “..the leg shall be straightened (i.e. not bent at the knee) for at least one moment”; in the 1972 this comma had further specification: “For at least one moment, and in particular, the supporting leg must be straight in the vertical position”. The progression of technology of the 1990s showed through the recording of high-quality video and photo (with a high sample frequency) a constant loss of ground contact during racewalking action. So, starting from this apparent contradiction between definition and reality but wanting to remain linked to the concept of walking, the definition was changed, introducing the require of “visible loss of contact”. However, the comma about “bent knee” still remained difficult to apply. So, the definition of race-walking changed again in the 1995. This is the last and actual definition of race walking (from the rule 230 of Competition Rules IAAF) and it states: “Race Walking is a progression of steps so taken that the walker makes contact with the ground, so that no visible (to the human eye) loss of contact occurs. The advancing leg must be straightened (i.e. not bent at the knee) from the moment of first contact with the ground until the vertical upright position” (Schiffer, 2008).

During competitions, the rule control is committed on subjective human observations by judges (by human eye) and, since 1880, in race walking events cautions and disqualifications had to be left to the discretion of the judges. However, the judgment has been a critical point since the beginning. Already in 1924 during the Olympic Games there were controversies about the judgements and the International Olympic Committee decided to cancel race-walking by successive Games (1928). Then, it was reintroduced in the Olympic program in the 1932. However, even in the following edition of Olympic Games, although the race-walking was no more deleted from the official program, there were other issues because of the lack of homogeneity in the judgement (the most popular: Helsinki 1952, Montreal 1976 and Sydney 2000). In the last case, the leader of the men’s 20-kilometer race was disqualified fifteen minutes after the finish of the race and a similar situation happened at the end of the women’s 20-kilometer event with the disqualification of the leader of the race few meters before the finish line. In the 2001, in order to reduce the time for the communication of red cards to the disqualification posting (and to improve the timeliness of

the judgment action) a new quick transmission system of the proposal of disqualification was developed. In the 2007, during the IAAF World Championship in Osaka, Francisco Javier Fernandez (Spain) was originally disqualified by the Chief Judge after crossing the finish-line in second place in the men's 20-kilometer race. After examining the video of the race and discussing with the Chief Judge, the Jury of Appeal decided unanimously that the mode of progression of the Spanish athlete did not merit a disqualification. This are the first attempts where the technology helped the judgment system in race-walking to improve the homogeneity.

An important evolution was the change of distances and race surface. Race walking was born with two races, 3.500 meters and 10.000 meters, both on track (Olympic events in 1908). After the issues happened during the Olympic Games of the 1924, race walking became a road event on the distance of 50 km. The track race on 10.000 meters was reintroduced in the two editions after the Second World War, but it was characterized by many issues and from the 1956 it changed again and it became a 20 km on the road (Schiffer, 2008). Nowadays, these distances (20 and 50 km) are the official distance race in the main international events. The races take place on the road surface in circuit with laps of 1 or 2 km.

The evolution of the rule and the increasing of the race distances aimed to help the judges in their work and to reduce the problems connected with the judgments. Indeed, the evolution of the rule, as previously explained, gives more detail to understand the correct technique. In addition, the IAAF developed specific courses and guidelines to improve judgment and to make it homogeneous. The increasing of the race distances caused a reduction of the speed and we can see from the literature that the Loss of Ground Contact (LOGC) duration is directly proportional to the velocity (Pavei G. C., 2014).

However, the race-walking even shows in its time life an increasing of the performance and the issues connected with the judgement continue.

To assess the improvement of the performance in race-walking, according to Haake (Haake S. J., 2009), the first point is an analysis of the world record for the 20 km and 50 km race-

walking man (respectively Figure 3 and Figure 4). The 20 km and 50 km woman were excluded from the analysis because they are too younger in the official competition. About these data we can underline: (i) the world records start from 1912 (year of the official institution for the 20 km man), 1921 for the 50 km man; (ii) the world record does not include performances that were subsequently deleted due to the use of banned substances. In Table 2 the improvement of the world records is shown.

Table 2 Estimates of performance improvement index ( $\Delta$ Overall) in a specific interval of time ( $\Delta$ Time) for the main race-walking man race event.

	20 Km Man	50 Km Man
$\Delta$ Time [years]	107	97
$\Delta$ Overall	+66%	+74%

In Figure 3 and Figure 4 we can see for each graph three linear trends, linked by two discontinuity points. The first one is the period after the Second World War and the second one the race-walking technical innovation by the Mexicans in the second half of 70s (Schiffer, 2008).

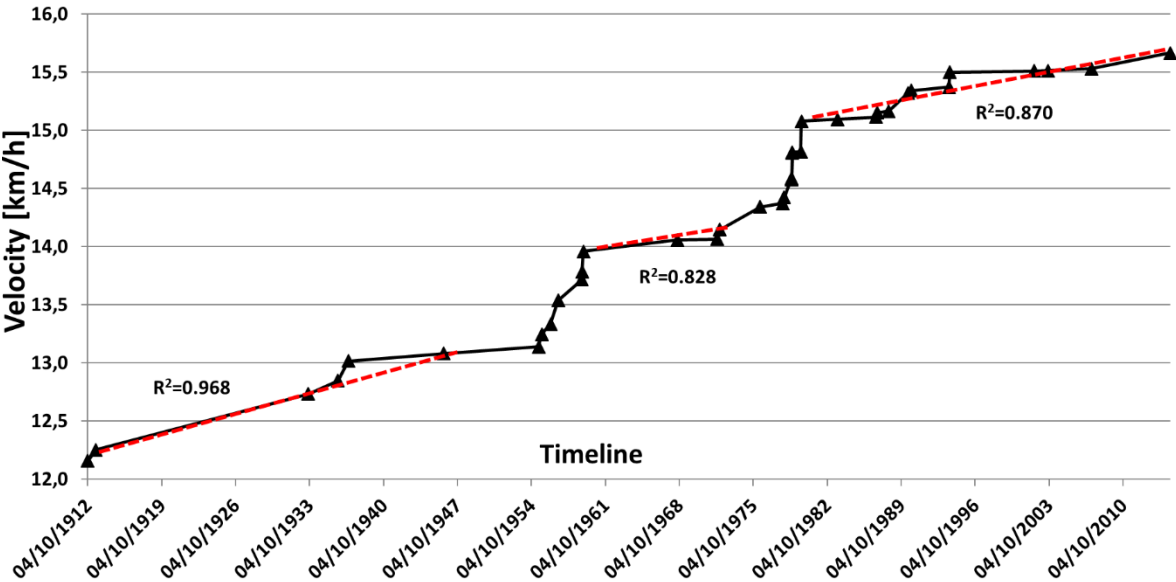


Figure 3 Mean velocity of world records for the men's 20km race-walking.

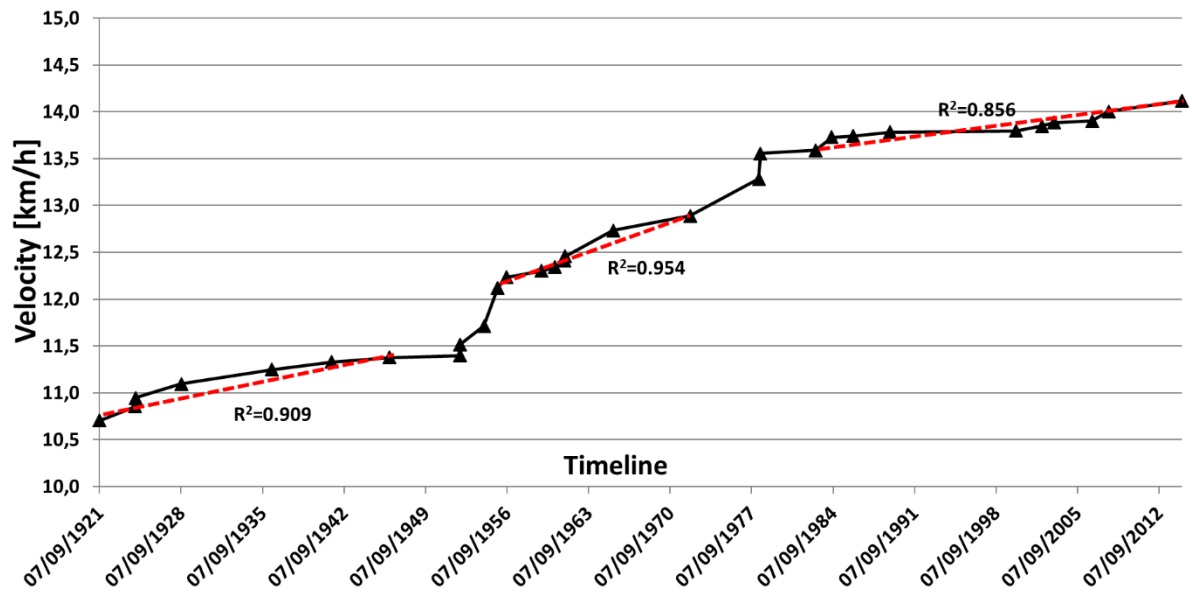


Figure 4 Mean velocity of world records for the men's 50km race-walking

### 1.3 Infringements and performance in race-walking

The locomotor constraints related with definition of the race-walking have forced athletes to develop a characteristic pattern widely recognized as 'race-walking cycle' (Figure 5) (Di Gironimo G. C., 2016). In this figure is possible to identify four main events. The first one is the heel-strike event (1). It is the stage in gait in which the heel of the foot makes the first contact with the walking surface (not bending the knee). This is the instant with maximum antero/posterior deceleration, which depends on the position of the front leg. The front leg position is obtained as the angle in the sagittal plane between two segments: the first one is defined by joining the Center of Mass (CoM) of whole body with the point located in the projection of the malleolus to the front support; the second one is the vertical axis passing through the same CoM. This angle is called "Attack angle" ( $ATT_{ang}$ ). The deceleration is inversely proportional to the  $ATT_{ang}$ . The second event is the midstance event (2). It is the instant when the CoM passes the vertical position. In the sagittal plane is possible to view the alignment of lower and upper leg. On the frontal plane (Figure 6), the race-walker's pelvic obliquity is maximum, and it allows to reduce the elevation of the CoM vertical position. The third event is "the start of the propulsive action" (3). The foot is behind of the CoM, so the race-walker accelerates the body in the progression direction (Pavei G. C., 2014). The last event is the toe-off event (4). It is the instant of the last toe-contact with the ground during the stance phase (of gait), preceded by the forefoot loading and followed by the swing phase.

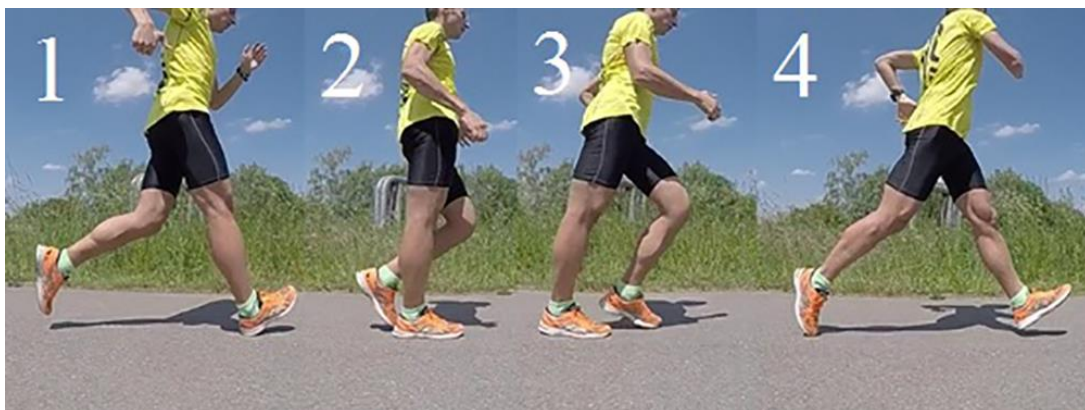
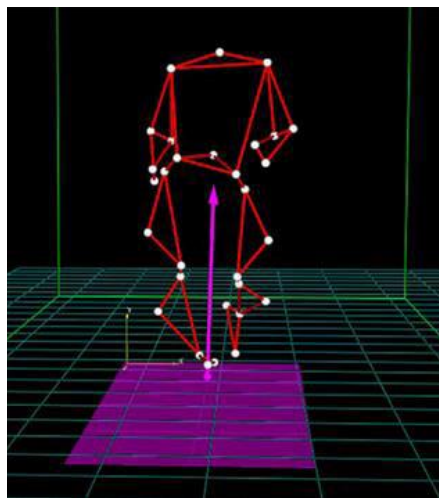


Figure 5 Highlights of a race-walking cycle: 1) the heel-strike event, 2) the mid-stance event, 3) the start of the propulsive action, 4) the toe-off event

In this instant, we can observe the push-off angle ( $PO_{ang}$ ) defined as the position of the rear leg (pushing leg) at toe-off event. It is evaluated as the angle in the sagittal plane between two segments: the first one is defined by joining the CoM of whole body with the point located in the projection of the malleolus to the end of the rear support; the second one is the vertical axis passing through the same CoM. The antero/posterior acceleration is directly proportional to the  $PO_{ang}$ .



*Figure 6 Frontal plane in virtual view of a race-walker.*

Related with the two commas of the definition of race-walking there are two possible infringements. The *bent at the knee* is a flexion of knee in the interval time between the heel strike event and the midstance event. For its assessment, the estimation of the flexion-extension of the knee is broadly recognized as a crucial parameter to evaluate the compliance of the athletic action with the rules of the competition. For a correct execution, as explained in the rule (c.f. section 1.2), the knee joint must indeed remain extended from the moment of the first contact with the ground (heel-strike event) until the passing through the vertical position (midstance). This stage lasts as long as about 35% of the stance phase (Dona, 2009). So, “the bent knee phase” lasts (in relationship of typical stance time for an élite race-walker) from 8 to 14 hundredths of a second (Pavei G. L., 2016). There is not a single reference value for the definition of straightened knee. Several studies provide different reference values for knee angles. Knicker and Loch (Knicker, 1990) consider knee joint as straightened for angles between  $-5^\circ$  to  $5^\circ$ . Cairns et al. (Cairns, 1986) define it as

"hyperextended" for joint angles greater than  $-5^{\circ}$ , while Hanley et al. (Hanley B. B., 2013) give the same definition for angles greater than  $0^{\circ}$ . In real race conditions they have found values between  $-6^{\circ}$  and  $+6^{\circ}$  at the heel-strike event and values between  $-17^{\circ}$  and  $3^{\circ}$  at midstance. In laboratory test (on treadmill) Pavei et La Torre (Pavei G. L., 2016) have found values between  $-2^{\circ}$  and  $+5^{\circ}$  at the heel-strike event and values between  $-6^{\circ}$  and  $+4^{\circ}$  at midstance. Hoga and Ae (Hoga, 2009) have studied the judgment evaluation of the "bent knee" in a research study on the men's 20-kilometer race during the Olympic Games in Athens (2004) (Figure 7). They carried out a comparison between the official summary of the race (i.e. the official document of the race where is possible to identify competitors, offenses, disqualifications and time of notifications) and the knee flexion-extension evaluation. For the last one they used a three-dimensional analysis with two video cameras (60fps). The analysis underlined the lacking correlation between the knee angle and the number of warning for bent knee. Indeed, it is possible to underline the presence of warning for race-walkers with a hyperextended knee and on the other side the case in which the support knee was a little bit bended and the athletes have not received any caution/warning.

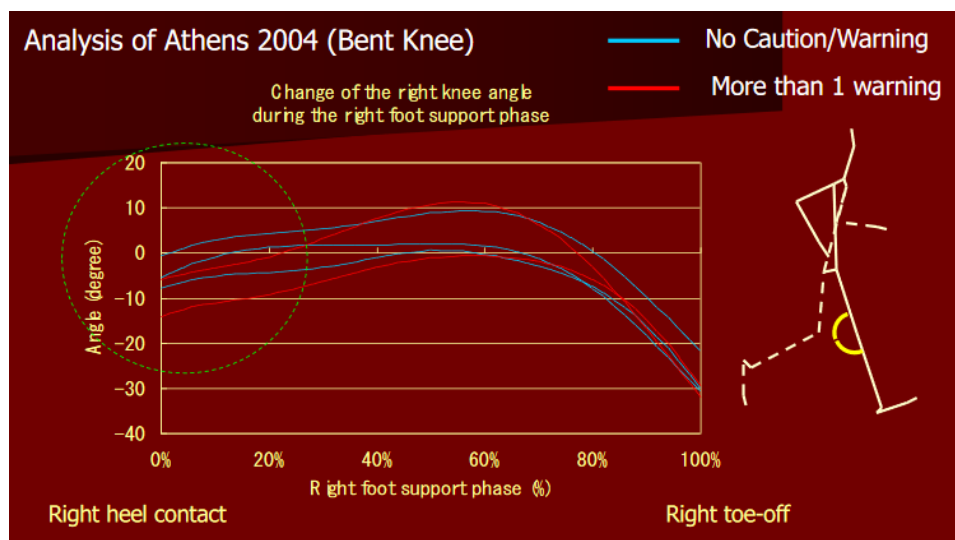


Figure 7 Knee-flexion extension during the stance phase and related warning for bent knee

The second possible infringement is the LOGC. It is the time between toe-off event and the following heel strike event (Figure 8).

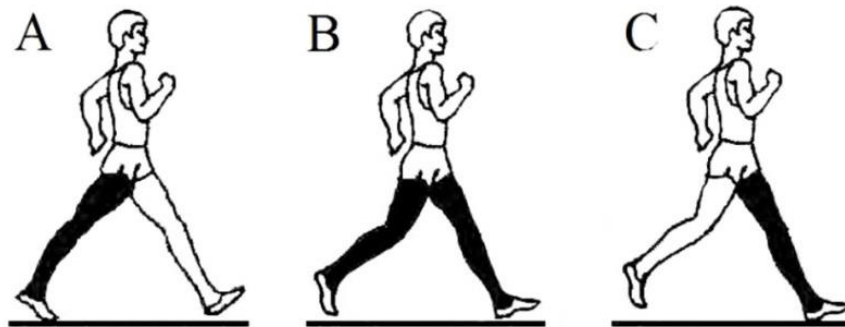


Figure 8 Temporal gait events: A) the toe-off and C) the heel-strike; B) shows a LOGC

The LOGC, of an élite race-walker lasts few hundredths of a second. Many studies were made to evaluate the LOGC of élite race-walkers in different conditions. In laboratory conditions with treadmills, using a motion-capture system analysis, a study on fifteen male race-walkers, divided into three groups (international, national and regional), has shown a range for LOGC values from 10ms up to 60ms (with average speed from 12.0 km/h to 18.0 km/h). In laboratory conditions without treadmills (Di Gironimo G. C., 2017), in our experimental tests with Italian national competition race-walkers we have collected LOGC between 10ms to 78ms. In training condition, a video-analysis study on sixteen international-level athletes, including ten men and six women, has shown a range for LOGC values from 30ms up to 45ms (with average speed from 12.0 km/h to 15.0 km/h) (DeAngelis M., 1992). Other works have evaluated the LOGC in race conditions: during 23<sup>th</sup> World Race-walking Cup, in Cheboksary on May 2008, of three hundredths of a second for males in 20 km and of two hundredths of a second for females in 20 km and for males in 50 km (average speed of 14.5, 12.7 and 13.1 km/h, respectively) (Hanley B. B., 2013) (Hanley B. B., 2011). During the 25<sup>th</sup> World Race-walking Cup, in Saransk, on May 2012, the LOGC was evaluated for medallists (both men and women) of the 20 km race-walk, and of the men's 50km race-walk. The LOGC value was equal to 50ms for the male in the 20 km race, to 30ms for the female in 20km race and to 40ms for male ones in 50km race; the average speed of 15.2, 13.2 and 13.9 km/h, respectively (Hanley B. , 2013). All works underline the short duration of LOGC events. So, a proper identification of LOGC is very difficult due to human psychophysiological limitations of vision.

Indeed, previous researches explain how people can perceive a movement in different ways (Claypool M, 2006) (Loschky L.C., 2005). Experimental tests on professional athletes of a first-person shooter have found that for refresh rates over 30fps (i.e. about every 33ms) the visual perception of the human eye does not show significant improvements (Claypool, 2007). On the other hand, the examination of limits of the visual resolution in natural scene viewing (Loschky L.C., 2005) has shown that the detecting image for human eye did not occur for fixations below 100ms. In addition, another study underlines that the human eye cannot accurately process an image if this does not persist for at least six hundredths of a second (Winter, 2005). This underlines as it is not simple to define a quantitative limit of human eye where no visible loss of contact occurs.

In race-walking scenario, in the selection of judges for the IAAF Panel, eye exams are now required, to see if candidates have normal vision. But not much is asked about their ability to judge contact. In literature few data are available about judges' ability. Researchers (Knicker, 1990) have studied the assessment of three judges about the race-walking technique. Each judge made 100 evaluations of step sequences observing the race-walker in a defined long observation area of 30 meters. Actions of race-walkers were simultaneously filmed with a standard video camera at 200fps. The study indicates a difficulty in recognizing LOGC shorter than 50 ms. This difficulty became evident also in race condition. Indeed, the analysis of the data in competition (25<sup>th</sup> World Race-walking Cup, in Saransk, on May 2012) carried out by Hanley allows to make a comparison between the official summary of the race and the LOGC timing. Table 3 shows as with for same flight time (as well as LOGC) judges submitted different number of red cards for LOGC (Hanley B. , 2013).

In addition, other practical difficulties for the judges to assess the LOGC during competition are due to: (i) the restricted period of assessment available for them; (ii) the situation in which multiple athletes are close to each other's (this often happens, especially during 20 km elite race) where it is very difficult for the human eye to pay close attention to two portions of the athlete's body at the same time (Figure 9).

Table 3 Flight Time data (mean  $\pm$  SD) and total red cards (loss of contact)

	Flight Time (sec.)	Red cards (~)
20 Km Senior Women	0.03 ( $\pm$ .01)	0
20 Km Senior Men	0.05 ( $\pm$ .01)	2
50 Km Senior Men	0.04 ( $\pm$ .00)	0
10 Km Junior Women	0.04 ( $\pm$ .00)	3
10 Km Junior Men	0.04 ( $\pm$ .00)	1



Figure 9 A picture of the men's 20 km race-walking in the last Olympic Games (Rio de Janeiro 2016 - FIDAL - G. Colombo)

Thus, the race-walk judges know the biomechanics of race-walking, so that they may see loss of contact or a bent knee as it happened. Their judgments are based on biomechanical patterns. Starting from the recommendations for race-walking judges (Westerfield, 2007) (Di Gironimo G. C., 2016), some parameters characterizing an inefficient technique are:

- the interruption of the line “trunk-pelvis-pushing leg” (Figure 10.a): it is strictly related with  $PO_{ang}$  and forward lean. If lean is emphasized it will most likely occur at the waist, restricting forward hip rotation, reducing the horizontal component of acceleration (underlined by lower value of  $PO_{ang}$ ) and increasing the vertical one. The effect is to emphasize the loss of contact. If contact is made almost at flatfoot in front

of the CoM (without noticeable heel strike) the knee may even be bent. Indeed, it is very difficult to land flat without flexing the knee;

- the high value of the  $ATT_{ang}$  (Figure 10.b): it occurs when there is a restricting hip rotation accompanied by too much emphasis on propulsion. Thus, hip flexion alone appears to move the legs and the step length is shortened. The race-walkers appear to bounce with each step and this has the effect to emphasize loss of contact. In extreme cases this inefficiency can lead the knee to be bent;
- high and tensed shoulders (Figure 10.c): they give the appearance of too much lifting of body mass which may be a precursor to possible loss of contact;
- too much knee lift (Figure 10.d): it has the effect to increase the vertical component of the CoM and emphasize the loss of contact. In addition, because of rapid leg swing it is difficult to dorsiflex the ankle enough before contact. In this case the foot lands flat and the knee can be flexed.



Figure 10 Biomechanical warnings for the judging of infringements in race-walking

Nowadays, the competition rules allow the judges to give the race-walker a yellow paddle (as a warning) when the athletes are going to break the rule. Two different symbols are associated with the two infringements (Figure 11). Each judge can give an athlete an only paddle for each infringement (Figure 12.a). Instead, the judge gives a red card (as proposal for disqualification) when he is sure of the race-walker's infringement (according to IAAF recommendations that said to give a red card only when the athlete continues to break the rules of race-walking, not only for a step). All the proposals of disqualification are recorded and showed on electronic board (Figure 12.b). If three different judges submit a red card, the athlete is disqualified. The disqualification is given the athlete from the chief judge

showing him a red paddle (Figure 12.c). In addition, in the race-walking competition rules a new power for chief judge has been introduced since 2001. He has the power to disqualify race-walkers in the last 100 meters of a race (when the race-walker's mode of progress obviously fails to comply with the definition).

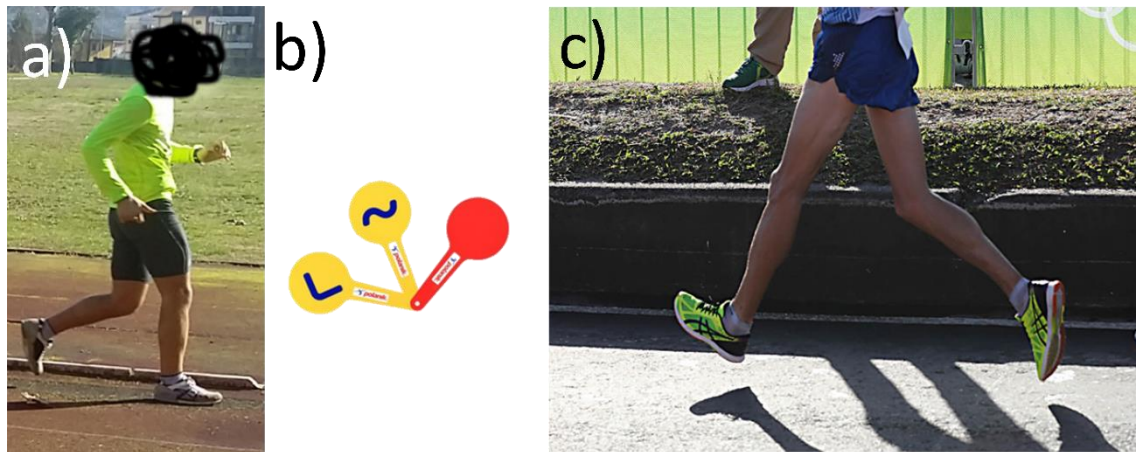


Figure 11 In a) a bent knee (with a flexion of knee before the vertical upright position); c) a LOGC picture. In b) the symbols associated with the two infringements (“<” bent knee and “-” LOGC)



Figure 12 In a) a race-walker received a yellow paddle; b) a picture of the electronic board with the red cards associated to the different race-walkers; c) a disqualification in competition of a race-walker

In the described context the judgment evaluation of the infringements is not easy for the judge. So, the event of a missed or incorrect disqualification is possible and it could generate controversies which can be devastating to the individual athlete. However, the LOGC is the most critical and issued infringement. Nowadays, the LOGC represents the main infringement given to an elite race-walker. Figure 13 shows an overview of the proposal of disqualification in the last main international events. Here we can see that approximately 60% of red cards were caused by a LOGC, with a peak of over 80% in the men's 20km race

(Caporaso T. P., 2018). In addition, although there is not a quantitative definition for both infringements, the possibility to define the “visible LOGC” appear simpler than the definition “straightened knee” that is strictly connected with the race-walker’s anthropometrical characteristics.

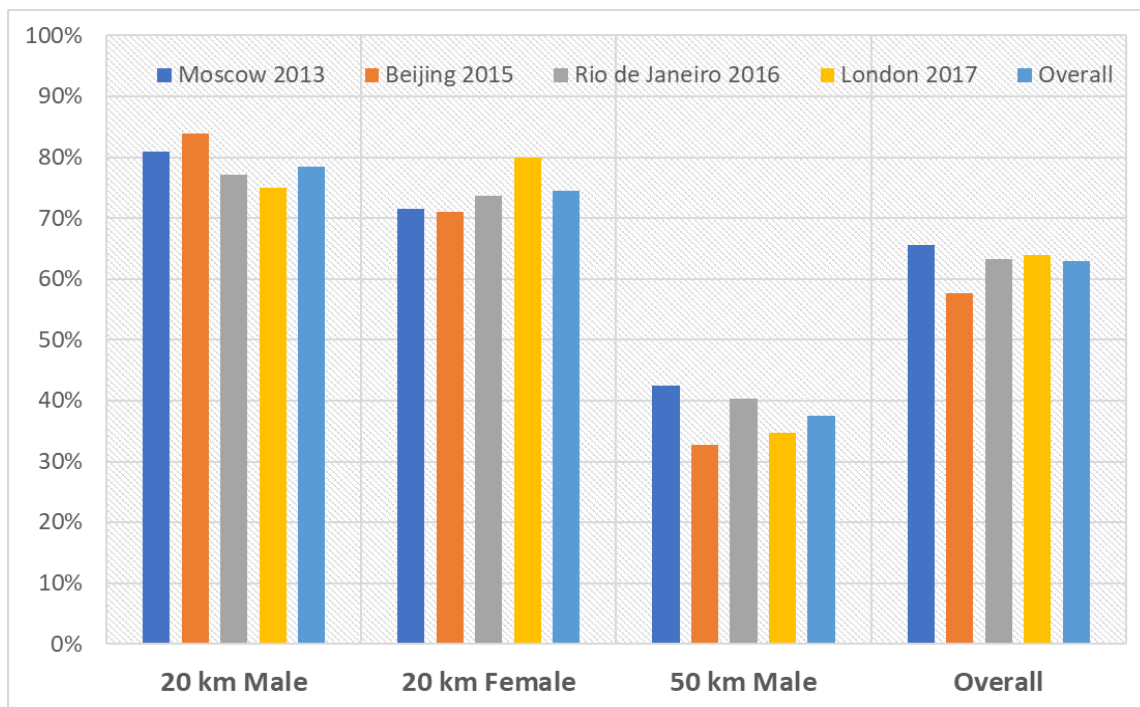


Figure 13 Percentage of red card for LOGC related to men’s 20 km, women’s 20 km and men’s 50 km and an overall during the last three edition of World IAAF Championship (Moscow 2013, Beijing 2015 and London 2017) and last edition of Summer Olympic Games (Rio de Janeiro 2016) and an overall of the four competition.

On the other side, reaching the best performance while avoiding disqualification is the main goal of every professional race-walker. So, the results underline a continuous increasing of the performance as shown in the analysis of the mean velocity of world record on the 20 km race-walking in the last 107 years (Figure 3). The literature underlines the correlation between performance and kinematic parameters. Pavei et al. (Pavei G. C., 2014) pooled together data from eleven different studies, showing a linear descriptive equation between the Step Cadence (SC), Step Length (SL) and the race-walking speed. Although in élite race-walkers the importance of SL on race-walking velocity appears greater than SC, it should be noticed that there is a limit on how much SL can be increased before achieving dangerous SC value. Furthermore, increases in SL might be achieved through longer LOGC. The ability of

the best race-walkers is to achieve the optimal SL and SC (with a legal LOGC) (Hanley B. , 2013).

Additional parameters are the values of the  $ATT_{ang}$  and  $PO_{ang}$ . These parameters are very interesting because they provide an immediate measure to evaluate the braking and the propulsive phases (Di Gironimo G. C., 2016). In fact, the technique used by race-walkers to increase their speed involves high push-off angles and low attack angles. A possible parameter taking into consideration these two elements is the smoothness on the anterior/posterior component. It allows to evaluate the homogeneity of the acceleration pattern that is related with the  $ATT_{ang}$  (determining the deceleration at the heel strike event) and  $PO_{ang}$  (influencing the acceleration profile at the toe-off event). Indeed, studies show that it significantly improves when the athlete's performance level increases (Choi, 2014).

In addition, Gomez-Ezeiza et al. found significant relationships between race-walking economy (the oxygen cost defined as the steady-state oxygen uptake at a given submaximal speed) and certain biomechanical factors (i.e. velocity, LOGC) (Gomez-Ezeiza, 2018). This is important because this kind of metabolic evaluation is lacking practicality in daily training while main biomechanical factors are simpler to collect.

## 1.4 Race-Walking stakeholders

The race-walking world is composed by several features (see Figure 14). The main protagonists of the system are the athletes, “sport cars” and leading actors of the race, the coaches, “chief technical officers” of the athletes’ team, and the judges, guarantees of the regularity of the race. Secondary players, but however important part of athlete’s team, are the medical staff (physician and physiotherapists) and biomechanical researchers. The first ones guarantee the “maintenance” of the athlete-car in order to treat and prevent possible damages (injuries). The second ones are the managers of the research and development part of the athletes’ team. They study the biomechanical pattern of the athlete in order to suggest possible solutions to improve performance and to reduce the risk of injuries. All of them are part of the national (i.e. single National Federation) and international (i.e. IAAF) institutions. The institutions’ role is the organization of the race events at different (national and international) levels. Finally, hidden actors are the producers, that develop specific equipment or sensor devices for data collection about the athlete-car.

All the previous features are interested in having new tools for the monitoring of the gesture in training and competition scenarios. Athletes are interested in having objective feedback about their performance and technique. Coaches are interested in having key indicators of the performance and infringements of athletes useful to design new customized strategies to optimize the training and competitions. Judges are interested in having useful tools to assist their evaluation of infringements in competition scenario. The institutions are interested in the definition of a competition system for the evaluation of LOGC, in order to reduce the issues connected with the judgement and to improve the outside credibility of the race-walking. The IAAF with its Race-walking Committee would perform this system in order to draw up a rule change proposal (IAAF). These tools are interesting also for the other components of the race-walking-world: medical staff is interested in the comprehension of the athlete’s biomechanical pattern; the researchers are interested in having more field data useful for the comprehension and the modelling of race-walking biomechanics. The producers are interested in the development and in the sale of an innovative device for the evaluation of performance and infringements.

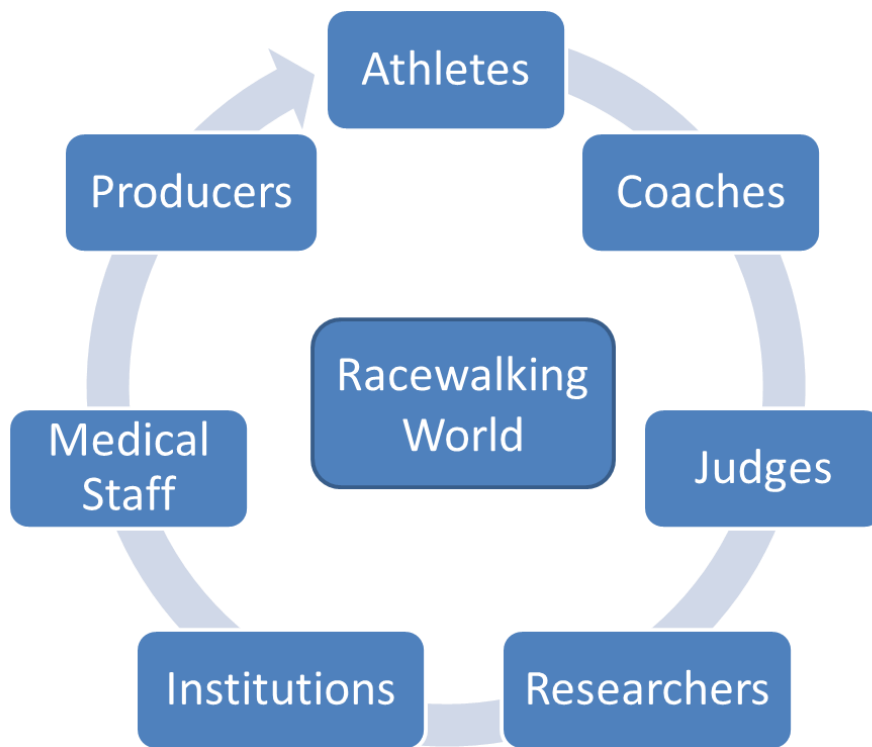


*Figure 14 Race-walking stakeholders*

## 1.5 Technology in Race-walking

As explained in paragraph 1.3, measurements and monitoring both for performance and infringements assume an important role in race-walking, in particular for elite athletes.

Although in the race-walking world coaches and athletes even use subjective measurements (i.e. tools for the physical status and performance evaluation of the athletes, like the Rate of Perceived Exertion defined by Borg, offering a range from 0 to 10 for rating the perceived exertion during physical activity) (Borg, 1982) (Hanley B. , 2015), most of the biomechanics studies are based on objective measurements to evaluate performance and infringements.

In this second category there are several different output data (Tao, 2012):

kinematic (K): “study of motion” (i.e. temporal/spatial parameters, accelerations, angular velocity, range of motion of joint angles). In order to collect these data, possible technologies available are: accelerometers, inertial sensors, high speed cameras, optical systems;

kinetic (KIN): “study of musculoskeletal internal loads” (i.e. joint torques and ground reaction force). In order to collect these data, possible technologies available are: platforms of force, insole systems;

electromyography (EMG): “study for evaluating neuromuscular activity “. It gives an added value in the interpretation of the kinematic and kinetic data useful for the estimation of muscle force. In order to collect these data, possible technologies available are: electromyography surface probes and electromyography intramuscular probes.

In addition, other useful measurements are physiological data (i.e. metabolic data such as heart rate data, lactate measurement and Maximal Oxygen Consumption). Overlooking studies about the only physiological measurement, Table 4 shows the issues about race-walking biomechanics published in the last 5 years (period from the last literature review (Pavei G. C., 2014)). We collected 45 studies (about 60% based on kinematic analysis, the others even using the kinetic one).

Table 4 The biomechanical studies of race-walking in the last five years

Authors	Year	Type of analysis	N subjects	Total Subjects	Performance Level	Equipment	Scenario	Sample Frequency	N trials collected; speed
(Hanley B. B., 2013)	2013	K	5M 5F 5JM 5JF	20	I	2P; 1V	LTO	1000 Hz (P); 100 Hz (V)	3Tr: 1St; Sp: SB (J: 10km; MF: 20/50 km): M: $3.79 \pm 0.11$ m/s; F: $3.47 \pm 0.25$ m/s.
(Lee, 2013)	2013	K	5M 2F	7	N	V, S	TT	125 Hz (V); 100 Hz (S)	3Tr: 4.65m; 3Sp.
(Padulo J. A., 2013)	2013	K	12M	12	EN	1V	LT	210 Hz	3Tr: 200St; Sp: 3.5–3.3–2.9m/s; Sl: 0–2–7%.
(Padulo J. A., 2013)	2013	K	12M	12	E	1V	LT	210 Hz	9Tr: 200St; Sp: 3.61–3.89–4.16m/s; Sl: 0–2–7%.
(Smith, 2013)	2013	K	10M	10	N; I	2P, V	LT	1000 Hz (P); 250 Hz (V)	1Tr: 30"; 103% RP 10 km (SB); mean Sp: $3.53 \pm 0.18$ m/s.

(Song Q. D., 2013)	2013	K, KIN	9M 5F	14	E	P, 3V	LO	50 Hz (V)	5Tr: 1St; tr Sp.
(Chwata, 2014)	2014	K	12M	12	I	C	LT	120 Hz	7Tr: 3'; 6Sp: 2.77-3.05-3.33-3.55-3.89-4.17, then 1% SI.
(Hanley B. B., 2014)	2014	K	20JM 20JF	40	I	2V	RC	50 Hz	1Tr: 5.20 m; 2St (1l-1r); mean Sp: M 3.71 m/s, F 3.22 m/s.
(Preatoni, 2014)	2014	K	15M	15	I; N; R	6C	LT	300 Hz	40St; Sp: 4.17 m/s.
(Sovenko, 2014)	2014	K	9F	9	N	V	RC	25 Hz	50Tr; Sp: 3.32±0.15 m/s.
(Dolenec, 2015)	2015	KIN	1F	1	N	P	LO	1000 Hz	20Tr: 1St.
(Hanley B. , 2015)	2015	K, KIN	9M 5F	14	I	P, V	LT	1000 Hz (P); 250 Hz (V)	4Tr: 30"; 103% RP 10/20 km, Sp: 3.44 ± 0.21 m/s.

(Hanley B. B., 2015)	2015	K, KIN	10M 7F	17	I	2P, V	LTO	1000 Hz (P); 100 Hz (V)	3Tr: 1St; 97-103% RP 20/50 km.
(Padulo J. , 2015)	2015	K	12M	12	N	V	LT	210 Hz	100St; Sp: 3,56±0.17.
(Pavei G. S., 2015)	2015	K, KIN	1M	1	T	P; 8C	LT	900 Hz (P); 300 Hz (C)	9Tr: 1'; Sp: 2.22-2.50-2.78-3.06-3.34-3.62-3.90-4.17 m/s.
(Song Q. X., 2015)	2015	K, KIN	20M	20	R	IP; TP	TT	126 Hz (IP)	2Tr: 10St; mean Sp 3.5-3.8 m/s.
(Cazzola, 2016)	2016	K	15M	15	I; N; R	6C	LT	300 Hz	Tr: 60", 40St; 2Sp: 3.33 and 4.30 m/s.
(Cronin, 2016)	2016	K, EMG	5M 6F	11	N; I	V	LT	100 Hz	2Tr: 3-6St; 2Sp: 2.78 m/s and RP 10/20Km (3.03-3.83 m/s).
(Di Gironimo G. C., 2016)	2016	K, KIN	1M	1	I	8P; 10C	LO	680 Hz (P); 340 Hz (C)	10St (l and r); mean Sp: 2.94 m/s.

(Di Gironimo G. C., 2016)	2016	K	1M	1	I	V; S	RT	240 Hz(V); 200 Hz (S)	4Tr: 90St; 4Sp.
(Forczek, 2016)	2016	K, EMG	1F	1	N	IP	TT	-	5Tr: 10", 6-8St. 5Sp: 2.5-3.03-3.36-3.77-4.30 m/s.
(Hanley B. B., 2016)	2016	K, KIN	11M 8F	19	I	2P; V	LTO	1000 Hz (P); 100 Hz (V)	3Tr: 1St; 97-103% RP 20/50 km.
(Harrison, 2016)	2016	K	7TM 11TF 14NM 2NF	34	T; B	O; V	RT	1000 Hz (O); 300 Hz (V)	6-10Tr: 8 m; Sp: 1 - 3.56 m/s.
(Ito, 2016)	2016	K, KIN	3	3	T	2P; 12C	LO	1000 Hz (P); 200 Hz (C)	Sp: 2.98±0.31 m/s.
(Norberg J. S., 2016)	2016	K, KIN	12F 3M	15	T; A	2P	LO	1000 Hz	3Tr: 1 St; mean Sp: 2.3 m/s.
(Pavei G. L., 2016)	2016	K	15M	15	I; N; R	6C	LT	300 Hz	17Tr max: 60", 40St; Sp: 2.77-5 m/s (+0.14 m/s/Tr).

(Sawamura, 2016)	2016	K	16J	16	B	V	RC	60 Hz	1Tr: 1St; Sp: 2.4-3.4 m/s.
(Wang, 2016)	2016	K	11M	11	A	8C, V	LT	200 Hz (C); 200 Hz (V)	10Tr: 6", 3St; 2x5Sp: 0.55-1.11-1.66-2.22-2.77 m/s.
(Alvarez, 2017)	2017	K	3M 2F	5	-	O; V	LT	1000 Hz (O); 1000 Hz (V)	3Tr: 20"; 3Sp: 3.33-3.61- 3.89 m/s.
(Barreto Andrade, 2017)	2017	K	4M 4F	8	N	2V	TT	25 Hz	6Tr; RP, mean Sp 3.20 m/s.
(Di Gironimo G. C., 2017)	2017	K, KIN	3M 1F	4	N	8P; 10C; S	LO	680 Hz (P); 340 Hz(C); 200 Hz(S)	1St.
(Hanley B. B., 2017)	2017	K, KIN	10M 7F	17	I	2P, V	LTO	1000 Hz (P) 100 Hz (V)	3Tr: 1St; Sp: 97-103% RP 20/50 km.
(Hanley B. B., 2017)	2017	K, EMG	5M 5F 5JM 5JF	20	I	V; EMG	LTO	100 Hz (V) 1000 Hz (EMG)	3Tr: 1St; Sp: 97-103% RP (SB).

(Hanley B. T., 2017)	2017	K	7M 6F	23	E	12C; V	LO	250 Hz(C); 100 Hz (V)	1St.
(Hoga- Miura, 2017)	2017	K	3M	3	I	4V	RC	60 Hz	8St; mean Sp: 4.22 m/s.
(Majed, 2017)	2017	K	5M 2F	7	B	8C	LT	120 Hz	62Tr: 30"; mean Sp: 2.02 m/s.
(Norberg J. V., 2017)	2017	K, KIN, EMG	3M 12F	15	T	2P; 11C	LO	1000 Hz (P); 200 Hz (C)	3Tr: 1St; Sp: 2.3 m/s.
(Pavei G. S., 2017)	2017	K, KIN	1M	1	T	P; 8C	LT	900 Hz (P); 300 Hz (C)	9Tr: 1'; Sp: 2.22-2.50- 2.78-3.06-3.34-3.62-3.90- 4.17 m/s.
(Tucker C. B., 2017)	2017	K, KIN	13M 5F 9JM 8JF	35	I	P	LT	1000 Hz	Tr: 30", 23St; Sp: 103%RP 10/20 km.
(Gomez- Ezeiza, 2018)	2018	K	21M	21	I	O	LT	1000 Hz	3Tr: 2'; 3Sp: 2.78/3.33/3.89 m/s, 1% Sl.

(Gravestock, 2018)	2018	K, KIN	7M	7	I	12C, TP	LO	250 Hz (C)	Tr: 2St (l and r); 3Sp: tr, RP 10/20km.
(Hanley B. T., 2018)	2018	K, KIN	10M 7F	17	I	P; O; V	LTO	1000 Hz (P); 1000 Hz (O); 500 Hz (V)	5Tr: 1St; 5Sp: 3.05-3.33-3.61-3.89-4.17 m/s
(Hanley B. T., 2018)	2018	K	7M 5F	12	I	12C, V	LTO	250 Hz (C); 100 Hz(V)	5Tr: 1St; 97-103% RP (20 km), Sp: M: 3.96±0.13 m/s; F: 3.60±0.09 m/s.
(Skublewska-Paszkowska, 2018))	2018	K	1F	1	I	8C	LO	100 Hz	-
(Tucker C. B., 2018)	2018	K, KIN	11M 7F	18	I	P; O; V	LT	1000 Hz (P); 1000 Hz (O); 500 Hz (V)	5Tr: 30"; Sp: 3.05-3.33-3.61-3.89-4.17(M) m/s.

---

KEY: K: kinematic; KIN: kinetic; EMG: electromyography; M: male(s); F: female(s); J: junior(es); T: trained; B: beginner(s); I: International; N: National; E: Elite; R: Regional; A: Amateur(s); V: High Speed Camera video (s); P: force platform(s); S: Inertial Sensor(s); C: infrared camera(s); IP: Insole Pressure System; O: Optojump; TP: Timing photocells; LTO: Laboratory Track Overground; LT: Laboratory Treadmill; LO: Laboratory Overground; RC: Road Competition; TT: Track Test; RT: Road Test; Tr: Trial(s); St: Stride(s); Sp: Speed(s); SB: Season Best; Sl: Slope; RP: Race Pace; l: left; r: right; tr: training.

As underlined in a previous review (Pavei G. C., 2014), studies often concern a few number of people (22% less than 4 subjects and 53% less than 12, Figure 15), with different sport level and gender.

**Partecipants analysis**

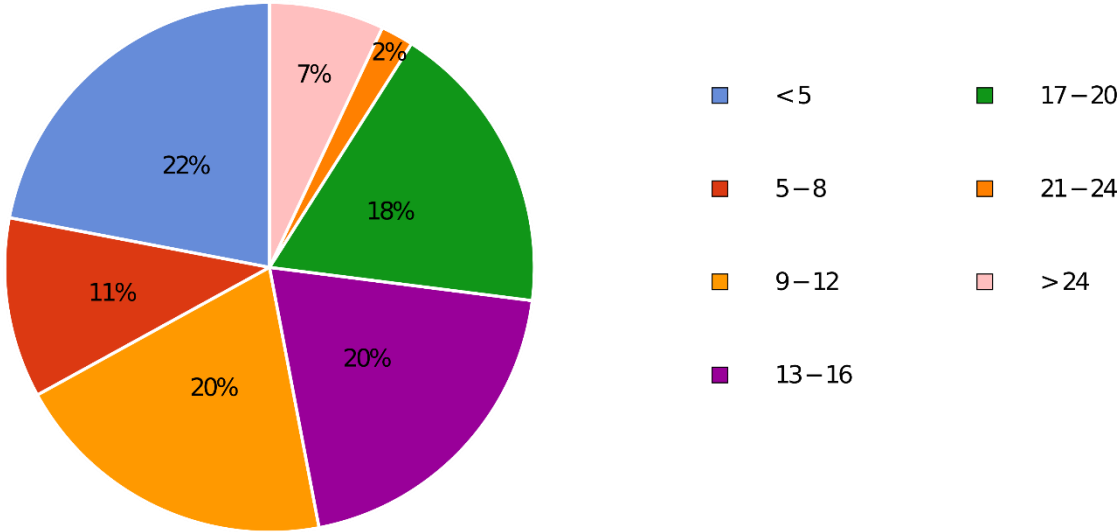


Figure 15 Pie chart of the race-walking studies participants divided into seven different range.

**Scenario analysis**

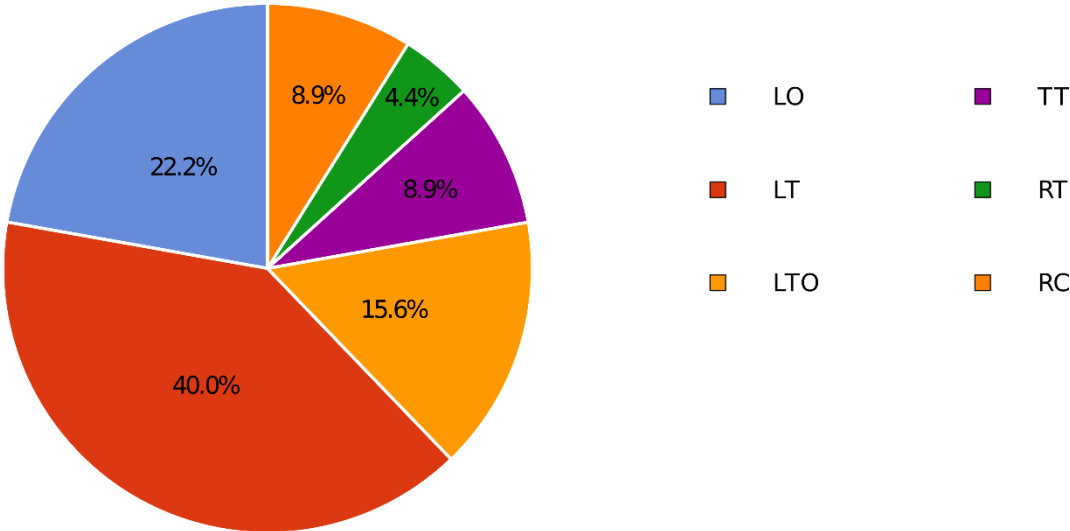


Figure 16 Pie chart of the race-walking studies scenario. In the legend: LTO represents Laboratory Track Overground; LT represents Laboratory Treadmill; LO represents Laboratory Overground; RC represents Road Competition; TT represents Track Test; RT represents Road Test

Moreover, they often analyze a restricted number of steps (44% just 1 stride). As shown in the paragraph 1.3, the assessment of these parameters is possible in different scenarios, as laboratory or field test. The scenario analysis (Figure 16) shows how many authors (over 75%) have studied performance and infringements in laboratory condition. In this type of test, it is possible to collect better measurements using accurate instruments, in many cases high value of sample frequency (more than 30% over 800Hz, Figure 17), in a controlled environment. When the tests are carried out with treadmill (over 40%, Figure 16) it is possible to analyze longer sequences of steps at the different velocities but there isn't a real interaction of the athletes with ground.

In tests without treadmill, there is a real interaction with ground but, although especially in laboratory track the athletes can have a balanced and controlled action, it is not possible to analyse longer sequences of steps.

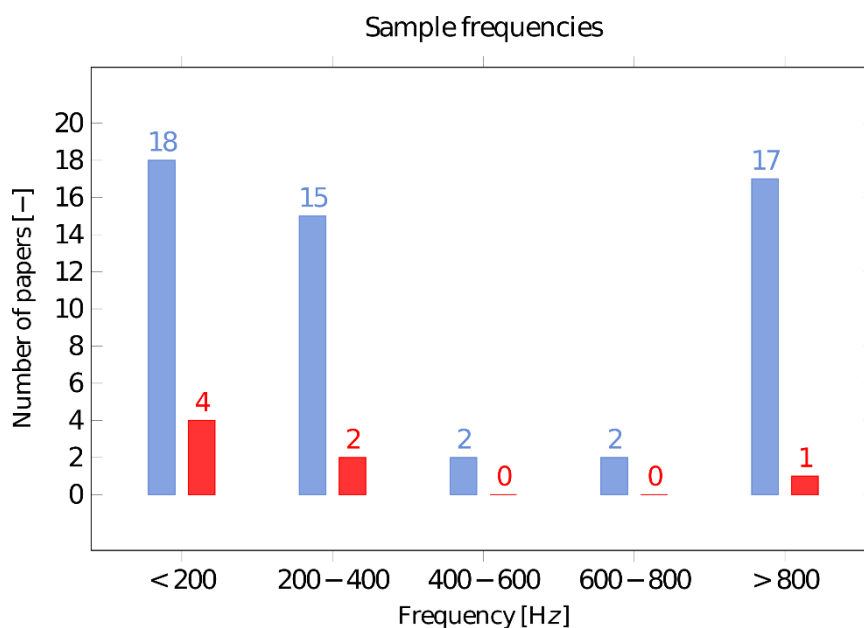


Figure 17 Bar graph about sample frequencies of the equipment in race-walking studies. In blue the bars related to all the papers; in red the bars related to papers in real scenario

However, field data (training and competition scenario), although they cover less of the 25% of studies, represent the benchmark for the analysis of the gesture since they allow to study the phenomena with the real ground interaction. Field tests allow to collect a larger number of steps, with different velocities. As well as the quality of the collected data, the more

variable conditions are critical points for in this scenario. These are due to the limitations of the available instrumentations, often with even low sample frequencies available (almost 50% with less than 200 Hz). As shown in Figure 18, the main technology chosen by authors in field conditions is the high-speed camera.

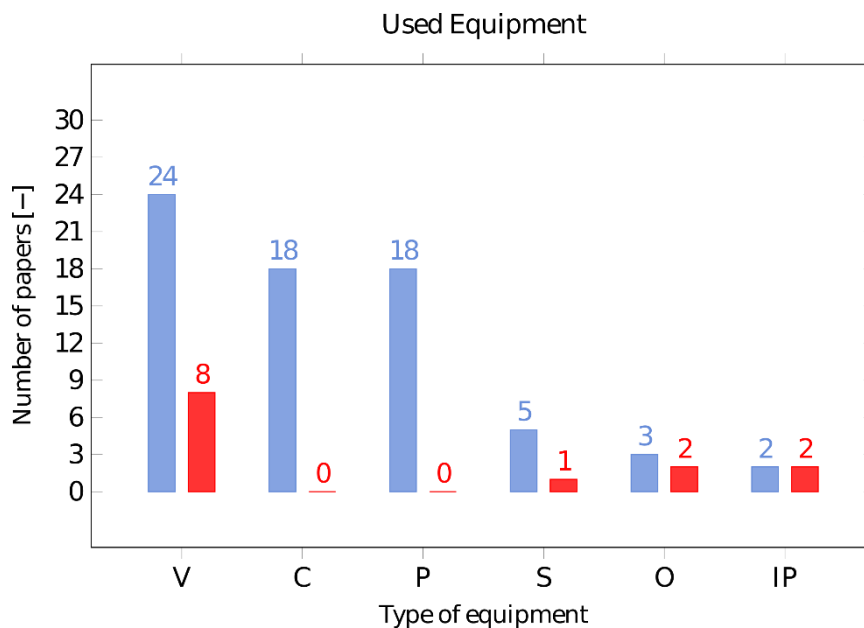


Figure 18 Bar graph about type of equipment in race-walking studies. On the x table V represents High Speed Camera video(s); P represents force platform(s); S represents Inertial Sensor(s); C represents infrared camera(s); IP represents Insole Pressure System; O represents Optojump. In blue the bars related to all the papers; in red the bars related to papers in real scenario

The video analysis provides very good reliability of the results and it allows to evaluate kinematic parameters (also related with human joints). On the other side, the limits of this analysis are its time-consuming nature and the restricted period of assessment. Another possible scenario is the dynamic simulation through musculoskeletal models. It allows a clear analysis and it permits to analyse real time data. On the other side the models are always limited, and they need reliable input data. In order to collect a larger number of steps in field condition two possible technologies are available: the insole pressure system and the inertial system.

The development of this technologies is very important for the world of race-walking that aims at having useful tools for the evaluation of infringements and performance in field conditions that ensure maximum reliability and quality of data. In this sense different related

works present different solution. The first attempt to monitor the LOGC in race-walking through an electronic device was made in 1990 by Dennis Furlong (Furlong, 1990). He invented a monitoring apparatus composed by an athlete's electronic shoes with pressure sensor inserted in each shoe, able to detect the contact between a shoe and the ground. When the contact occurs, the system generates a signal and a logic circuit combines signals of both shoes. The LOGC happens if the apparatus detects the simultaneous absence of both signals from the shoes. The apparatus also allowed the measuring of performance parameters: SL, SC and speed of an athlete. The device was evaluated by the IAAF for its use in competition, but it was refused because of its excessive weight and volume and its leaking accuracy.

More recently, Santoso and Setyanto (Santoso, 2013) developed a precision instrumentation system to measure and characterize human foot stress. The system includes a sensing unit and a signal unit which is useful in race-walking sports to identify gait temporal events and consequently the LOGC. The sensing unit consists of a piezoelectric stress sensor module and a data acquisition module. The signal-processing unit consists of a computer system and several program procedures to identify foot stress signals. The system can be operated online and real-time. Experimental validation of the system is carried out only for differentiating walking from running. No race-walking evaluation test was carried out.

Amigo (Amigo, 2013) proposed a system consisting of a pair of insoles made up of piezoelectric sensor with a thickness lower than 1 mm which transmits the LOGC information to the control unit through radio frequencies. A wrist control unit allows athletes to know when they are violating the rule. Data transmission during the race allows real-time knowledge and monitoring of rule violations and parameters. The electronic detection system has now moved to the design stage with two preindustrial demonstration prototypes to detect loss of contact by race-walkers. Experimental validation (in training and competition scenario) of the system are not presented.

Another device useful for the evaluation of the infringements in field condition is the inertial sensor. Lee et al. (Lee, 2013) used this system with seven Australian race-walkers. They have

found that characteristic patterns in each accelerometric axis can be used to identify heel-strike and toe-off events. With this approach, the LOGC timing was carried out and two different step classifications (to define legal or illegal steps) are proposed. The evaluation of the LOGC was compared with high-speed camera data. Findings concluded that an inertial system permits to correctly determine the LOGC.

CHAPTER 2:

USER-CENTERED DESIGN FOR RACE-WALKING

ANALYSIS TOOLS

*In this chapter we describe the user-centered design approach for the development of race-walking analysis tools. The flow chart in Figure 19 summarizes the methodological approach based on Kansei Engineering used in our case-study. In the following subsections this method is applied. It starts from the choice of a product domain, then followed by the span semantic and properties spaces. Then the Design of Experiments (DoE) is performed (Otto, 2001) by combining such information to generate concepts. Finally, by means of an analysis of variance (ANOVA), the optimal system architecture can be chosen (Jindo, 1997) (Lai, 2005).*

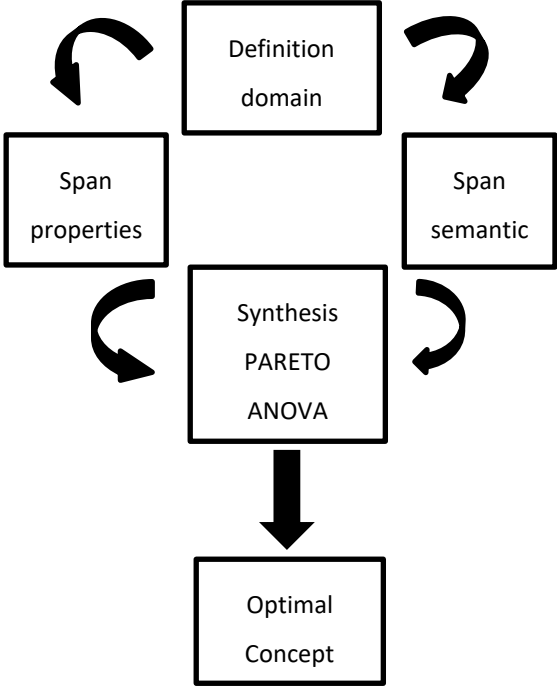


*Figure 19 The flow chart of the Kansei Engineering approach*

## 2.1 Kansei Engineering

Nowadays, many methodologies for product design and development start from the users' needs. This helps the design team to take into consideration the anthropometric characteristics and the subjective feelings of common users, at the same time of more objective performance indices.

In order to involve subjective customer feelings into the design, a possible way is to use classical methods of participatory design, which allow the identification of quality elements satisfying both functional and emotional user needs. In these techniques, the visual interaction between users and final product is possible through sketches or 3D CAD models. One of these methods of participatory design is the Kansei Engineering. It is a consumer-oriented technology for products development based on Ergonomics and Computer Science (Nagamachi, 1995) (Nagamachi, 2002) (Lanzotti A. T., 2008). Several studies underline how the Kansei Engineering approach is a highly useful method for the design of products and it can be used to facilitate product design process and to satisfy consumers' emotional needs. Indeed, based on the Kansei Engineering approach, Nagamachi has developed (since 1970) more than 60 new products, in different fields of application (i.e. body shampoo, airplane interior design, refrigerator, video-camera) (Nagamachi, 2017). The generation of the design ideas started from users' emotion (using psychological scaling) and their analysis (using statistical tools). In the following step for the implementation of Kansei Engineering approach, the products are usually decomposed into design factors (that can be discrete or continuous). So multiple alternatives are proposed for the product, each one with proper advantages and disadvantages. At this point the most critical phase of the design is the concept selection of the best alternatives (Sebastian, 2009). In this phase, multiple criteria decision-making methods, as ANOVA ( (Jindo, 1997) (Lai, 2005)), fuzzy analytic hierarchy process (Ma M-Y, 2007), and TOPSIS (Chang H-C, 2014) can be used. Questionnaires are usually employed to collect the evaluation data concerning affective responses, and one of its limitation is the evaluation process being subjective and even subconscious (Li, 2018). Finally, obtaining the optimal design, that satisfies consumers' affective responses, is a crucial key point in Kansei Engineering approaches.

In the case study of race-walking, although the problematics are relevant (as shown in the Chapter 1), the specific users' need, in term of explicit design specifications, are unknown. Indeed, a full device system for the monitoring of infringements and performance in race-walking does not exist. In this situation, the Kansei Engineering approach is very useful because it allows to discover the tacit and unconscious customers' need. Finally, it allows to translate them into technical requirements or design elements (Nagamachi, 2011).

In our case study we use a Kansei Engineering approach of Type II (Nagamachi M. L., 2011). The consumers' minds are collected and a database with all Kansei word is established. On the other side, we start from selected functional requirements (a first selection based on opinion of race-walking experts and a second one based on users' evaluation) and then we translate them into design specifications. At this point we use statistical technique in order to link the Kansei words and design specifications.

## **2.2 Definition domain**

In our case-study, as seen in Paragraph 1.5, the main available technologies useful for field application in race-walking are insole pressure and inertial sensors. The first type of technology, even achieving a direct measure of the contact/loss of contact with the ground, was not chosen due to its uncomfoting characteristic for athletes. Indeed, its positioning inside the shoes is a critical risk for troubles (such as foot blisters), especially in the longest distances. So, the choice of possible product domain concerns an inertial system. It includes a measurement unit for the collection of data and a control unit for evaluation. It is a product with a high technological content, which could be useful to support both coaching and judging activities. In order to explore the semantic and properties space it is important to define the users. In the context of race-walking world (see Paragraph 1.4) we chose three main users: athletes, coaches and judges. The first ones wear the system; the second and third ones use the system unit parts as a tool for coaching and judging.

## 2.3 Span the Semantic and Properties Space

A specific questionnaire was elaborated to register emotional user needs (Appendix A) and it was so organised:

- Before the questionnaire itself we asked our subjects to express 5 essential features of the device;
- Then, the first three questions aimed at characterizing the interviewed sample about their role (athlete/trainer/judge), their setting (national/international) and years of experience in race-walking field.
- A second group of questions aimed to know the possible effect of using the device. In particular, we asked them if they considered it important, what it should evaluate (flight time/maximum height from the ground), its acceptable price and in which kind of competition it should be used.
- Finally, it asked about the device positioning and the addressee(s) of the communication of the eventual offence.

The questionnaire was administered to fifty experts from the race-walking world. Data were collected during the IAAF Race-walking World Cup and the Italian Club Championship. The chosen sample features were:

- 50% athletes - 30% trainers - 20% judges;
- Most of them worked in international field (more than 80 %)
- About 40% of them has been part of race-walking world for more than 20 years, about 30% for 5-10 years, about 20% for 10-20 years and the last 10% for less than 5 years.

It is worth to note their opinion about the importance of introducing an electronic support device to control the loss of contact with the ground (more than 80%), more than 50% suggests its spreading use in competition (from national championships on). Almost the totality of them (more than 80%) would like its use to evaluate the flight time, by positioning it on the external part of the shoe or on the pelvis.

About its price, the 85% would it to be cheaper than 500€.

More than seventy words associated with the product were collected. The most frequent words were grouped by their semantic meaning. On the basis of the Kansei approach, a reduction of words based on the affinity diagram was performed. Four groups of words were obtained and four Kansei words were respectively assigned (Table 5). Since the word ‘efficient’ is a must for the product, this word was left out for further analysis. Therefore, the selected words were comfortable, easy to use and solid.

Table 5 Kansei words based on the affinity diagram

<b>Comfortable</b>	<b>Easy to use</b>	<b>Efficient</b>	<b>Solid</b>
Light	Essential	Accurate	Resistant to shock
Small	Regular	Reliable	Durable
Usable	Handy	Functional	Robust
Natural	Practical	Guaranteed	Waterproof
Silent	Easy	User-adjustable	
Ergonomic	user-friendly	Flexible	
		Operational	

The electronic device is composed of two physical parts: the first, named ‘measurement unit’, collects data, while the second, named ‘control unit’, processes them. In order to span the space of users’ evaluations about its properties ten core characteristics are chosen. They are decided by the race-walking experts to define the product message of a support device to control the loss of ground contact in the race-walking. Thus, at the end of the questionnaire these potential characteristics were administered in order to collect users’ evaluations. So, based on a 10-points ordinal scale with extremes 1 (no importance) and 10 (maximum importance) their preferences were collected, defining the meaning of each feature as reported below.

**Accuracy of measure:** the degree to which the result conforms to the corrected value or a standard.

**Communication speed measurement:** the rate at which information is transmitted to the user.

**Human Machine Interface:** the degree of easy comprehension of the device outputs.

**Registrability of measurement data:** the proportion of recording and collecting the acquired measures.

**Weight:** the amount of its lightness.

**Size:** how small its volume is.

**Product life:** the property of lasting in time and being used again.

**Flexible use:** the adaptability to several using conditions (road/track/indoor competitions).

**Resistance to shock:** the rate of not being vulnerable to break or damage because of impacts.

**Cost:** how restrained is the price.

Then, mean scores were calculated (Table 6). Several properties which obtained a greater score than eight were selected. In particular, the 'accuracy of measure' and the 'resistance to shock' are strictly connected to the measurement unit, while the 'ease of use' and the 'size' are related to the control unit. The next step was that of translating each selected property into design factors (Table 7). In our study we chose to use discrete variables as design factor. Some biomechanical researches (Stanhope, 1990) (Zijlstra, 2003) indicated that the accuracy of the measure is influenced by the sensor position on the body, especially in identifying gait temporal events. Some parts of the body are subject to shocks during the race, therefore the resistance to shock itself could be affected by the sensor placement. On the basis of these assumptions, we indicated the measurement unit placement (A) as a design factor. Based on the opinion of race-walking experts, the A factor should be set at the bottom of the back and on the external malleolus.

Table 6 Mean scores of properties

Property	Mean score
<b>Accuracy of measure</b>	9.3
<b>Human Machine Interface</b>	9.1
<b>Size</b>	8.7
<b>Resistance to shock</b>	8.2
Weight	7.5
Communication speed measurement	7.4
Cost	7.1
Flexible use	6.9
Product life	6.6
Registrability of measurement data	6.1

The human machine interface could be associated with the control unit of the system. A critical point of this part is the graphical user interface which was assumed as the B design factor.

Table 7 Design factors and their levels selected for the development of concepts

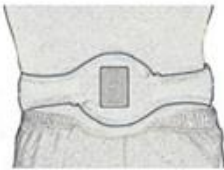
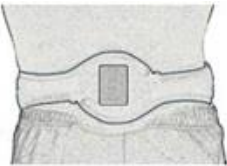
Factor	Level	
	-1	+1
A - Measurement unit placement	Bottom of the back (L5/S1)	External malleolus
B – Graphical interface	User Numerical interface	Colour interface
C- Control placement	unit For the race-walker and the judge	Only for the judge

It should be developed with a numerical interface to express the LOGC and with a colour interface based on judging (i.e. red, yellow and green ratings). Finally, the size affects the control unit and, in particular, its placement on the field. Therefore, the control unit placement (C) was assumed as the C design factor. The athlete could wear the control unit and the judge could use an external device. Therefore, the C factor is set for the athlete and the judge, and only for the judge.

## 2.4 Selection of the Optimal System Architecture

Table 8 shows the  $2^{3-1}$  fractional factorial design adopted. We chose this type of planning in order to reduce the time required for the questionnaire. Indeed, being questionnaires carried out during competitions (IAAF Race-walking World Cup and the Italian Club Championship), athletes, coaches and judges could not have enough time for analysing all the concepts of the full factorial design. Treatments represent four concepts which were evaluated through a questionnaire which was administered to the same above-mentioned users (cf. section 2.3).

Table 8 Fractional factorial design of three factors defining four concepts

Treatment	A	B	C	Concept	
1	-1	-1	+1		
2	+1	-1	-1		
3	-1	+1	-1		
4	+1	+1	+1		

Based on 10-points ordinal scale with extremes 1 (no relevance) and 10 (maximum relevance) subjective ratings were collected for each concept. We chose this type of scale, according to the findings carried out by Awang (Awang, 2016), revealing that a 10-point scale

is more efficient in the questionnaire development stage to ascertain the researchers conducting their research needed, in measurement models. The Overall Mean of subjective ratings related to Kansei words was assumed as response (Table 9).

Table 9 Subjective ratings collected for each Kansei word and their overall mean

Treatment	Factor			Kansei word			Overall Mean
	A	B	C	Comfortable	Easy to use	Solid	
1	+1	-1	-1	9.5	9.4	9.2	9.4
2	-1	+1	-1	3.4	4.5	3.2	3.7
3	-1	-1	+1	8.8	9.0	8.9	8.9
4	+1	+1	+1	2.1	5.0	2.9	3.3

First, normality test is used to know whether the data set has a normal distribution. By using Anderson-Darling normality test, the data is considered normal since the significant value of AD coefficient equal to 0.518 with  $p=0.419$  ( $>0.05$ ) (Rahmillah, 2017). Then, the ANOVA is used in order to analyse the differences between the overall mean groups. Table 10 shows that, at a significance level  $\alpha = 0.05$ , the mean effect of the A factor is significant, while B and C are not significant.

Table 10 Analysis of variance for the overall mean response ( $\alpha = 0.05$ )

Source	Degree of freedom	Sequence sum of squares	p-value
A	1	94.641	0.001
B	1	0.521	0.411
C	1	0.007	0.920
Error	8	5.533	

Figure 20 shows the chart of the effects ranked according to their contributions

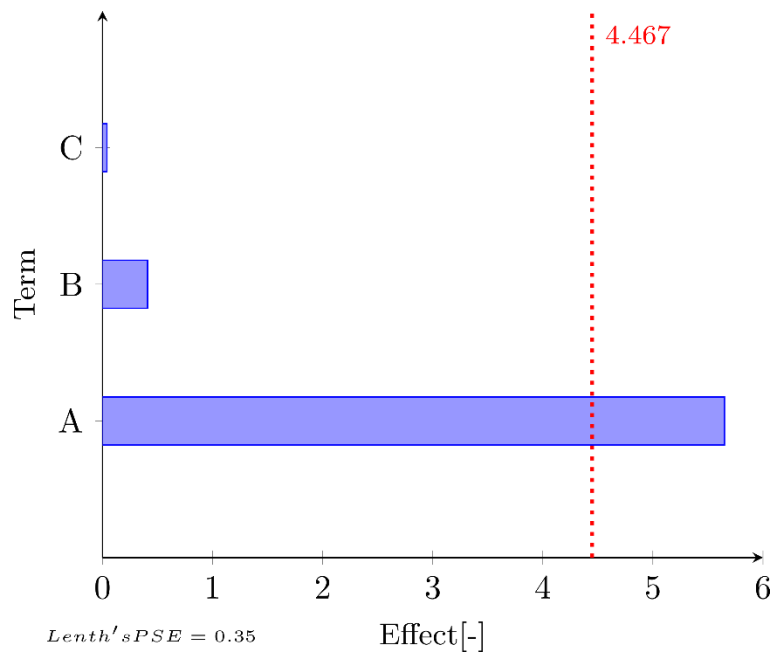


Figure 20 Chart of the effects (overall mean response with  $\alpha = 0.05$ )

Main effects plot for the overall mean response (Figure 21) shows that the optimal choice for the A factor is the -1 level, i.e. measurement unit at the bottom of the back. Therefore, the measurement unit placement is the most relevant factor and an experimental investigation about it should be performed.

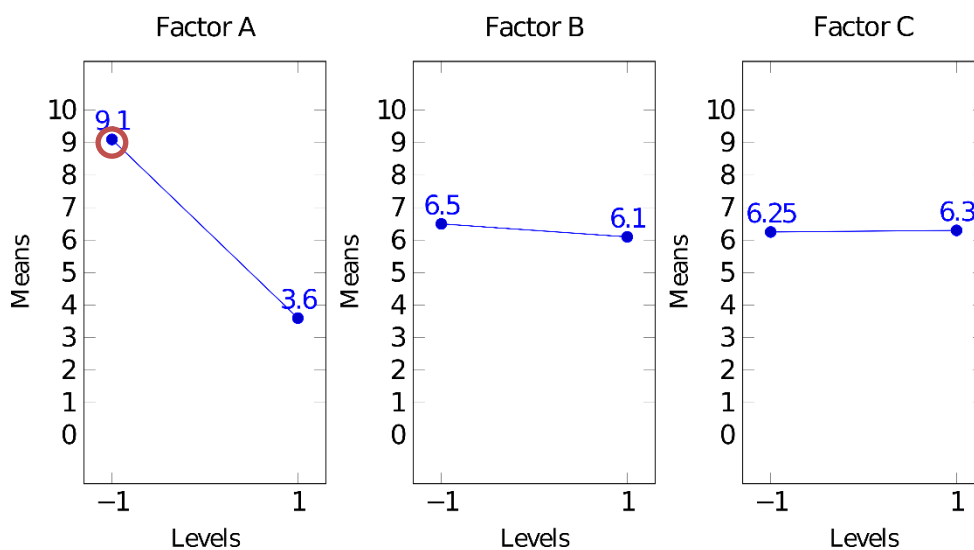


Figure 21 Main effects plot for the overall mean response and optimal level of the significant A factor

Finally, a possible real scenario of application for the optimal system architecture is shown in Figure 22.

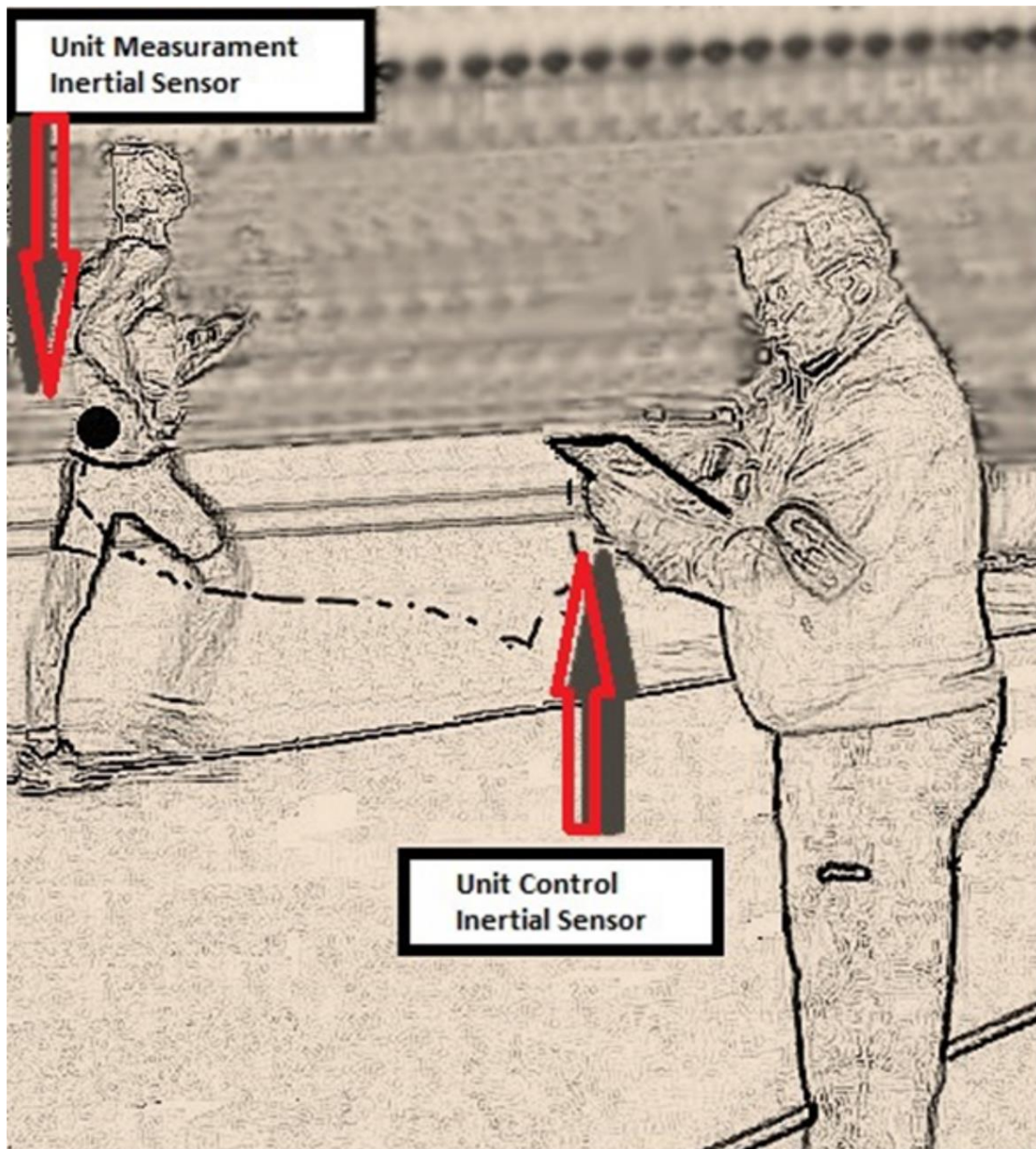


Figure 22 Picture of a possible real scenario: measurement unit placed at the end of athlete's column vertebra in communication with the control unit handled by judge.

## CHAPTER 3:

# BIOMECHANICAL-BASED METHOD FOR ASSESSMENT OF INFRINGEMENTS AND PERFORMANCE IN RACE-WALKING

In this chapter we describe:

- the inertial data processing for the assessment of infringements and performance parameters. After the data filtering and the assessment of gait temporal events, the LOGC time ( $LOGC_T$ ) is evaluated and the steps are classified.
- The assessment of  $LOGC_T$  allows to develop three different methods for step classification: (i) binary; (ii) on three levels and (iii) based on fuzzy theory. All classification methods are built according to race-walking competition rules.
- Quantitative parameters for the evaluation of the infringements and performance are carried out. The following parameters are chosen: the LOGC with the assessment of the timing ( $LOGC_T$ ) and the step classification ( $LOGC_C$ ), the smoothness for anterior/posterior linear movement ( $S$ ), the Step Cadence ( $SC$ ) and step length over athlete's height ratio ( $SLR$ ). The first two parameters are strictly connected with the infringements, while the last three ones with the performance.
- All parameters are related to a sequence of a fixed number of steps and they are correlated with a synthetic index for a representation on a radar graph.

The flow chart in Figure 23 summarizes the methodological approach.

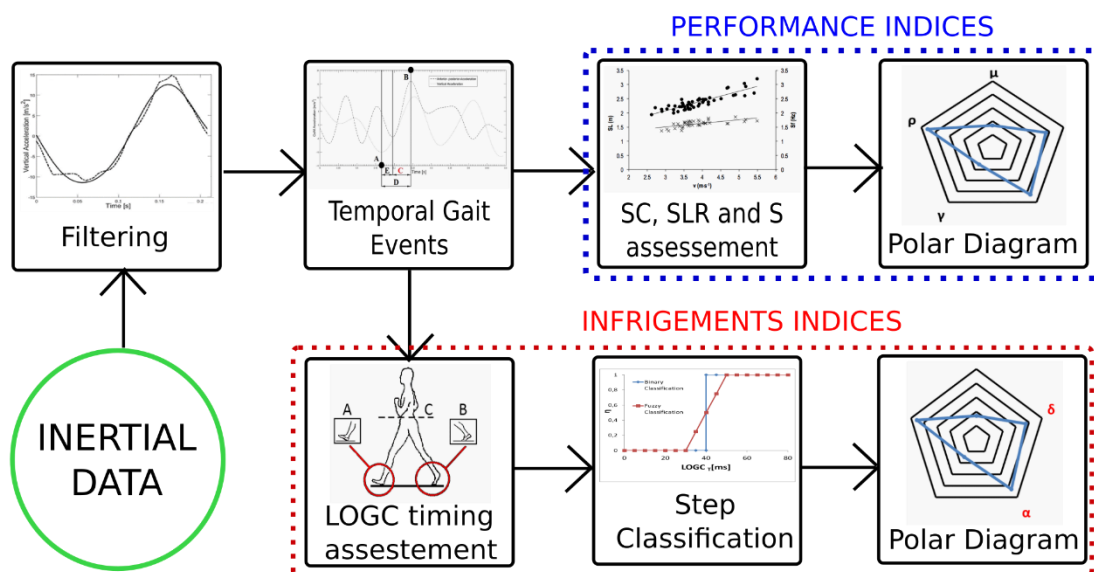


Figure 23 Flow chart of the methodological approach for inertial data processing and analysis

### 3.1 Inertial data processing

#### 3.1.1 Signal Filtering

After the offset error correction, acceleration data of the inertial sensor were converted from device-based units to meters per square second. A fourth order Butterworth low pass filter was applied with a cut-off frequency of 20Hz for x-axis (i.e. the vertical acceleration of CoM) and 30Hz for z-axis (i.e. the anterior-posterior acceleration of CoM) according to Lee (Lee, 2013) that used for a similar application a low pass filter at 20Hz.

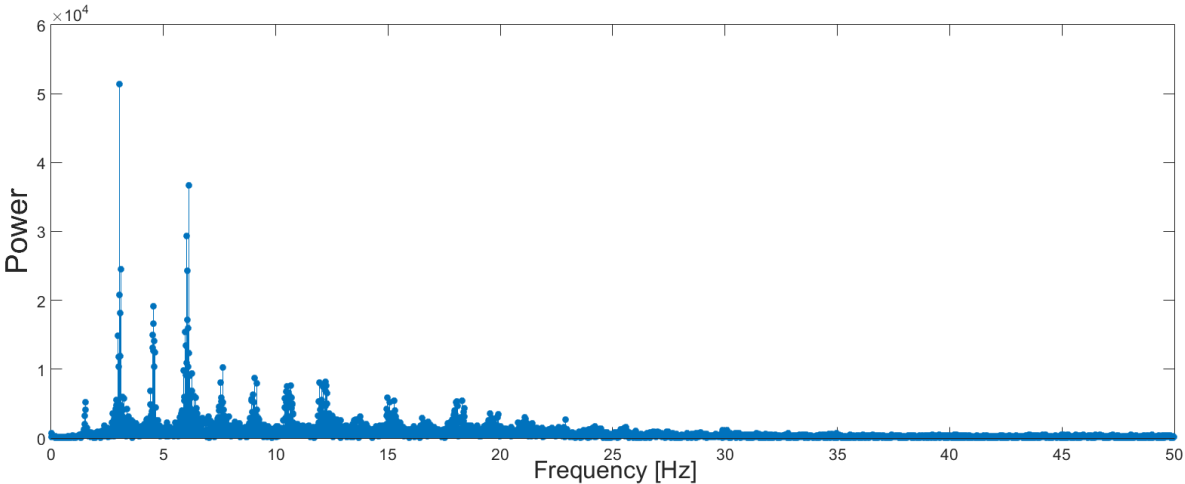


Figure 24 The power spectrum for accelerations on the x-axis

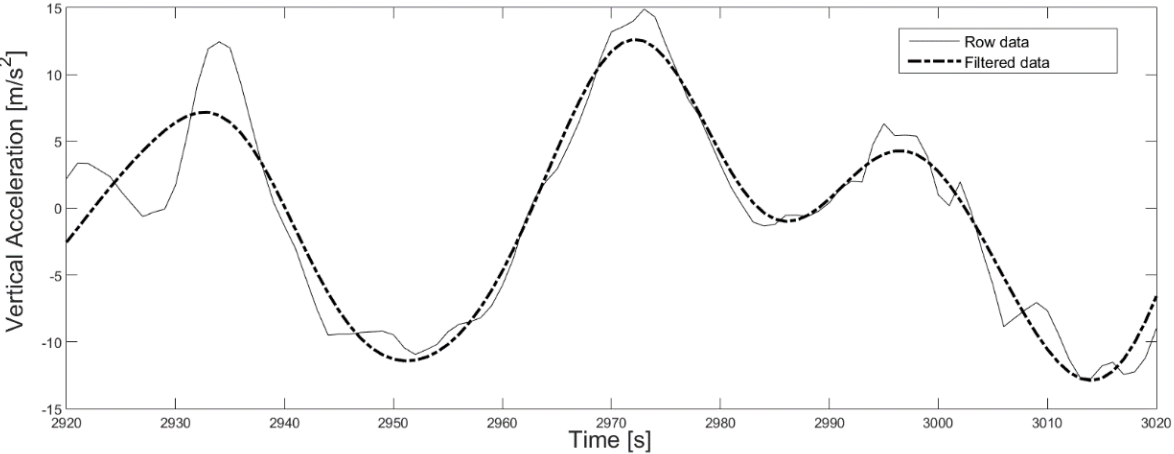


Figure 25 The comparison between the vertical acceleration based on raw data and the one two-times filtered

The filtering allowed to identify gait temporal events. Over the 70% of the signal is lower than the cut-off frequency, as shown in Figure 24. In order to delete the phase shift, signals were filtered two times (in both the directions, Figure 25).

### 3.1.2 Detection of temporal gait event for the assessment of LOGC

Figure 26 shows the inertial sensor data signal processing for the laboratory test.

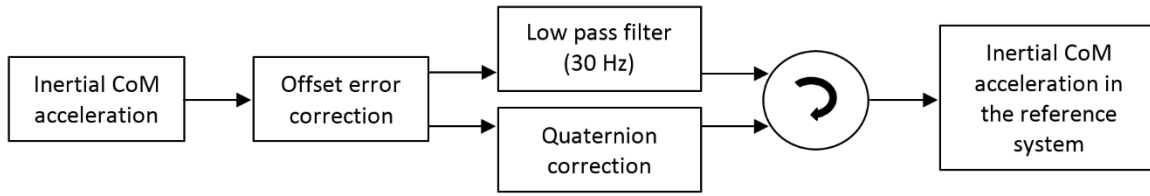


Figure 26 The signal processing applied to inertial system data in laboratory test

After the filtering according to Esser (Esser, 2009), the Inertial CoM acceleration with the quaternion correction was obtained by using a matrix multiplication (eq. 1).

$$\begin{Bmatrix} a_{x,CoM,rs} \\ a_{y,CoM,rs} \\ a_{z,CoM,rs} \end{Bmatrix} = [T_{rs-LS}(q_0, q_x, q_y, q_z)] * \begin{Bmatrix} a_{x,CoM,LS} \\ a_{y,CoM,LS} \\ a_{z,CoM,LS} \end{Bmatrix} \quad (\text{eq. 1})$$

The  $a_{CoM,rs}$  variable is the acceleration in the reference system; the  $a_{CoM,LS}$  variable is the acceleration in the local reference system; and the  $T_{rs-LS}$  is the quaternion rotation matrix (eq. 2) where  $q_0$  is the real value, while  $q_x$ ,  $q_y$  and  $q_z$  are complex numbers.

$$\begin{bmatrix} q_0^2 + q_x^2 - q_y^2 - q_z^2 & 2 * (q_x * q_y + q_0 * q_z) & 2 * (q_x * q_z - q_0 * q_y) & 0 \\ 2 * (q_x * q_y - q_0 * q_z) & q_0^2 - q_x^2 + q_y^2 - q_z^2 & 2 * (q_y * q_z + q_0 * q_x) & 0 \\ 2 * (q_x * q_z + q_0 * q_y) & 2 * (q_y * q_z - q_0 * q_x) & q_0^2 - q_x^2 - q_y^2 - q_z^2 & 0 \\ 0 & 0 & 0 & q_0^2 + q_x^2 + q_y^2 + q_z^2 \end{bmatrix} \quad (\text{eq. 2})$$

In particular, solving the differential equation system (eq. 3), quaternions were obtained:

$$\begin{Bmatrix} \dot{q}_0 \\ \dot{q}_x \\ \dot{q}_y \\ \dot{q}_z \end{Bmatrix} = \frac{1}{2} * \begin{bmatrix} 0 & -p & -q & -r \\ p & 0 & r & -q \\ q & -r & 0 & p \\ r & q & -p & 0 \end{bmatrix} \quad (\text{eq. 3})$$

Where the  $p$ ,  $q$  and  $r$  variables are angular speeds calculated from gyroscopic data.

Moreover, this model was used only for laboratory test. Indeed, after the first experimental phase in the laboratory, we observed how the accuracy of flight time evaluation didn't have significant improvements, with the quaternion correction (a time-consuming computational operation). For outdoor tests, we would need to design a Kalman filter. We rejected this hypothesis because of the limitations of the Kalman filter (it is an adaptive predictive filter and it assumes that both the system and observation models' equations are linear, which is not realistic in real scenario), so it could introduce greater error in the LOGC timing assessment.

So, for outdoor test the inertial data processing (without quaternion correction) is shown in Figure 27.

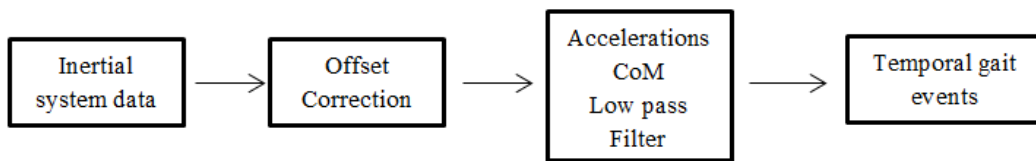


Figure 27 The signal processing applied to inertial system data in laboratory test

The definition of temporal gait events (Figure 28) was required in order to evaluate the LOGC. We started from the definition of the gait temporal events (toe-off and heel strike) according to Lee (Lee, 2013) (Figure 28) and LOGC was evaluated through the following equation:

$$LOGC_T = \text{mean}(\sum_1^{30} t_{\max,i} - (t_{\min,i} + E)) \quad (\text{eq. 4})$$

where  $t_{\min}$  is time instant of the minimum value of the vertical component of the center of mass' acceleration;  $t_{\max}$  is time instant of the consecutive peak of anterior-posterior acceleration, corresponding to the heel-strike event (HSE) and  $E$  is a threshold value. Lee (Lee, 2013), basing on Little (Little, 2013), hypothesized that the flight phase occurs when the time range between the HSE and the negative peak of the vertical component of the CoM acceleration, is over a threshold ( $E$ ). They have found that for race-walking tests, using a high-speed camera,  $E$  was 30 ms. This threshold allows to defined the event of toe-off.

In laboratory test (that will be extensively displayed in paragraph 4.1), we assumed that the toe-off event occurs twenty-five millisecond (i.e. E=25ms) after the negative peak of the vertical component of the CoM acceleration. For this assessment, we studied how the accuracy of LOGC step classification (that will be extensively displayed in paragraph 3.2) in relationship with force platform evaluation varies at different toe-off event thresholds.

In field test, we started the analysis with a previous model (E=30ms, according to Lee (Lee, 2013)) and then we developed an advanced model modifying the threshold value E (named  $E_p$ ) according to the following quadratic correlation with the SC:

$$E_p = \frac{1}{a * SC^2 + SC * b} \quad (\text{eq. 5})$$

Thus, (eq. 4) takes the novel form:

$$\text{LOGC}_M = t_{\max} - \left( t_{\min} + \frac{1}{a * SC^2 + SC * b} \right) \quad (\text{eq. 6})$$

For the evaluation of a and b, we used field experimental data carried out using an high speed camera as ground truth system (that will be extensively displayed in paragraph 4.2).

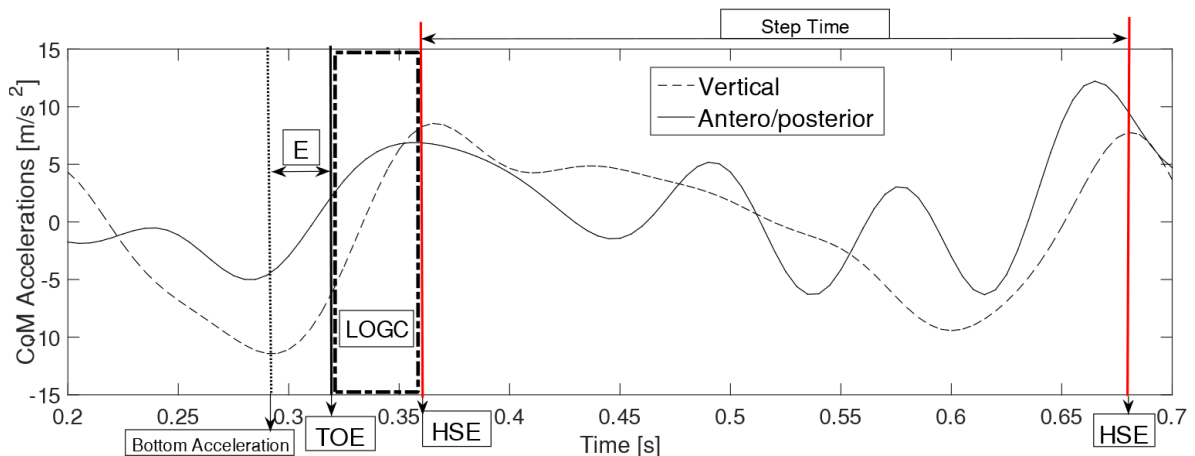


Figure 28 The correlation between the CoM accelerations and gait temporal events (TOE: toe-off event; HSE: heel strike event) for assessing the LOGC (using the threshold value E). The time between two following HSE represents the Step time.

## 3.2 Step Classification

In this section are presented three different strategies developed for the step classification: on two levels (binary step classification); on three levels and a third option based on fuzzy theory. Finally the evaluation of Judge's field of view was carried out.

### 3.2.1 Binary classification

Steps were analysed through a binary classification. This task consists in classifying steps in two groups based on a classification rule. The procedure assigns each step to one of the classes: 'legal' or 'illegal'. A perfect classification is such when every step is assigned to the class it really belongs to; on the contrary, some errors can appear. The 'legal' step is such when the corresponding value of the LOGC, net of the human eye limit as well as the IAAF rule states, is less or equal to zero; the 'illegal' step is such when the corresponding value of the LOGC is greater than zero. The human eye limit, in this study, was fixed to 25 Hz, or 40 ms according to the study on human psycho-physiological limitations of vision and research in race-walking scenario (see section 1.3). This limit was also chosen in similar classification by Alvarez et al. (Alvarez, 2017). Therefore, in order to apply the aforementioned classification rule, the human threshold was subtracted from each dynamic and inertial LOGC value.

For the assessment of  $LOGC_c$ , the steps were classified as 'legal' or 'illegal' according to the classification proposed:

$$\begin{cases} LOGC_T > 40 \text{ ms} & \text{Illegal step} \\ LOGC_T \leq 40 \text{ ms} & \text{Legal step} \end{cases} \text{ (eq. 7)}$$

So,  $LOGC_c$  for each sequence of steps (in the following paragraph we describe the choice of 30 for the number of steps of the sequence) was fixed equal to:

$$LOGC_c = \frac{\text{Illegal steps}}{30} \text{ (eq. 8)}$$

### 3.2.2 Three-level classification

In the previous subsection, all the steps were classified as 'legal' or 'illegal'. Differently, in

this one, three levels of classification are proposed. The new level is introduced to reproduce the “doubt case” that represents the yellow paddle shown by judge during the competition. The  $LOGC_T$  values are expressed as confidence intervals. Starting from inertial sensors data,  $LOGC_T$  results to be included between  $LOGC_{T,min}$  and  $LOGC_{T,max}$  as:

$$LOGC_{T,max} = \left[ t_{max} - \frac{1}{SF} \right] - \left[ \left( t_{min} + \frac{1}{a * SC^2 + SC * b} \right) + \frac{1}{SF} \right] \quad (\text{eq. 9})$$

$$LOGC_{T,min} = \left[ t_{max} + \frac{1}{SF} \right] - \left[ \left( t_{min} + \frac{1}{a * SC^2 + SC * b} \right) - \frac{1}{SF} \right] = LOGC_{T,max} - 4 * \frac{1}{SF} \quad (\text{eq. 10})$$

Where SF represents the sample frequency of the inertial sensor. (eq. 9) was carried out considering the points A and D in Figure 29 respectively as the minimum vertical acceleration and the maximum antero-posterior acceleration; (eq. 10) was carried out considering the points B and C in Figure 29 respectively as the minimum vertical acceleration and the maximum antero-posterior acceleration.

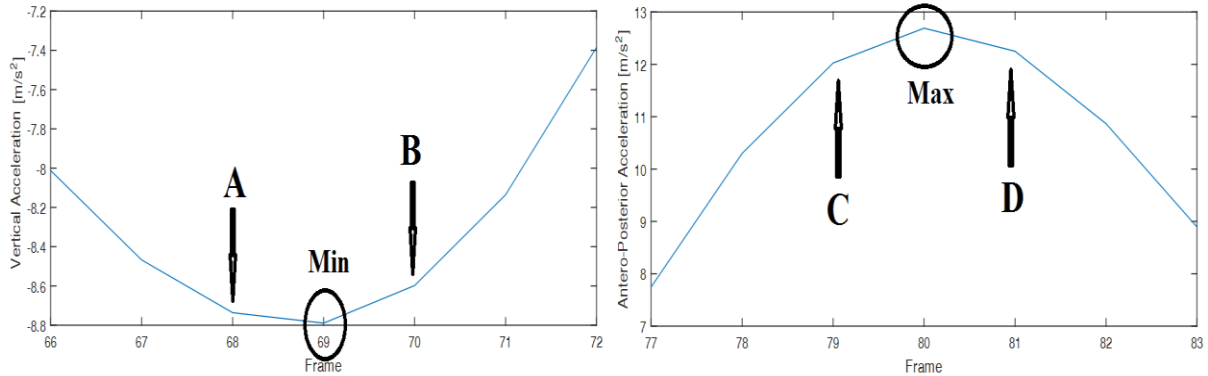


Figure 29 Acceleration data, on the left: the vertical acceleration near the bottom point of the cycle; on the right: antero-Posterior acceleration near the maximum point of the cycle.

The human eye limit was fixed equal to 40 ms, according to the literature and the previous subsection. The step was identified as: ‘legal’ when  $LOGC_{T,max}$  and  $LOGC_{T,min}$  were under 40ms (no visible LOGC); ‘illegal’ when  $LOGC_{T,min}$  and  $LOGC_{T,max}$  were over 40ms (visible LOGC); ‘doubt’ if the confidence interval across the line of limit of human eyes as we can see in Figure 30.

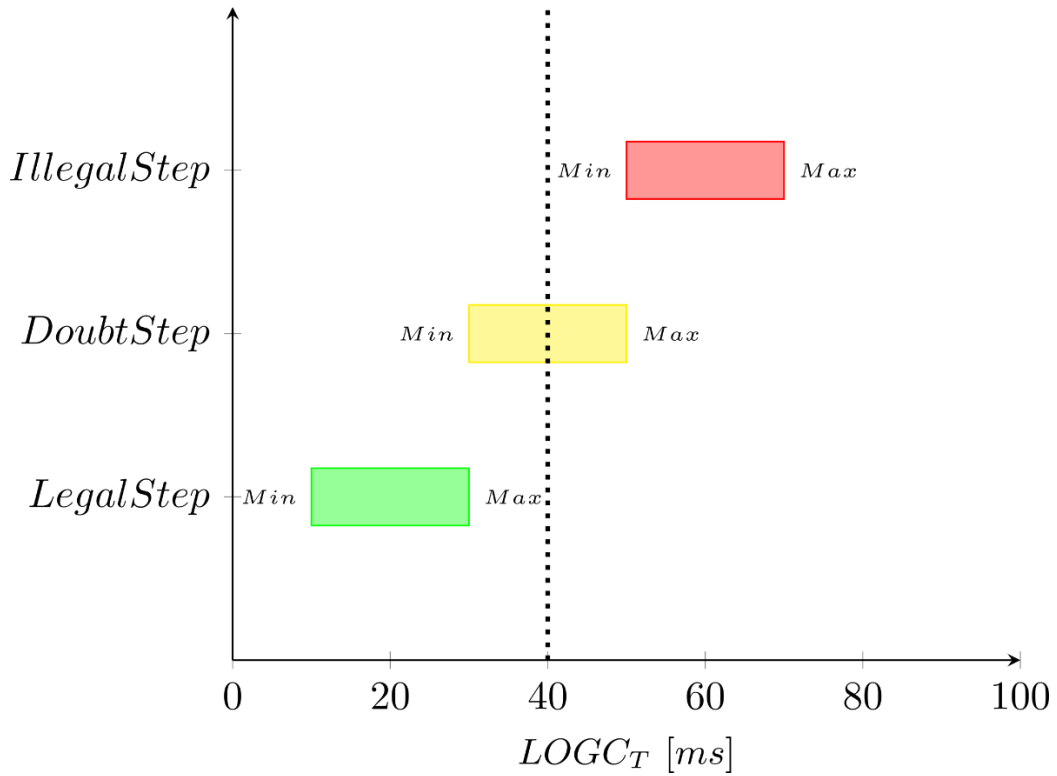


Figure 30 The novel step classification. On the abscissa axis the value of  $LOGC_T$  expressed in ms. On the ordinate axis the different step classification. On the graph the legal steps are in “green”, doubt steps in “yellow”, illegal steps in “red”. The vertical dotted line represents the limit of human eyes (40 ms).

### 3.2.3 Fuzzy classification

The described measurement of LOGC (with a classification on three level) presents a new degree of uncertainty. Thus, it required an overcoming of the typical binary classification for a correct evaluation. For this purpose, fuzzy logic is a powerful tool. We proposed to use fuzzy set theory as a mathematical framework for managing the step classification (Feizollah, 2013). According to Figure 30, a fuzzy membership function has been built to describe the response of video ground truth system and inertial kinematic model. The membership function is a curve that defines how each LOGC value (input space,  $LOGC_T$ ) is mapped to a membership value (output space) between 0 and 1. We called  $\eta(LOGC_T)$  the membership function for the fuzzy set  $LOGC_T$  described by the following equation system (eq. 11):

$$\delta(LOGC_T) = \begin{cases} \eta = 1, & LOGC_M \geq 50 \text{ ms} \\ 0 < \eta < 1, & 30 \text{ ms} > LOGC_M > 50 \text{ ms} \\ \eta = 0, & LOGC_M \leq 30 \text{ ms} \end{cases} \text{ (eq. 11)}$$

They have a core, that is defined as those elements of the  $LOGC_T$  where the step is defined illegal. The boundaries of the function are where the step is defined doubt. In all cases where the step is classified as legal the function is equal to 0. Figure 31 illustrate the membership function compared with the previous binary classification method.

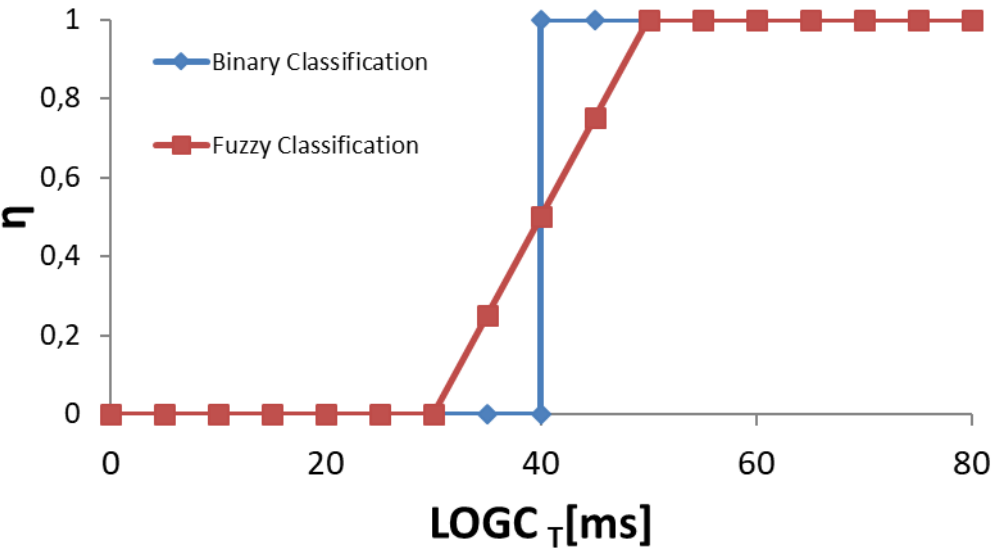


Figure 31 Inertial system membership function compared with the binary classification

**3.2.4 Estimation of judge’s field of view – Step sequence classification**

According to the IAAF regulations, the judges must consider a sequence of steps instead of a single step.

Thus, the evaluation of the length of judge’s field of view L was carried. This value is equal to:

$$L = \tan(\beta + \gamma) * h * 2 \text{ (eq. 12)}$$

where  $\beta$  is the angle to observe the athletes with respect of the race-walking direction,  $\gamma$  is the acceptable eye rotation, h is the distance of the judges from the race line. For a geometrical interpretation, see Figure 32. We fixed  $\beta = 45^\circ$  and  $h = 5.50m$ , as recommended by IAAF for the judging (IAAF, 2014). Indeed, according to Shimizu (Shimizu, 1994),  $\gamma$  was set equal to  $30^\circ$ .

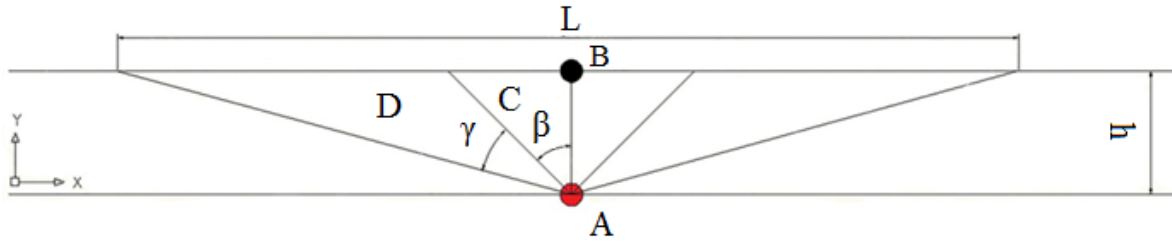


Figure 32 Judge's field of view design: A) Judge; B) Athlete; C) Area of observation for a field of view at  $\beta$ ; D) Additional Area for field of view allowed through acceptable eye rotation ( $\gamma$ ). The x axis represents the athlete's direction of progression, y axis is orthogonal to the athlete's direction of progression

Finally, considering the velocity, the step length (SL) of a single athlete's step varies in a range. The estimation of the number of step (NS) to be included in a sequence of steps was carried out as:

$$NS = \frac{\tan(\beta + \gamma) \cdot h^2}{\max(SL)} \quad (eq. 13)$$

where in the result we considered only the whole number. According to the maximum value of SL in elite race-walkers (about 1.40m (Pavei G. L., 2016)), we fixed NS equal to 30.

### 3.3 Performance indices assessment

Starting from the temporal gait event assessment it is possible to evaluate also the performance indices. The main performance index are the Step Cadence (SC) and Step Length Ratio (SLR). It is possible to evaluate them through the following equations:

$$SC = \text{mean} \left( \sum_{i=1}^{30} \frac{1}{(t_{max,i+1} - t_{max,i})} \right) \text{ (eq. 14)}$$

$$SLR = (SC * v_{mean}) / h \text{ (eq. 15)}$$

where  $v_{mean}$  is the test mean velocity and  $h$  is the athlete's height.

In addition, another useful parameter is the smoothness (S). It is evaluated using Normal Jerk according to Balasubramanian (Balasubramanian, 2012) through the following equation:

$$S = \text{mean} \left( \sum_{i=1}^{30} \sqrt{\frac{(t_{max,i+1} - t_{max,i})^5}{(SC * v_{mean})^2} \int_{t_{max,i}}^{t_{max,i+1}} j^2(t) dt} \right) \text{ (eq. 16)}$$

where  $j(t)$  is the jerk related to the anterior/posterior acceleration.

### 3.4 Development of a customized strategy for élite race-walkers: radar chart representation

Starting from the previous defined five parameters (SL, SC, LOGC<sub>T</sub>, LOGC<sub>c</sub> and S) each one is associated to a scale between 0 (best score) and 1 (worst score). According to the IAAF recommendations, the judgments must consider a sequence of steps instead of a single one, so all parameters are related to the mean values in a sequence of steps (equal to 30, see section 3.2.4). We considered the features of the inertial device and fixed this correlation criteria for LOGC<sub>T</sub>:

$$\delta(\text{LOGC}_T) = \begin{cases} \delta = 0.4, & \text{LOGC}_T = 40\text{ms} \\ \delta = 0, & \text{LOGC}_T \leq (40 \text{ ms} - \frac{2}{SF}) \end{cases} \text{ (eq. 17)}$$

where SF is the sample frequency expressed as 1/T<sub>s</sub> (T<sub>s</sub> is the sample timing) of the wearable inertial system. So, we fix a linear equation between  $\delta=0$  and  $\delta=0.4$  and the following equations system to describe  $\delta(\text{LOGC}_T)$  is carried out (eq.18):

$$\delta(\text{LOGC}_T) = \begin{cases} \delta = 1, & \text{LOGC}_T \geq (40 \text{ ms} + \frac{3}{SF}) \\ \delta = \frac{1}{40 - \frac{5}{SF}} * \left( \text{LOGC}_T - \left( 40 \text{ ms} - \frac{2}{SF} \right) \right), & (40 \text{ ms} - \frac{2}{SF}) > \text{LOGC}_T > (40 \text{ ms} + \frac{3}{SF}) \\ \delta = 0, & \text{LOGC}_T \leq (40 \text{ ms} - \frac{2}{SF}) \end{cases} \text{ (eq.18)}$$

For the SLR and SC we use the linear regression presented by Hanley (Hanley B. B., 2008) and Pavei (Pavei G. C., 2014) that, starting from élite competition data, derive the following equations:

$$\{SLR = 2.47 * v + 32.73 \quad \{SC = 0.259 * v + 2.253 \text{ (eq. 19, eq. 20)}$$

From these equations we obtain for all type of race competition the optimal value (SLR<sub>0</sub>) and the passing one (SLR<sub>0,4</sub>):

$$\begin{cases} SLR_{0,4} \text{ with } v = v_E \\ SLR_0 \text{ with } v = v_R \end{cases} \quad \begin{cases} SC_{0,4} \text{ with } v = v_E \\ SC_0 \text{ with } v = v_R \end{cases} \text{ (eq. 21, eq. 22)}$$

where  $v_E$  is the velocity of the entry standard time for the last World Championship for the 50 km man (12.20 km/h) and  $v_R$  is the velocity of the world record for the 20 km man (15.76 km/h). These ones are chosen to cover the range of velocities of interest. All velocities in the equations are expressed in km/h for the equations (eq. 19) and (eq. 21) and in m/s in (eq. 20) and (eq. 22). Consequently  $SLR_{0,4}$  and  $SLR_0$  are setted equal to 62.8 and 71.4;  $SC_{0,4}$  and  $SC_0$  equal to 3.130 step/s and 3.380 step/s. Finally, we compute the indices  $\rho(SLR)$  and  $\gamma(SC)$  through the following equation systems:

$$\left\{ \begin{array}{l} \rho(SLR) = -0.4 \frac{(SLR - SLR_{0,4})}{(SLR_0 - SLR_{0,4})} + 0.4, \\ \text{for } SLR > SLR_0, \quad \rho(SLR) = 1 \text{ (eq. 23)} \\ \text{for } SLR < -1.5 * SLR_0 + 2.5 * SLR_{0,4}, \quad \rho(SLR) = 0 \end{array} \right.$$

$$\left\{ \begin{array}{l} \gamma(SC) = -0.4 \frac{(SC - SC_{0,4})}{(SC_0 - SC_{0,4})} + 0.4 \\ \text{for } SC > SC_0, \quad \gamma(SC) = 1 \text{ (eq. 24)} \\ \text{for } SC < -1.5 * SC_0 + 2.5 * SC_{0,4}, \quad \gamma(SC) = 0 \end{array} \right.$$

Moreover, for the assessment of  $\mu(S_{AP})$  we use a similar equation where  $S_{Min}$  is equal to 1 (ideal best value of smoothness) and  $S_{Max}$  is fixed equal to 10 (since no references are provided).

$$\mu(S) = \frac{(S - S_{Min})}{(S_{Max} - S_{Min})} \text{ (eq. 25)}$$

Instead, the parameter  $LOGC_C$  is already defined between 0 and 1.

$$\alpha(LOGC_C) = LOGC_C \text{ (eq. 26)}$$

All parameters are shown in a synthetic radar graph shown for example in Figure 33. The evaluation of the polygon area (Area) allows to obtain a synthetic index ( $\beta$ ) to take into consideration both infringements and performance. This index is expressed as:

$$\beta = \frac{Area}{Area_{max}} \text{ (eq. 27)}$$

where  $Area_{max}$  is the maximum possible area (area of a regular pentagon with unitary radius).

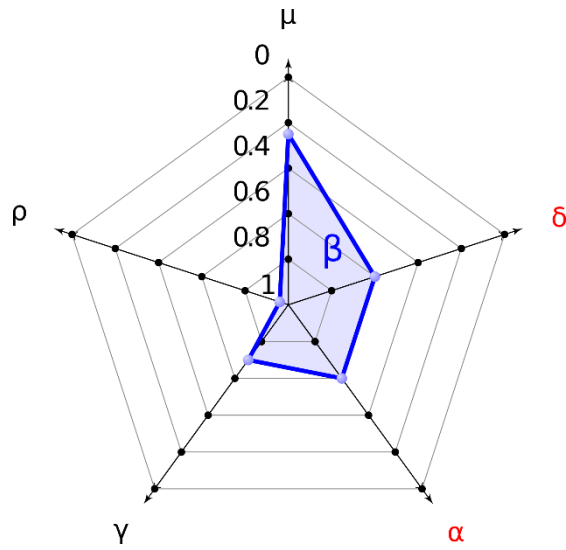


Figure 33 In the figure the red indices are related to the infringements, the black ones to the performance. The blue opacity area ( $\beta$ ) represents the synthetic index.

Furthermore, we fix the minimum condition of the correct gesture (assuming the threshold values of 0.4 for the infringements parameters  $\delta$  and  $\alpha$ ) and we carried the best acceptable  $\epsilon$  value ( $\beta_{opt}$ ):

$$\begin{cases} \beta_{opt} = \frac{Area}{Area_{max}} \\ \alpha \leq 0.4 \quad \delta \leq 0.4 \end{cases} \quad (\text{eq. 28})$$

## CHAPTER 4:

# EXPERIMENTAL VALIDATION OF INDICES FOR EVALUATING INFRINGEMENTS AND PERFORMANCE IN RACE WALKING SCENARIOS

*In this chapter, the methodology illustrated in chapter 3 is validated both in laboratory and field condition using a commercial inertial sensor (200Hz).*

*Four athletes participate at the laboratory tests (Figure 34) conducted at the ErgoS Lab part of the Fraunhofer Joint Labs IDEAS at CESMA (University of Naples Federico II). The first model for the LOGC timing assessment (and classification approach) are evaluated through a comparison with a ground truth system composed by eight platforms of force (680Hz).*

*Then, using a high-speed camera system (240Hz) as ground truth, the algorithms for performance and infringement evaluation are evaluated in field tests (Figure 39). The whole experimental tests are performed in a training scenario with nine international élite race-walkers. They perform at least four outdoor field tests at different velocities in order to cover a range around their race pace.*

- *The first part of test allows to define the advanced model with a variable threshold ( $E_p$ ) for the assessment of the LOGC. It is compared with the model with a fixed threshold. Then, the three defined step classifications allow to evaluate the efficiency of the models for LOGC assessment. Statistical indices are carried out; by using the Receiver Operating Characteristics graph and Precision Recall graph the performances of the proposed methods as classifier are evaluated.*
- *The second part allows to verify the quality and reliability of radar chart representation through statistical analysis.*

## 4.1 Laboratory tests

The aim of this experimental investigation is to evaluate the LOGC with the inertial system in laboratory conditions in order to objectively recognize infringements of competition rules according to the IAAF. The evaluation of the LOGC is the objective variable of this investigation. By means of an integrated system, including dynamic and kinematic devices which are more accurate than the inertial system, the validation of the inertial system was made.

The whole experiment was carried out at the ErgoS Lab of the University of Naples Federico II. It consisted of fifteen sessions in which four race-walker volunteers performed sixty test-runs according to a well-defined experimental protocol. They performed a race-walking task into a calibrated control volume where the inertial, dynamic and kinematic measurement systems registered experimental data. Figure 34 shows the methodological approach.

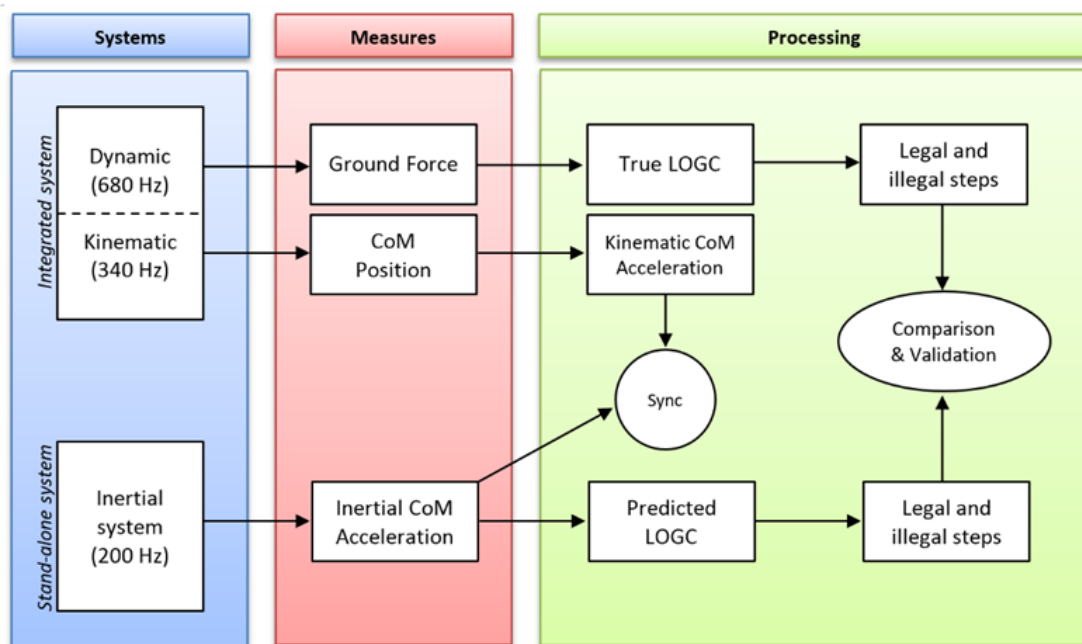


Figure 34 The methodological approach

### 4.1.1 Participants

Four race-walker volunteers, including one female and three males, participated to the experimental sessions. These participants came from the Italian national team. This

population was deemed relevant for this study since elite athletes tend to have a balanced and controlled action even in short runs. Participants had not suffered severe injuries in the twelve months before the testing day. The test leader collected the informed consent from volunteers as well as their personal details (i.e. age and experience) and anthropometric characteristics (i.e. stature and weight). Table 11 shows collected data.

Table 11 Mean and standard deviation related to age, stature, weight and experience of race-walkers

	Age (year)	Stature (cm)	Weight (kg)	Experience (year)
Mean	22	173	62	8
SD	5	7	8	5

Participants are representative of the reference population. They cover the range from 15th to 86th percentile of the Italian national team stature distribution since 2006 (i.e.  $\mu=173$  and  $\sigma=7$  from the personal cards of Italian race-walkers (Di Gironimo G. C., 2017)).

#### 4.1.2 Devices and Experimental Settings

Experimental data were collected with inertial, dynamic and kinematic measurement systems at the Laboratory of Advanced Measures on Ergonomics and Sport of the University of Naples Federico II.

The inertial system (i.e. G-Sensor2, BTS S.p.A., Italy) consists of a triaxial accelerometer, a triaxial gyroscope and triaxial magnetometer. This system has a mass of 62 g and its operating temperature range is 0-60 °C. The external dimensions are 78×48×20 mm. Data transmission is via Bluetooth Zig Bee modules (+EDR class 1). The battery is rechargeable with an operating time of about 24 hours. The sampling frequency, for this study, was set to 200 Hz (i.e. the maximum value). Table 12 shows the sensor's additional technical features. This system acquired the CoM Inertial acceleration.

Table 12 Data sheet of the inertial system

Technical feature	Accelerometer sensor	Gyroscope sensor	Magnetic sensor
Dynamic range	±8g	±300 dps	± 6 Gauss
Max offset	± 40 mg		
Sensitivity	±0.002 %/°C	0.83 mV/dps/(1200dp)	1mV/V/gauss
No linearity	±1% FSO	±1% FSO	50 aV/√Hz
Noise	350 µg/√Hz	0,018 dps/√Hz	120 µgauss
Amplitude band	of 400 Hz	140 Hz	5 mHz

The dynamic system (*i.e.* P-6000, BTS S.p.A., Italy) consists of eight integrated platforms of force. The sampling frequency was set to 680 Hz (*i.e.* the maximum value). Table 13 shows its technical features. This system has acquired the Ground Reaction Force.

Table 13 Data sheet of the dynamic system

Technical feature	Dynamic system
Dimension	sensitive area 600×400mm; minimum height 5.7cm
Capacity (X and Y) for each sensor	up to ±2000 N
Capacity (Z) for each sensor	up to 2000 N
Sensitivity/Resolution	16 bit over selected range
Sensitivity deviation over plate surface	<1,0% full scale output

The kinematic system (*i.e.* Smart DX 6000, BTS S.p.A., Italy) is a motion capture system composed by infrared digital cameras, which acquired the CoM position. In particular, this system permits the synchronisation between inertial and kinematic signals. The sampling

frequency was set to 340 Hz (*i.e.* the maximum value in order to achieve the maximum resolution). Table 14 shows its technical features.

The dynamic and kinematic systems are part of an integrated system; the inertial system is a stand-alone.

*Table 14 Data sheet of the kinematic system*

Technical feature	Kinematic system
Sensor resolution	2048×1088 pixel
Acquisition frequency at maximum resolution	340 fps
Maximum acquisition frequency	2000 fps
Accuracy	<0.1mm on a volume 4000×3000×3000 mm
Strobe LED wavelength	850nm
Number of markers detected simultaneously	Unlimited
Data transmission technology	gigabit Ethernet
Passive and retro reflecting markers	∅ from 3 to 20 mm

#### **4.1.3 Experimental Protocol**

Participants came to the laboratory in one day. The whole experiment consisted of fifteen sessions. Each participant performed fifteen test-runs, one test-run in each session. The test-run order of each session was randomized. Therefore, they performed a total sixty test-runs.

After an initial briefing, the test leader collected race-walkers anthropometric data and personal details. The test leader continued with the calibration process of measurement systems. The inertial system has an auto-calibration process when activated. On the other hand, the calibration process of kinematic and dynamic systems included three operations: 1) setting the reference system of the laboratory; 2) marking the control volume; and 3) defining the position of force platforms in the control volume. At the end of the calibration

process, the control volume was equal to  $9.2 \times 2.4 \times 2.6$  m (*i.e.* X×Y×Z directions) with a mean error of 0.251 mm.

For each participant the inertial sensor was placed at the bottom of the vertebral column on the L5/S1 inter-vertebral space. In order to acquire roughly the CoM position with the kinematic system, a reflective marker was exactly fixed on the middle of the inertial sensor.

Race-walkers performed a warm-up of fifteen minutes before the first experimental session. At the beginning of each test-run, they took a straight static position in order to easily make the correction offset. Right after, they completed a squat-jump, which is an exercise where athletes engage in a rapid eccentric contraction and forcefully jumps off the floor at the top of the range of motion. This exercise is used to mark a common event in order to make the sync with reliable stand-alone systems, *i.e.* the system not integrated as the inertial system in this case. Then, participants race-walked (a sequence of steps, *i.e.* the target task) into the control volume over force platforms. They executed all test-runs in the morning. Figure 35 shows the laboratory set-up and Figure 36 shows highlights of a race-walking test.

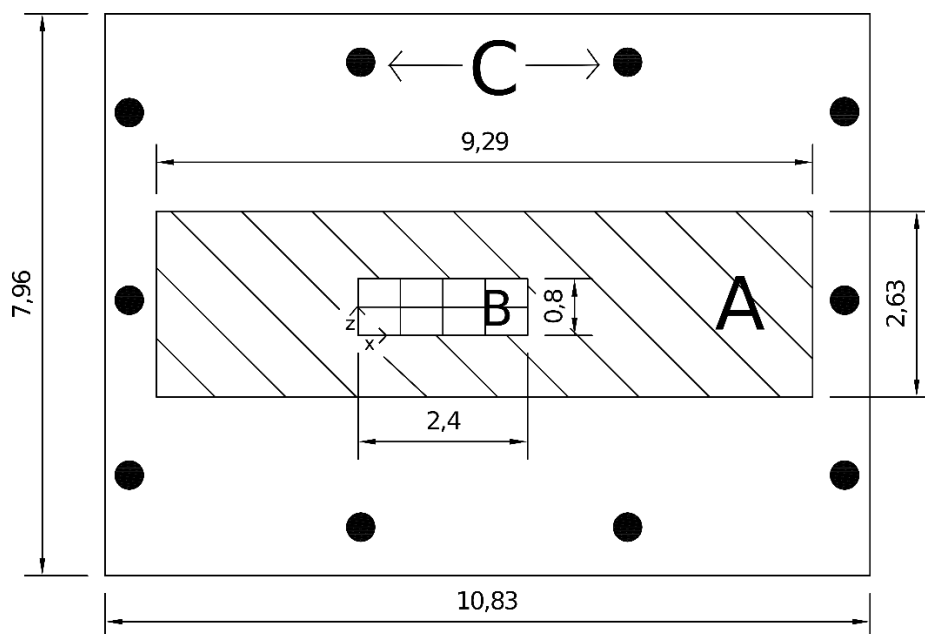


Figure 35 The experimental setting of the ErgoS Lab: the A zone shows the control volume, the B zone shows eight integrated platforms of force, and the capital letter C indicates the ten infrared digital cameras. The bottom left corner of the B zone matches with the origin of the reference system. The x and z axes show the anteroposterior direction and the medio-lateral direction, respectively; and the y axis (not visible since leaving the plane) indicates the vertical direction. All distance are expressed in meters.



Figure 36 Main phases of a race-walking cycle during a laboratory test

#### 4.1.4 Data analysis

After the LOGC timing assessment and binary step classification (described in sections 3.1 and 3.2.1), some events, as defined below, were evaluated in order to create a two-way contingency table in which columns represent the predicted conditions (see Figure 34, Predicted LOGC) and rows the true ones (see Figure 34, True LOGC):

TP, true positive (actual legal steps which were correctly classified as legal steps);

FP, false positive (illegal steps which were incorrectly labelled as legal steps);

FN, false negative (legal steps which were incorrectly marked as illegal steps);

TN, true negative (all remaining steps, correctly classified as not-illegal steps).

Based on these events some classification metrics were derived (Fawcett, 2006) (Powers, 2011):

Sensitivity (or True Positive rate, TPR) is the proportion of real legal cases which were correctly predicted as legal:  $TPR = \frac{\sum True\ positive}{\sum Condition\ positive}$

Miss rate (or False negative rate, FNR) is the proportion of real legal cases which were predicted as illegal:  $FNR = \frac{\sum False\ negative}{\sum Condition\ positive}$

Fall-out (or False Positive rate, FPR) is the proportion of real illegal cases which occur as predicted legal:  $FPR = \frac{\sum False\ positive}{\sum Condition\ negative}$

Specificity (or True Negative rate, TNR) is the proportion of real illegal cases which were correctly predicted as illegal:  $TNR = \frac{\sum True\ negative}{\sum Condition\ negative}$

Precision (or Positive Predicted Value, PPV) is the proportion of predicted legal cases which were correctly real legal cases:  $Precision = \frac{\sum True\ positive}{\sum Predicted\ positive}$

Negative predict value (NPV) is the proportion of predicted illegal cases which were real illegal indeed (inverse precision):  $NPV = \frac{\sum True\ negative}{\sum Predicted\ negative}$

Accuracy is the proportion of true results (both true positives and true negatives) among the total number of the considered cases:  $Accuracy = \frac{\sum True\ positive + \sum True\ negative}{\sum Total\ cases}$

The results were also compared with other two approaches for evaluating the LOGC (Lee, 2013) (Wixted, 2010). Finally, the so-called Receiver Operating Characteristics (ROC) graphs (Fawcett, 2006) (Powers, 2011) were used to help the decision about the best classification approach.

#### 4.1.5 Results and discussion

Participants completed a total of sixty-five steps. Table 15 shows descriptive statistics of LOGC data for two measuring systems: dynamic and inertial. The first system registered sixty-five flight phases, which were all identified by the second one. The inertial system estimated a mean predicted LOGC equal to 35 ms that is 5 ms lower than the true LOGC estimated by using the dynamic system. The standard deviation (SD) of the predicted LOGC is equal to 20 ms and is greater than the SD estimated by using the dynamic system.

Table 15 Descriptive statistics for LOGC data stratified for measuring system [ms]

System	Variable	Mean	SD	Min	Max
Dynamic	True LOGC	40	14	10	78
Inertial	Predicted LOGC	35	20	5	70

According to the LOGC timing assessment and binary step classification (described in section 3.1 and 3.2.1) twenty-seven legal steps and fourteen illegal steps were correctly classified. According to Lee *et al.* (Lee, 2013) twenty-nine legal steps and ten illegal steps are correctly classified. Finally, according to Wixted’s approach (Wixted, 2010) (that assume the LOGC as the period between the alignment of the vertical acceleration zero-crossing going negative (*i.e.* toe-off) and the alignment of the anterior–posterior braking spike (*i.e.* heel strike)) thirty-three legal steps and one illegal step were correctly classified (see Table 16).

Table 16 Steps classification according to three different methods for LOGC evaluation

		Predicted classification			
		Legal	Illegal	Sum	
A – (Di Gironimo G. C., 2017)	Legal	27	6	33	True classification
	Illegal	18	14	32	
	Sum	45	20	65	
B – (Lee, 2013)	Legal	29	4	33	True classification
	Illegal	22	10	32	
	Sum	51	14	65	
C – (Wixted, 2010)	Legal	33	0	33	True classification
	Illegal	31	1	32	
	Sum	64	1	65	
D – Ideal approach	Legal	33	0	33	True classification
	Illegal	0	32	32	
	Sum	33	32	65	

Table 17 shows the values of classification metrics (as described in section 4.1.4) based on the data summarised in Table 16.

Table 17 Comparison of classification metrics

Classification metrics	Target	A – (Di Gironimo G. C., 2017)	B – (Lee, 2013)	C – (Wixted, 2010)
Sensitivity (TPR)	100%	82%	88%	100%
Miss rate (FNR)	0%	18%	12%	0%
Fall-out (FPR)	<u>0%</u>	56%	69%	97%
Specificity (TNR)	<u>100%</u>	44%	31%	3%
Precision (PPV)	<u>100%</u>	60%	57%	52%
Negative predict value (NPV)	100%	70%	71%	100%
Accuracy	<u>100%</u>	63%	60%	52%

The proposed A approach (Di Gironimo G. C., 2017), shows the highest value of accuracy and it is the index that takes into account all the right diagnosis the system performs. The Wixted *et al.* approach (Wixted, 2010) shows the maximum performances in terms of true positive ratio (TPR) and false negative ratio (FNR), but it has the worst performance in terms of false positive ratio (FPR) and true negative ratio (TNR). As in the hypothesis testing the so-called error of the second type is really important in the decisional process. In the race-walking case, the possibility to assign undue yellow cards or, at the end after three times, a red card, penalizing an athlete by mistake, is really not acceptable and the relative chance has to be minimised. Even if the proposed approach has the worst performance in terms of TPR and FNR it allows to significantly improve the FPR and the TNR. In this way this approach better fits the needs of potential users. In order to confirm the effectiveness of these hypotheses, interviews for eliciting the experts opinion are performed. Eight race-walking experts (athletes, coaches and judges) with an average of fifteen years practice, answered the interviews. In this study, the accuracy of results is the most important factor. The second important index is the NPV which guarantees the quality of the system in evaluating illegal steps. The ranking continues with the miss rate, the fall-out and the specificity. The

proposed approach offers the best value for the Accuracy, the fall-out and the specificity and worst value for the negative predict value (NPV).

Figure 37 shows a ROC graph with three classifiers labelled from A to C which represent the three previously introduced approaches. This graph is a two-dimensional graph which is useful to visualize the classifiers performance (Fawcett, 2006), in which the FPR is plotted on the *X-axis* and the TPR on the *Y-axis*. Each classifier produces a (FPR, TPR) pair corresponding to a single point in the ROC space. It is worth noting some important points in the ROC space:

- The (0,0) lower left point represents the strategy of never issuing a positive classification; such a classifier commits no false positive errors but also gains no true positives.
- The (1,1) upper right point represents the opposite strategy, that of unconditionally issuing positive classifications.
- The (0, 1) point indicates perfect classification.

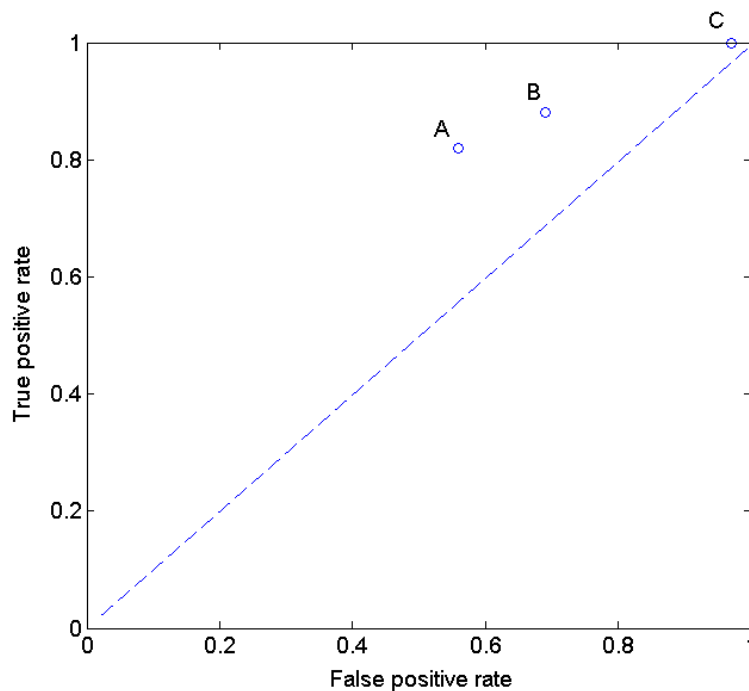


Figure 37 A basic ROC graph showing three classifiers

One point in the ROC space is better than another if it is to the northwest (TPR is higher, FPR is lower, or both) of the first point. All points represent good classification results since they are above the diagonal. The A classifier is the most northwest. A and B classifiers make fewer false positive error than C, but they have a lower true positive rate as well. The C method classifies all positives correctly, but it has a high false positive rate. Its performances are similar to the completely random guess that would give a point along the diagonal line in Figure 37 (the so-called line of no-discrimination). Wrong judgement could dominate the race-walking world (Knicker, 1990), therefore the performance of the A method becomes very interesting.

Fiinally, it was found that the maximum value of accuracy was obtained by choosing a threshold equal to 25 ms (Figure 38) which was the one which had been assumed. In Figure 38 it was noted that the increase in the threshold over 25 ms causes a rapid worsening of the accuracy.

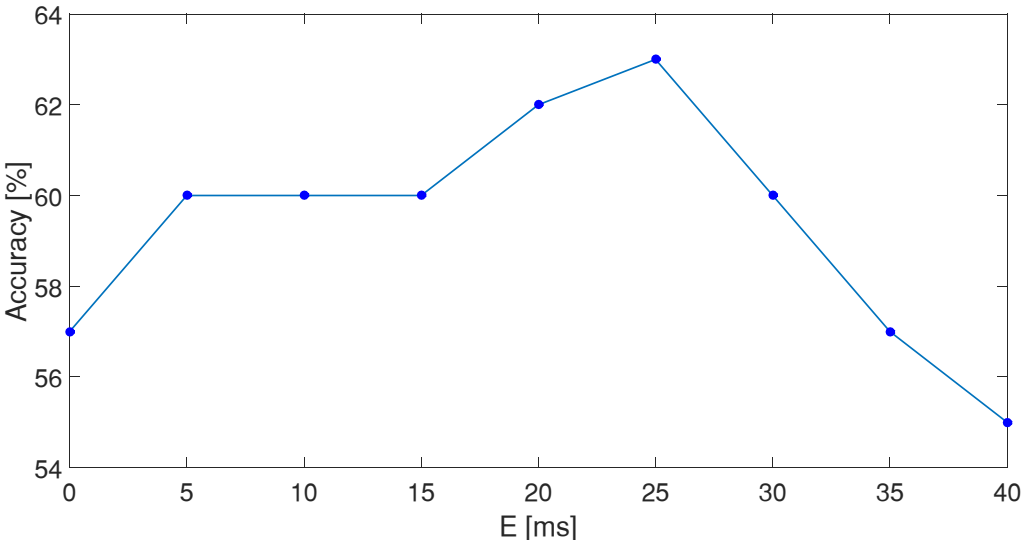


Figure 38 The variation of the accuracy in function of the E (toe-off threshold)

## 4.2 Field test

The aim of this experimental investigation was to evaluate the LOGC with the inertial system on paved road (in typical training and race conditions). This type of tests allowed to evaluate the system: (i) for a long sequence of steps; (ii) at different speeds close to race pace of the athlete. An e-bicycle was equipped with a high-speed camera. It allowed a precise visual assessment of the LOGC and represents the ground truth for this type of test. In addition, a video recorded by webcam synchronized with inertial data allowed to compare inertial and high-speed camera data. The first part of the field experimental tests was performed by an elite Italian race-walker. He carried out road field race-walking tests at four different speed near the department of Sports Equipment and Technology, TU Chemnitz. This phase permitted to find for race-walking field tests, using a high-speed camera, a correlation for the assessment of  $E_p$  (see section 3.1.1). Then, the whole experimental protocol on the field tests was performed by nine elite race-walkers. It aimed to evaluate the correlation for the assessment of  $E_p$  (advanced model) in comparison between the previous model ( $E=30ms$ ) using the step binary classification, the step classification on three level (see section 3.2.1 and 3.2.2) and the fuzzy approach (see section 3.2.3), through the statistical analysis. In addition, this phase allowed to evaluate the efficiency of the customized strategy for elite race-walkers described in the section 3.3. The full methodological approach is summarized in Figure 39.

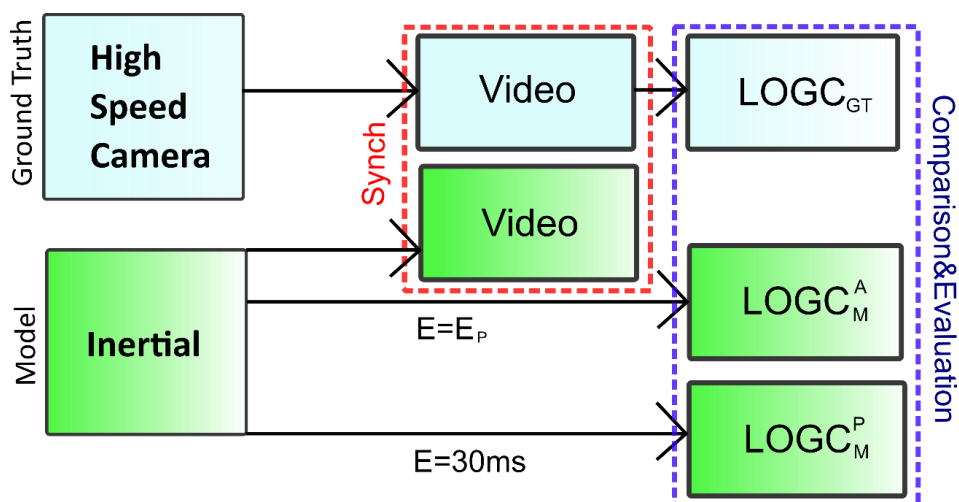


Figure 39 Flow chart methodological approach field test

## 4.2.1 Field test: EP assessment

### 4.2.1.1 Experimental set-up

An athlete of Italian national team performed field race-walking tests. LOGC values were estimated by using an inertial system (i.e. the model type G-Sensor2, BTS) set at sampling frequency of 200Hz,  $\pm 8g$  for the tri-axis accelerometer,  $\pm 300gps$  for the tri-axis gyroscope sensor, and  $\pm 6$  Gauss for the tri-axis magnetic sensor. The sensor was located at the bottom of athlete vertebral column in correspondence of the L5–S1 inter-vertebral space. Acquired data were transmitted via Bluetooth to a laptop mounted on an electrical bicycle that accompanied the athlete during the test. It was provided with a motor system including a torque sensor that permits to obtain instant seamless power without noise, to follow the athlete at constant speed.

The e-bicycle (see Figure 40) was also equipped with a high-speed camera (i.e. the model type GoPro Black Hero4, Woodman Lab.) operating at 240fps with a resolution of 848x480 in 16:9, fixed on rear dropout and controlled remotely via wireless connection with a mobile device (i.e. the tablet, Samsung Galaxy Note 2014 Edition) positioned on the handlebars.

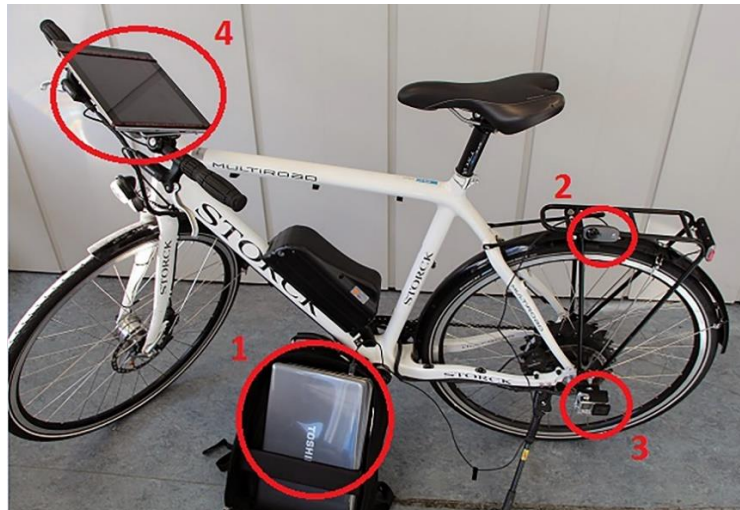


Figure 40 Data collection setting: 1) the laptop with software for acquisition of inertial data and the USB Bluetooth; 2) the webcam; 3) the high-speed camera; 4) the tablet

The high-speed camera video of the athlete's performance allowed to evaluate a precise visual assessment of the LOGC. Finally, a webcam (i.e. the model type HD C310, Logitech

International S.A, resolution of 320x240 at 30 Hz) was connected with the laptop and fixed on the e-bike carrier (with the optical axes parallel to the one of the high-speed-camera) in order to obtain a video of the race-walking, synchronized with the inertial system data. The race-walker was also equipped with a GPS watch (i.e. the model type Forerunner 305, Garmin) with heart rate monitoring.

#### **4.2.1.2 Experimental protocol**

Tests were performed near the Chemnitz University of Technology campus on a long paved road, straight and flat in according to recommendations of the IAAF about race-walking courses (IAAF, 2014). After a standard twenty minutes warm-up routine, the athlete performed four tests of three-hundred meters race-walking each, at four different speeds (i.e. mean values of 12.0, 12.9, 13.7, 14.6 km/h representing, respectively, the 93%, 100%, 106% and 113% of the athlete's racing pace (RP)). By means of the GPS watch, the athlete controlled the performance and tried to keep a mostly constant speed during the test. A rest time of 90s between two consecutive tests allowed the athlete to recover completely. It was controlled that the athlete's heart rate before each test was less than 60% of his theoretical maximum heart rate (Benson, 2011). At the beginning of each test, the athlete kept an orthostatic position in order to calculate the offset error of the inertial sensor. The Figure 41 shows highlights of the race-walking technique during tests.



*Figure 41 Main phases of a race-walking cycle during a field test*

#### 4.2.1.3 Results and discussion

The LOGC assessment firstly was carried out with the threshold value  $E=30$  ms (named previous model, superscript P). From high-speed camera data, LOGC was evaluated through video analysis tools (i.e. Kinovea© software, by Joan Charmant&Contrib.) as the time difference between the frame of the toe-off event and the following frame at the heel-strike event. The comparison between the webcam and the high-speed camera data allowed associating LOGC of the inertial sensor with the correspondenting LOGC event on the high-speed camera video. A total amount of 720 athlete's steps were evaluated. For each race-walking test and excluding the initial acceleration phase of the athlete (10s), 180 consecutive steps were considered. For each step, the LOGC value was evaluated both by the inertial sensor (named  $LOGC_M^P$ ) and by the high-speed camera (named  $LOGC_{GT}$ ). In the last column, there is the mean difference between  $LOGC_M^P$  and  $LOGC_{GT}$  with standard deviation (see Table 18).

Table 18 LOGC data collected during trials with inertial system (previous model) and ground truth

RP (%)	Cases of $LOGC_M^P$	$LOGC_M^P$ (ms)	Cases of $LOGC_{GT}$	$LOGC_{GT}$ (ms)	Mean difference (ms)
93	180	35±10	179	17±8	20±10
100	176	40±10	180	29±8	10±15
106	180	45±15	180	37±8	10±15
113	178	45±15	180	41±8	5±20

Of 720 steps analysed by the camera, 719 steps were characterized by a LOGC event. Only one-step had a double support. The inertial system allowed to identify correctly the 99% of LOGC events, with seven errors (i.e. six LOGC classified as double support and one double support classified as LOGC). Both  $LOGC_M^P$  and  $LOGC_{GT}$  duration were directly proportional to the test speed. This correlation is consistent with the literature (DeAngelis M., 1992). The mean difference in the previous method appears to decrease when RP increases: it takes the highest value to the lowest speed (i.e. 20ms at RP of 93%); then, it takes the lowest value to

the highest speed (i.e. 5ms at RP of 113%). This result may be due to the threshold value expressed as a variable depending on the speed. However, starting from the previous biomechanical research, a new threshold evaluation was carried out. Hanley et al. studies (Hanley B. B., 2011), pooling together data from 11 different studies, show a linear descriptive equation between the Step Cadence (SC) and the race-walking speed. This means that velocity and SC are correlated. So, we carried out a regression models (quadratic without constant) between the Optimal Threshold (OT) time for each step ( $E_{new}$  that allows to have the time difference between  $LOGC_M^P$  and  $LOGC_{GT}$  equal to 0) and the corresponding SC. Starting from the experimental data, we excluded for the evaluation data that were clearly wrong: (i) outside the normal range of step cadence ( $SC < 2.8$  step/s and  $SC > 3.8$  step/s); with  $OT < 0$  (because the toe off event is sure after the bottom of vertical acceleration). In this way, 8 steps are excluded from the regression analysis (as shown in Figure 42). According to the methodology shown in section 3.1 we choose the quadratic model without constant correlation that performed the best statistical index (see Table 19).

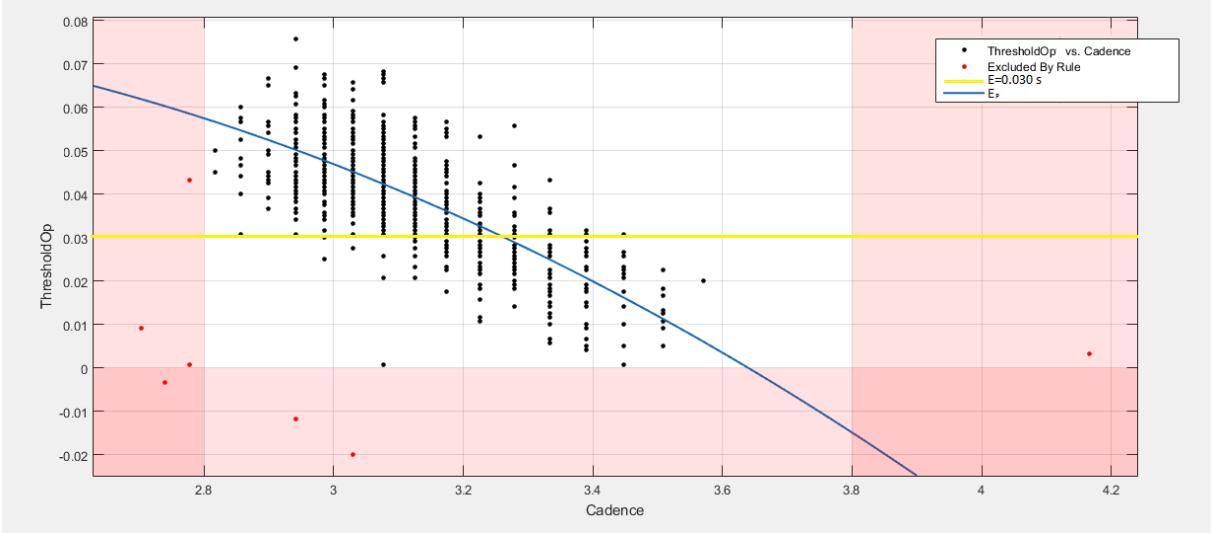


Figure 42 Scatter plot of Optimal Threshold vs cadence Step ( in red the area excled by analysis)

So, the parameters  $a$  and  $b$  were fixed respectively equal to  $-40.921$  and  $11.242$ . The quality of regression equation in comparison with the fixed value of  $E$  is shown in Figure 42. For the last one the regression analysis shows a negative value that underlines how the fit is poor. Instead, the quality of regression analysis for the quadratic (on the mean value) was ensured by R-Squared over 95% (see Table 19) and the normality of residual plot (see Figure 43).

Table 19 Summary parameters of the model

Model	R-squared	R-squared adj	S
Quadratic	95,55%	95,53%	0,0086554

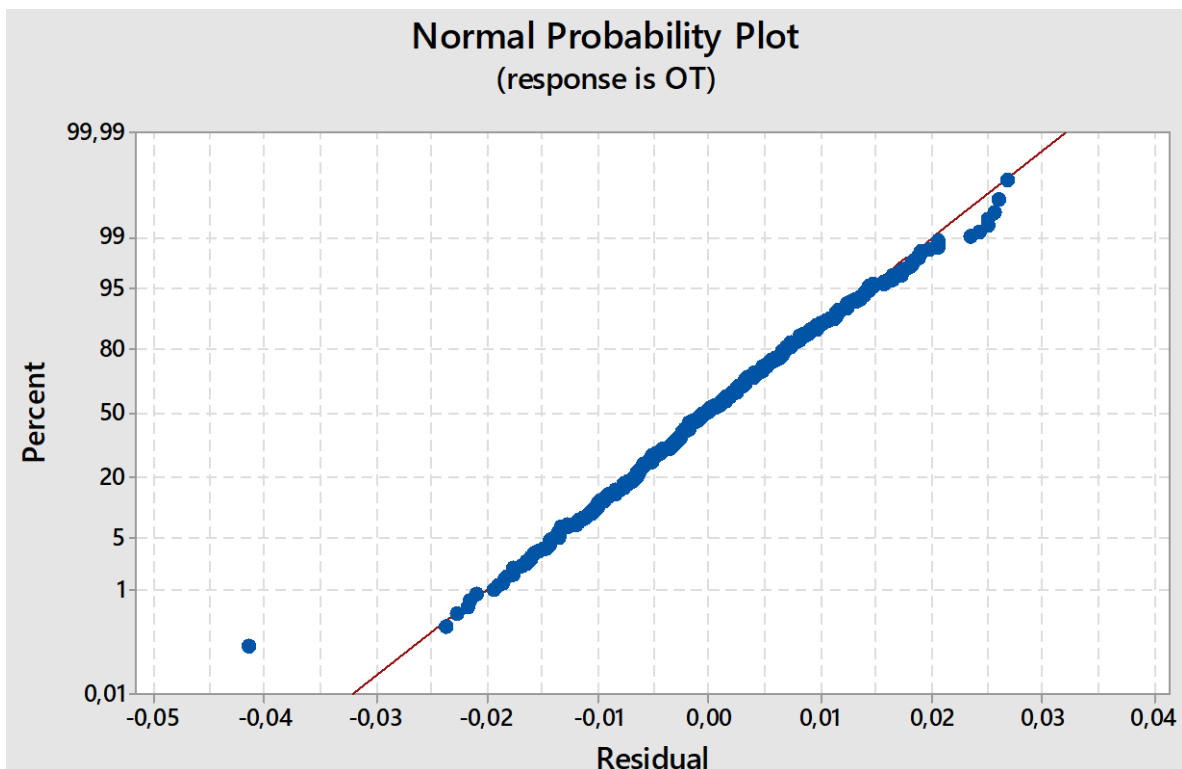


Figure 43 Normal probability plot of residuals (response OT)

Then, according to the (eq. 6) with threshold value  $E_P$  (named advanced model, superscript A), the LOGC value was reevaluated both by the inertial sensor (named  $LOGC_M^A$ ) and by the high-speed camera (named  $LOGC_{GT}$ ). Table 20 shows the total number of cases, mean values with standard deviations of  $LOGC_M^A$  stratified for four different test RP. At the same way of the previous model, the inertial system with the advanced model allowed identifying correctly the 99% of LOGC events, with eight errors (i.e. seven LOGC classified as double support and one double support classified as LOGC).

Table 20 LOGC inertial assessment with the advanced model.

RP (%)	Cases of LOGC <sub>M</sub> <sup>A</sup>	LOGC <sub>M</sub> <sup>A</sup> (ms)	Mean difference (ms)
93	180	20±10	0±10
100	175	25±10	-5±10
106	180	35±10	0±10
113	178	45±10	0±10

Also LOGC<sub>M</sub><sup>P</sup> duration was directly proportional to the test speed. In addition, the advanced model for the assessment of threshold reduced the mean (that became close to 0 for all RP) and standard deviation values of MD. This means that the proposed method leads to a LOGC value closer to the exact one.

## 4.2.2 Field test: experiments with elite athletes

### 4.2.2.1 Participants

Nine world-class Olympic race-walkers, seven males (three specialized on 20 km and four on 50 km) and two females (specialized on 20 km) from Italy, Germany and Czech Republic agreed to participate in this study. All race-walkers were member of their national team; seven possessed the World Championship Entry Standard for London 2017 (1:24:00 in 20 km man, 4:06:00 in 50 km for men and 1:36:00 in 20 km female). The participants had not suffered severe injuries in the last twelve months before the testing day. The race-walkers were informed about all tests and possible risks involved and provided written informed consent (in accordance with the Etic Committee of the University of Naples Federico II) before testing. After an initial briefing, the test leader collected the informed consent from volunteers as well as their personal details (i.e. personal best on 20 km, age and experience) and anthropometric characteristics (i.e. stature). Table 21 shows their main all data recorded with mean and standard deviation (SD).

Table 21 Mean and standard deviation related to their personal best, age, stature and experience of race-walkers

	PB (km/h)	Age (year)	Stature (cm)	Experience (year)
Mean	13,73	26,2	175,4	12,6
SD	0,70	4,1	6,3	4,7

In order to obtain a specific description of the participants' experimental phase, their percentiles in relationship with the variable stature height were carried out. For this aim, we screened the reference male and female elite race-walkers populations for normality of distribution using the Anderson-Darling normality test (Newell, 2014). We derived the two world-class Olympic race-walkers reference population (male and female), starting from personal cards data of 140 male (mean 176,6 cm, standard deviation 7,5 cm, AD=0.369 and p=0.422) and 72 female (mean 163,1 cm, standard deviation 6,2 cm, AD=0.478 and p=0.229) Olympic race-walkers in Rio de Janeiro<sup>1</sup>. The analysis underlined how the participants of our research studies were representative of the reference population. Indeed, they cover a large range from 8<sup>th</sup> to 97<sup>th</sup> percentile (in detail: 8<sup>th</sup> M, 19<sup>th</sup> M, 27<sup>th</sup> M, 30<sup>th</sup> M, 57<sup>th</sup> M, 63<sup>th</sup> M, 68<sup>th</sup> M, 92<sup>th</sup>F, 97<sup>th</sup> F). The sample size was also in agreement with previous studies to give an acceptable robustness to the study. Indeed, the analysis of the review on biomechanical studies in race-walking in the last five-year (see section 1.4) underlines how over 33% of the studies present a number of participants smaller than 9.

#### 4.2.2.2 Experimental protocol

The experimental setting was the same of the first filed test. So, data were collected using the same inertial system (i.e. the model type G-Sensor2, BTS) set at SF of 200Hz (1/5ms), ±8g for the tri-axis accelerometer, ±300gps for the tri-axis gyroscope sensor, and ±6 Gauss for the tri-axis magnetic sensor. The sensor was located at the bottom of athlete vertebral column in correspondence of the L5–S1 inter-vertebral space. Trials were performed on a

<sup>1</sup> <https://www.sports-reference.com/olympics/athletes>

long-paved road, which is straight and flat in according to the IAAF recommendations about race-walking courses (IAAF, 2014).

After a standard self-selected warm up of 20 minutes (including mobility exercise) the athletes performed 4 trials of three hundred meters race-walking each, at different incremental mean velocities (from 12.0 km/h to 14.5 km/h). These velocities were chosen in order to guarantee the covering for each race-walker approximal a range from the 93%, to 100% of the athlete's racing pace on 20 km evaluated respect the best results of the athlete in the last two seasons. For the velocities between 12.0 km/h to 14.0 km the velocity incremental gain was fixed equal to 1.0 km/h then it became 0.5km/h. Tests with a difference over  $\pm 0.2$  km/h (for the velocity from 12.0km/h to 14.0km/h) and over  $\pm 0.1$  km/h (for the velocity from 14.5 km/h) were excluded from the evaluation. In order to collect data even in the range of high velocity the three specialists on 20 km performed one (1 athlete) or two (2 athletes) additional test at 15.0 km/h ( $\pm 0.1$  km/h) and 15.5 km/h ( $\pm 0.2$  km/h). The test-run order of each athlete was randomized. By using the gps watch, the athlete controlled the performance and tried to keep a mostly constant speed during the test. A rest time of 90s was fixed between two consecutive trials and allowed the athlete to recover completely.

#### 4.2.2.3 Comparison and Evaluation: Data analysis

In order to evaluate the two models (advanced and previous) in relationship with the different types of step classification, we choose eight tests of two different athletes (two male one specialized on 20 km and one on 50 km) in order to quantify the performance of the different algorithms.

*Table 22 Planning of trials analyzed: the line in reds include the trial tests for the overview athletes' analysis; the column in blu the trials for the specific speed analysis.*

Athlete	Test Velocity [km/h]				
1	12.0	12.9	13.7	14.6	x
2	11.9	12.9	13.8	x	15.7

The trials were chosen in order to cover a full range of velocity of an elite race-walker (from 11.9 km to 15.6 km/h). For two athletes we choose four different speeds in order to obtain a good overview of the accuracy of the algorithms in relationship to athlete's range of velocities. The summary of the test analysis is shown in Table 22.

Afterwards the LOGC timing assessment for both value of threshold (previous and advanced model) all steps were firstly classified as 'legal' or 'illegal' according to the binary step classification (section 3.2.1) and the contingency table was carried out for each trial. Assuming as true the classification based on the high-speed camera results, the false alarm rate, the miss alarm rate, the accuracy, the true positive rate and the false positive rate were obtained. Starting from TPR and FPR value, the ROC graphs (Fawcett, 2006) (Powers, 2011) were used to help the comparison between the different algorithm for LOGC timing assessment.

Then the steps were classified through three level multi-class confusion matrices (see section 3.2.2) and by the fuzzy approach (see section 3.2.3). For the three-level classification,  $LOGC_{GT}$  results having a minimum value  $LOGC_{GT,min}$  and a maximum value  $LOGC_{GT,max}$  defined as:

$$LOGC_{GT,max} = \frac{1}{FR} * (FN_D - FN_A) \text{ (eq. 29)}$$

where  $FN_A$  is the frame number of the last frame of contact with the ground (Figure 44.a),  $FN_D$  is the frame number of the first frame with the contact ground (Figure 44.d); and

$$LOGC_{GT,min} = \frac{1}{FR} * (FN_C - FN_B) = LOGC_{GT,max} - 2 * \frac{1}{FR} \text{ (eq. 30)}$$

where  $FN_B$  is the frame number of the frame following the last contact with the ground (Figure 44.b),  $FN_C$  is the frame number of the last frame before the contact with the ground (Figure 44.c).

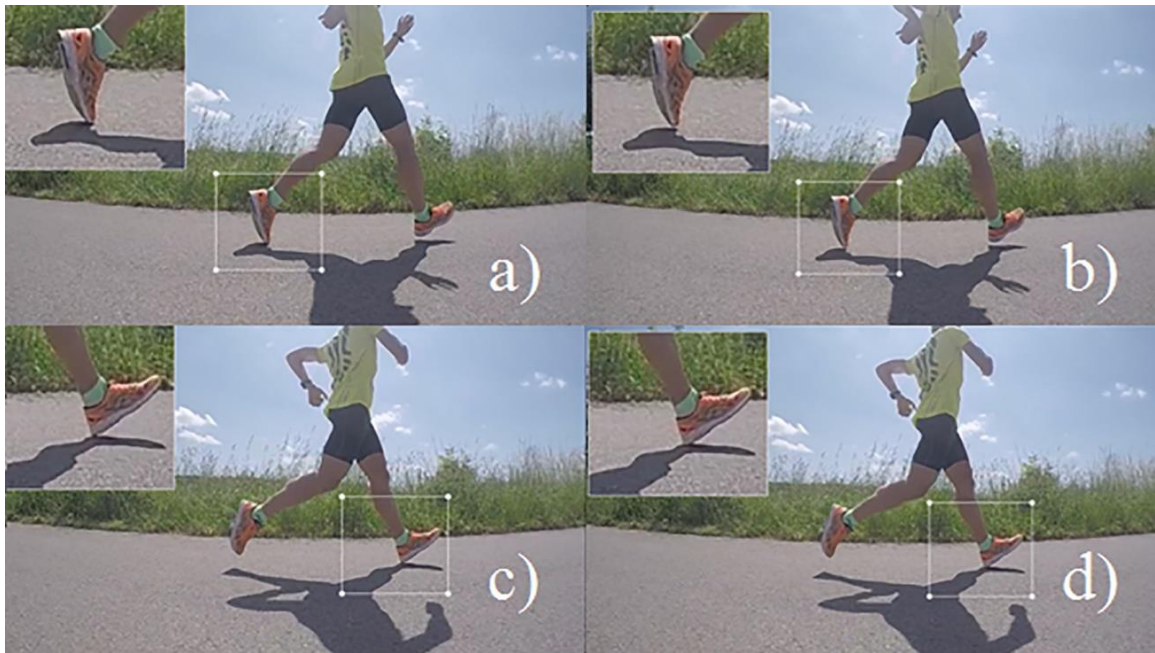


Figure 44 Two photo sequences with magnifying glass focus around the left foot (near the TOE) and right foot (near the HSE): a) Last image with visible ground contact of left foot; b) First image without last visible ground contact of left foot; c) Last image without visible ground contact of right foot; d) First image with visible ground contact of right foot.

In Figure 45 the comparison between the three levels classification by the inertial system and the high-speed camera is shown.

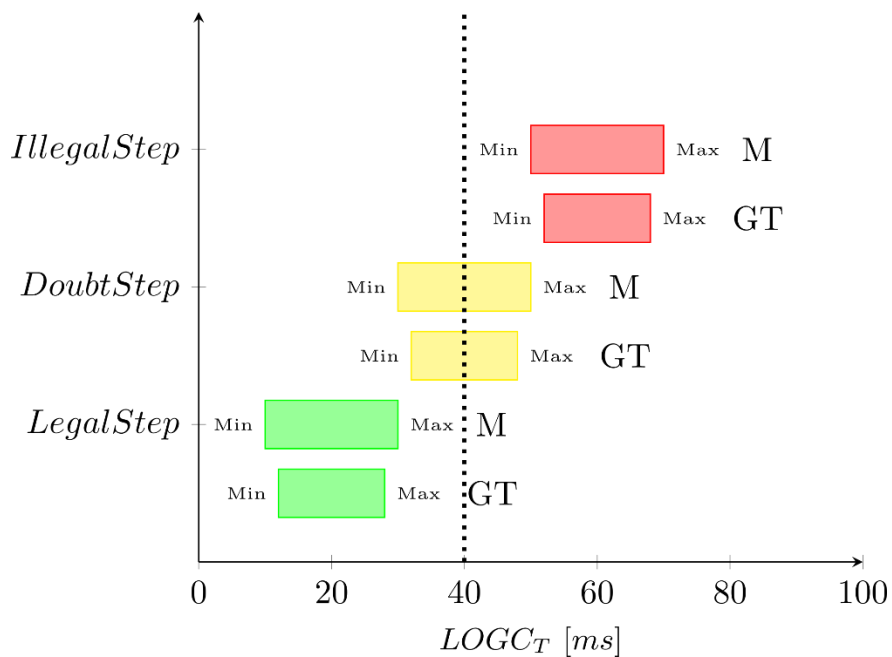


Figure 45 Comparison between the two classifications (M: represent the inertial system; GT: the high speed camera system) on three levels. The vertical dotted line represents the limit of human eyes (40 ms).

On this basis, two three multi-class confusion matrices were carried out and statistical indices as accuracy, TPR and positive PPV were evaluated for legal, illegal and doubt steps. Starting from TPR and PPV values, they were plotted on the Precision-Recall curve and Area Under the Curve (AUC) was calculated.

For the fuzzy classification, we called  $\rho$  ( $\text{LOGC}_{\text{GT}}$ ) the membership function for the fuzzy set  $\text{LOGC}_{\text{GT}}$ . The following equation system (eq. 31) described the curves.

$$\lambda(\text{LOGC}_{\text{GT}}) = \begin{cases} \lambda = 1, & \text{LOGC}_{\text{GT}} \geq 50 \text{ ms} \\ 0 < \lambda < 1, & 38 \text{ ms} > \text{LOGC}_{\text{GT}} > 50 \text{ ms} \\ \lambda = 0, & \text{LOGC}_{\text{GT}} \leq 33 \text{ ms} \end{cases} \quad (\text{eq.31})$$

Figure 46 illustrates the membership functions compared with the previous binary classification method.

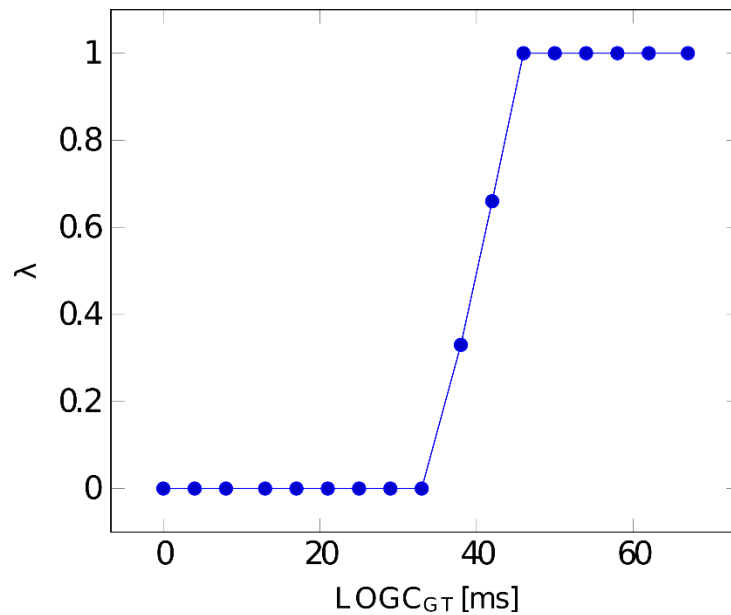


Figure 46 Membership functions for the video ground truth system

Finally, we defined  $\sigma$  equal to the difference between  $\eta$  (see section 3.2.3) and  $\lambda$ . This parameter allowed to quantify the distance between the two systems (inertial model and ground truth). The following criterion (eq.32) was used for declaring a correct identification of the step:

$$\begin{cases} -0.5 < \sigma < 0.5 & \text{Accetable Classification} \\ -0.5 < \sigma, \sigma > 0.5 & \text{Not Accetable Classification} \end{cases} \quad (\text{eq.32})$$

#### 4.2.2.3.1 Binary step classification: Results and Discussion

##### Athlete 1

We started with the test data of the first athlete (see Table 18), for the previous model the contingency table was carried out for each trial and reported in Table 23.

*Table 23 Steps' classification according to contingency table for the trials at 12.0 km/h, 12.9 km/h, 13.7 km/h and 14.6 km/h (previous model)*

12 km/h	Legal inertial system	Illegal inertial system	Sum
Legal high-speed camera	155	25	180
Illegal high-speed camera	0	0	0
Sum	155	25	180
12.9 km/h			
Legal high-speed camera	131	43	174
Illegal high-speed camera	2	4	6
Sum	133	47	180
13.7 km/h			
Legal high-speed camera	78	69	147
Illegal high-speed camera	13	20	33
Sum	91	89	180
14.6 km/h			
Legal high-speed camera	34	39	73
Illegal high-speed camera	57	50	107
Sum	91	89	180

At the same way, starting from data of Table 19, for the advanced model the contingency table was carried out for each trial (Table 24).

Table 24 Steps' classification according to contingency table for the trials at 12.0 km/h, 12.9 km/h, 13.7 km/h and 14.6 km/h (adavanced model)

12.0 km/h	Legal inertial system	Illegal inertial system	Sum
Legal high-speed camera	170	10	180
Illegal high-speed camera	0	0	0
Sum	170	10	180

12.9 km/h	Legal inertial system	Illegal inertial system	Sum
Legal high-speed camera	168	6	174
Illegal high-speed camera	4	2	6
Sum	172	8	180

13.7 km/h	Legal inertial system	Illegal inertial system	Sum
Legal high-speed camera	127	20	147
Illegal high-speed camera	18	15	33
Sum	145	35	180

14.6 km/h	Legal inertial system	Illegal inertial system	Sum
Legal high-speed camera	25	48	73
Illegal high-speed camera	44	63	107
Sum	69	111	180

Starting from the data in Table 23 and Table 24, assuming as “true” the high-speed camera classification the false alarm rate, the miss alarm rate, TPR, FPR and the accuracy were obtained (Table 25).

Table 25 Statistics for the two models at different velocities (best values are underlined in each column).

	12.0 km/h	12.0 km/h	12.9 km/h	12.9 km/h	13.7 km/h	13.7 km/h	14.6 km/h	14.6 km/h
	P	A	P	A	P	A	P	A
False Alarm	14%	<u>6%</u>	25%	<u>3%</u>	47%	<u>14%</u>	<u>56%</u>	66%
Miss Alarm	0%	0%	<u>33%</u>	67%	<u>39%</u>	55%	55%	<u>41%</u>
TPR	86%	<u>94%</u>	75%	<u>96%</u>	53%	<u>86%</u>	<u>44%</u>	34%
FPR	n.d.	n.d.	<u>33%</u>	67%	<u>36%</u>	54%	55%	<u>41%</u>
Accuracy	86%	<u>94%</u>	75%	<u>94%</u>	55%	<u>79%</u>	44%	<u>49%</u>

The accuracy value still showed a decreasing trend with RP, but its value improved with the advanced model for each speed. In particular, Table 25 shows an increase between +5% (for 14.6 km/h) and 24% (for 13.7 km/h). Moreover, accuracy values provide a good classification of legal steps (accuracy equal to 94%). Furthermore, the false alarm value has the same response (a percentage of decrease between 8% and 33%, only for 14.6 km/h the index has worsened). Only the miss alarm overall has worsened (except for 14.6 km/h), in particular for RP=100%.

Table 26 Contingency table of step sequences based on previous (right) and advanced (left) model

	Legal <sub>M</sub> <sup>P</sup>	Illegal <sub>M</sub> <sup>P</sup>	Sum <sub>M</sub> <sup>P</sup>	Legal <sub>M</sub> <sup>A</sup>	Illegal <sub>M</sub> <sup>A</sup>	Sum <sub>M</sub> <sup>A</sup>
Legal <sub>GT</sub>	13	8	21	19	2	21
Illegal <sub>GT</sub>	0	3	3	0	3	3
Sum	13	11	24	19	5	24

Finally, according to the estimation of judge's field of view (see section 3.2.4) the step sequence classification was carried out. Table 26 shows the two contingency table based on the classification of the sequences; the correlated statistical indexes are shown in Table 27.

Table 27 Statistics for the two models in sequence step evaluation (best values are underlined in each column).

	Sequence Step P	Sequence Step A	$\Delta$
False Alarm	38%	<u>10%</u>	<u>-28%</u>
Miss Alarm	<u>0%</u>	<u>0%</u>	0%
TPR	62%	<u>90%</u>	+28%
FPR	<u>0%</u>	<u>0%</u>	0%
Accuracy	67%	<u>92%</u>	<u>+25%</u>

For the step sequence analysis (Table 27), the advanced model allows to achieve better performance indices for the accuracy (92% with an increasing of 25%) and the false alarm (from 38% to 10%). Finally, the pairs of points related with TPR and FPR values for the two model are plotted in the ROC space (see Figure 47). All points represent good classification results because they are above the diagonal. The letter A indicate the classifier of the advanced model. It is norther than P (previous model).

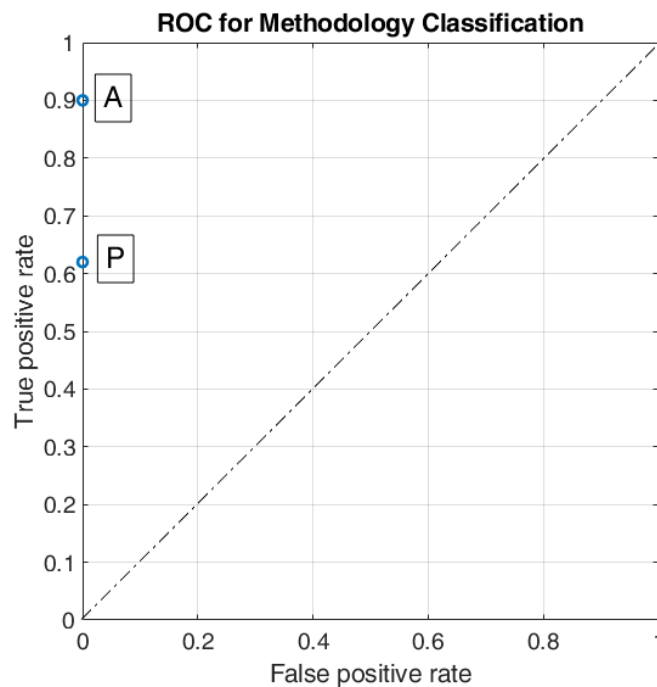


Figure 47 A basic ROC graph showing the two classifiers: (A) advanced, (P) previous

So, the classifier A has the best performance and it is close to the perfect classifier (coordinates: 0,1)

## Athlete 2

The advanced method was also evaluated with a second athlete. We choose four speed tests: 11.9 km, 12.9 km, and 13.8 Km/h (in order to verify the improvements and best performance of the advanced model with a different athlete at the same velocities) and 15.7 km/h in order to carried out an evaluation of the system at high speed. With the same experimental protocol, we collected 720 steps of the other athlete. The inertial system with the advanced model allowed to correctly identify the 98% of LOGC events, with twelve errors (i.e. eleven LOGC classified as double support and three double support classified as LOGC). Even the duration was directly proportional to the test speed. In addition, the advanced model for the assessment of threshold reduced the mean (that became close to 0 for all RP) and standard deviation values of MD (see Table 28). This means that the advanced model leads to a LOGC value closer to the exact one.

Table 28 LOGC data collected during trials of Athlete 2 with inertial system (advanced and previous model) and ground truth

Velocity [km/h]	Cases of LOGC <sub>M</sub> <sup>P</sup>	Cases of LOGC <sub>M</sub> <sup>A</sup>	LOGC <sub>M</sub> <sup>P</sup> (ms)	LOGC <sub>M</sub> <sup>A</sup> (ms)	Cases of LOGC <sub>GT</sub>	LOGC <sub>GT</sub> (ms)	MD <sup>P</sup> (ms)	MD <sup>A</sup> (ms)
11.9	180	169	30±10	15±10	177	17±8	15±10	0±10
12.9	180	180	50±10	40±10	180	29±8	15±10	10±10
13.8	180	180	50±5	45±10	180	37±8	15±10	10±10
15.7	180	180	55±5	65±10	180	50±8	5±10	15±5

LOGC<sub>M</sub><sup>P</sup>, LOGC<sub>M</sub><sup>A</sup> and LOGC<sub>GT</sub> durations were directly proportional to the test speed. In addition, the advanced model for the assessment of threshold shows in overall a little reduction of the mean and standard deviation values of MD, although these improvements are less evident than the athlete 1.

Then, we derived the step classifications for the previous model and the contingency table was carried out for each trial and reported in Table 29.

*Table 29 Steps' classification according to contingency table for the trials at 11.9 km/h, 12.9 km/h, 13.8 km/h and 15.7 km/h (previous models) – Athlete 2*

11.9 km/h	Legal inertial system	Illegal inertial system	Sum
Legal high-speed camera	173	7	180
Illegal high-speed camera	0	0	0
Sum	173	7	180
12.9 km/h			
Legal high-speed camera	50	105	155
Illegal high-speed camera	2	23	25
Sum	52	128	180
13.8 km/h			
Legal high-speed camera	12	92	104
Illegal high-speed camera	1	75	76
Sum	13	167	180
15.7 km/h			
Legal high-speed camera	0	11	11
Illegal high-speed camera	1	168	169
Sum	1	179	180

At the same way, for the advanced model the contingency table was carried out for each trial (see Table 30).

Table 30 Steps' classification according to contingency table for the trials at 11.9 km/h, 12.9 km/h, 13.8 km/h and 15.7 km/h (advanced model) – Athlete 2

11.9 km/h	Legal inertial system	Illegal inertial system	Sum
Legal high-speed camera	173	7	180
Illegal high-speed camera	0	0	0
Sum	173	7	180

12.9 km/h			
	Legal inertial system	Illegal inertial system	Sum
Legal high-speed camera	81	74	155
Illegal high-speed camera	12	13	25
Sum	93	87	180

13.8 km/h			
	Legal inertial system	Illegal inertial system	Sum
Legal high-speed camera	40	64	104
Illegal high-speed camera	6	70	76
Sum	46	134	180

15.7 km/h			
	Legal inertial system	Illegal inertial system	Sum
Legal high-speed camera	0	11	11
Illegal high-speed camera	1	168	169
Sum	1	179	180

Starting from the data in Table 29 and Table 30, statistical indices were obtained (Table 31). The accuracy still value shows a decreasing trend with velocities until 13.7 km/h. For the last velocity (15.7 km/h) its value increased. However, accuracy value confirmed an improvement with the advanced model for each speed. In particular, Table 31 shows an increase between +1% (for 15.7 km/h) and 13% (for 13.8 km/h).

Table 31 Statistics for the two models at different velocities (best values are underlined in each column) – Athlete 2

	11.9 km/h	11.9 km/h	12.9 km/h	12.9 km/h	13.8 km/h	13.8 km/h	15.7 km/h	15.7 km/h
	P	A	P	A	P	A	P	A
False Alarm	4%	<u>0%</u>	68%	<u>48%</u>	88%	<u>62%</u>	<u>100%</u>	<u>100%</u>
Miss Alarm	0%	n.d.	<u>8%</u>	48%	<u>1%</u>	8%	1%	<u>0%</u>
TPR	96%	<u>100%</u>	32%	<u>52%</u>	11%	<u>38%</u>	0%	<u>0%</u>
FPR	n.d.	n.d.	8%	<u>48%</u>	1%	<u>8%</u>	1%	<u>0%</u>
Accuracy	96%	<u>100%</u>	41%	<u>52%</u>	48%	<u>61%</u>	93%	<u>94%</u>

Furthermore, the false alarm value has the same response (a percentage of decrease between 4% and 26%). Only, the miss alarm overall is worsened (except for 11.9 km/h), in particular for 13.8 km/h.

Finally, according to the estimation of judge's field of view (see section 3.2.4) the step sequence classification was carried out. Table 32 shows the two contingency tables based on the classification of the sequences; the correlated statistical indexes are shown in Table 33.

Table 32 Contingency table of step sequences based on previous (right) and advanced (left) model – Athlete 2

	Legal <sub>M</sub> <sup>P</sup>	Illegal <sub>M</sub> <sup>P</sup>	Sum <sub>M</sub> <sup>P</sup>	Legal <sub>M</sub> <sup>A</sup>	Illegal <sub>M</sub> <sup>A</sup>	Sum <sub>M</sub> <sup>A</sup>
Legal <sub>GT</sub>	8	8	16	12	4	16
Illegal <sub>GT</sub>	0	8	8	1	7	8
Sum	8	16	24	13	11	18

For the step sequence analysis (Table 33), the advanced model allows to achieve better performance indices for the accuracy (79% with an increasing of 12%) and the false alarm (from 50% to 25%).

Table 33 Statistics for the two models in sequence step evaluation (best values are underlined in each column).

	Sequence Step P	Sequence Step A	$\Delta$
False Alarm	50%	<u>25%</u>	<u>-25%</u>
Miss Alarm	<u>0%</u>	<u>13%</u>	+13%
TPR	50%	<u>75%</u>	<u>+25%</u>
FPR	0%	<u>13%</u>	+13%
Accuracy	67%	<u>79%</u>	+12%

Finally, the pairs of points related with TPR and FPR value for the two model are plotted in the ROC space. All points represent good classification results because they are above the diagonal. The letter A indicate the classifier of the advanced model. It is norther than P (previous model).

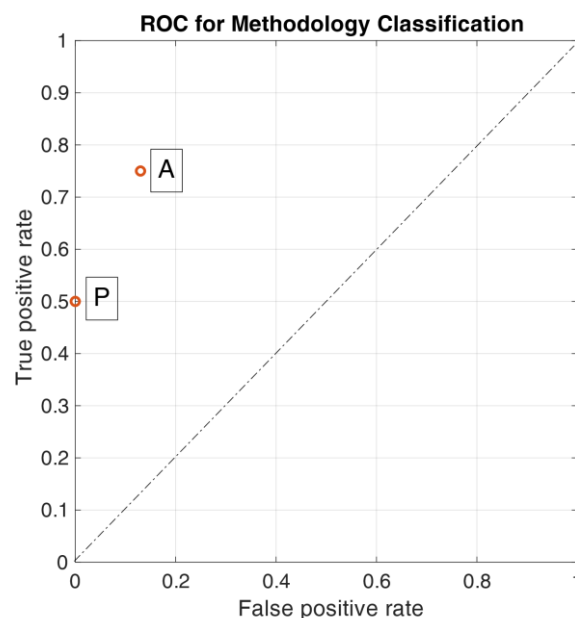


Figure 48 A basic ROC graph showing the two classifiers for the athlete 2: (A) advanced, (P) previous

### Key outputs Binary classification

The inertial system with the advanced and previous model allowed to identify correctly at least the 98% of LOGC events (better performance than similar systems in the literature

(Lee, 2013)). For both athletes the accuracy values improved with the A method for all the velocities and for step sequences evaluation. The same trend was shown by false alarm (with an only test showing worse performance than P method). Instead, miss alarm worsened in 4 of 8 tests. Despite the advanced method worsen the evaluation of the miss alarm, this at least does not lead to a disqualification of a correct athlete, as in the case of a false alarm. The overall accuracy values of A method for step sequences were between 79% and 92%. For giving a better understanding of these values, Knicker (Knicker, 1990) reported an outdoor experiment, where the judges' accuracy was evaluated. Analysing judges' evaluations with our binary method of classification, judges achieved the following accuracy rate: 73%, 68% and 54% (i.e. the mean value of 65%). Therefore, in a similar experiment, the inertial system seems to get higher values of accuracy despite a stricter classification of step sequences legal, i.e. LOGC < 40ms vs LOGC < 50ms. It is worth noting that at lowest speeds ( $\leq 12.9$  km/h) illegal steps are very unusual (e.g. zero cases at 12.0 km/h) as also recognized in other studies (DeAngelis M., 1992) (Cazzola, 2016). For both athletes, the classifier A has the best performance. It is close to the perfect classifier (coordinates: 0,1) therefore the performance of the A method becomes very interesting.

#### 4.2.2.3.2 Three level step classification: Results and Discussion

Data collected with the two previous athletes have been analysed through the three-level step analysis (see section 3.2.2).

Table 34 Step sequences classification according to three multi-class confusion matrices for P and A model

	Legal <sub>M</sub> <sup>P</sup>	Doubt <sub>M</sub> <sup>P</sup>	Illegal <sub>M</sub> <sup>P</sup>	Sum <sub>M</sub> <sup>P</sup>	Legal <sub>M</sub> <sup>A</sup>	Doubt <sub>M</sub> <sup>A</sup>	Illegal <sub>M</sub> <sup>A</sup>	Sum <sub>M</sub> <sup>A</sup>
Legal <sub>GT</sub>	8	28	0	36	20	16	0	36
Doubt <sub>GT</sub>	0	5	1	6	0	5	1	6
Illegal <sub>GT</sub>	0	0	6	6	0	0	6	6
Sum	7	34	7	48	20	21	7	48

Table 35 Comparison between Statistics based on the multi-class confusion matrices (best column values are underlined).

	TPR <sub>L</sub>	TPR <sub>D</sub>	TPR <sub>I</sub>	PPV <sub>L</sub>	PPV <sub>D</sub>	PPV <sub>I</sub>	Accuracy
Previous	22%	83%	100%	100%	15%	86%	40%
Advanced	<u>55%</u>	83%	100%	100%	<u>24%</u>	86%	<u>65%</u>
$\Delta$	<u>+33%</u>	0%	0%	0%	<u>+9%</u>	0%	<u>+25%</u>

On this basis, according to the estimation of judge’s field of view (see section 3.2.4) two three multi-class confusion matrices (related to the total of 48 step sequences analyzed) were carried out and statistical indices as accuracy, TPR and positive PPV were evaluated for legal (subscript L), illegal (subscript I) and doubt (subscript D) steps (see Table 34 and Table 35). Table 35 shows that the advanced model overperforms in: accuracy, true positive rate for legal steps and predict positive value for doubt steps.

The accuracy value with a three-level classification appears to be worse than the corresponding values with two levels. This happens because many legal sequences of steps are classified as “doubt” (as shown by PPV<sub>L</sub>). However, this error in competitions is not a problem because it represents only a warning for a correct athlete (not a disqualification). Finally, the pairs of points related with TPR and PPV value for the sequence step (legal, doubt and illegal) with the two model are plotted in the Recall Sensitivity Diagram (see Figure 49). Starting from the three pair of TPR and PPV value (for legal, doubt and illegal steps) the curve on the diagram are plotted and Area Under the Curve (AUC) was calculated. The score is 1.0 for the classifier with the ideal performance level and 0.5 for the classifier with the random performance level. The actually first point of the curve have a value of TPR different to 0. So, it became the second one and for the assessment of the AUC we have to estimate a new the first point. For this aim we draw a horizontal line from the second point to the y-axis. Hence, the first point is estimated as (0.0, 1.0) for both models. Table 36 shows the pair of points used to build the two curves on Recall-Precision graph.

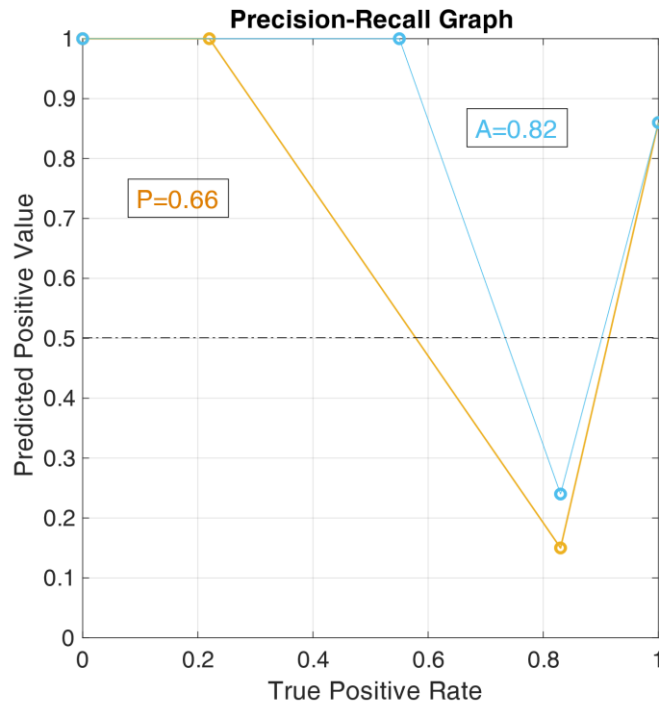


Figure 49 Two precision-recall curves represent the performance levels of two classifiers A and P.

The plot clearly shows classifier A outperforms classifier P, which is also supported by their AUC scores (0.66 and 0.82).

Table 36 Coordinates of the four points in the Precision Recall graph

Point	TPR	PPV
1	0	1
2	$TPR_L$	$PPV_L$
3	$TPR_D$	$PPV_D$
4	$TPR_I$	$PPV_I$

#### 4.2.2.3.3 Fuzzy classification: Results and Discussion

Finally, data collected with the two previous athletes have been analysed through the fuzzy step classification (see section 3.2.3) using the two built membership function related with high speed camera and inertial system. We indicate with  $\alpha$  the percentage of acceptable

classification (according to eq. 31). Table 37 shows the performance of the two models for the two athletes considered.

Table 37 Performance index  $\alpha$  of the two models previous (P) and advanced (A)

Velocity [km/h]	$\alpha^P$ [%]	$\alpha^A$ [%]	Velocity [km/h]	$\alpha^P$ [%]	$\alpha^A$ [%]
12.0	86	<u>98</u>	11.9	96	<u>100</u>
12.9	75	<u>96</u>	12.9	37	<u>68</u>
13.7	54	<u>84</u>	13.7	33	<u>66</u>
14.6	46	<u>59</u>	15.7	83	<u>84</u>

The correct classification for the athlete 1 still shows a decreasing trend with velocities. For the athlete 2 this trend change in the last velocities. However,  $\alpha$  confirmed an improvement with the advanced model for both athlete a for each speed. Finally, Table 38 shows the analysis of step sequences.

Table 38 Performance index  $\alpha$  in the step sequences analysis

Method	Athlete 1 $\alpha$	Athlete 2 $\alpha$
Previous	79%	66%
Advanced	<u>100%</u>	<u>91%</u>
$\Delta$	+21%	+25%

The performance index  $\alpha$  for step sequence analysis confirms the improvements with the advanced model for both athletes, with values greater than 90%.

#### 4.2.3 Radar chart representation of infringements and performances for nine elite athletes

In this section, starting from data collected in all tests, we applied the previously exposed methodology in order to design a radar graph representation (see section 3.3). According to the procedure described in the section 4.2.2.2, we collected data through a well-defined

experimental protocol at four velocities between 12.0 km and 14.5 km. For each race-walking test, excluding the initial acceleration phase of the athlete (fixed equal to 10 s), 180 consecutive steps (six sequences of step for each trial) were considered. So, 24 sequences of steps (720 steps) for each athlete were evaluated. A total amount of 36 tests (144 sequences of step, 25920 steps) were evaluated. Table 39 shows the mean and standard deviation values of each performance and infringement parameter at the four velocity of the trials.

*Table 39 Performance and infringements parameters data collected during trials (mean±SD)*

Velocity [km/h]	SC [steps/s]	SLR [%]	LOGC <sub>T</sub> [ms]	LOGC <sub>C</sub> [-]	S [-]
12.0	3.100±0.067	61.9±2.8	21±7	0.078±0.09	6.276±1.404
13.0	3.197±0.082	64.6±3.2	34±7	0.339±0.25	5.392±1.441
14.0	3.294±0.071	67.3±3.1	45±8	0.635±0.26	4.647±1.109
14.5	3.344±0.073	69.3±3.3	51±9	0.749±0.26	4.444±1.188

These data agree with literature (Pavei G. C., 2014): flight time, SC and SLR increase with growing velocities. At slower speeds than 13 Km/h, mean flight times of step sequences are under 40 ms and only few sequences have greater flight times greater than 40 ms (LOGC<sub>C</sub> value close to 0). Agreeing with literature, with increasing step frequencies smoothness improves (showing decreasing jerk values).

In Figure 50, we reported the key performance indices (for all nine athletes) evaluated according to the proposed methodology (see section 3.3) and plotted on radar charts.

For the performance analysis, the radar chart allows to understand the strong and critical points that characterize the technique of the single athlete. For example, the radar charts underline how the Athlete 2 and Athlete 9 have step length values ( $\rho$ ) better than step cadence ones ( $\gamma$ ) and it represents their strong point. On the other side, the Athletes 5, 6 and 7 have the strongest technical point in step cadence.

For the infringement analysis, at the starting velocity the considered indices are at their optimum, then worsening with growing speeds, sometimes suddenly.

Finally,  $\beta$  allows to individuate the speed where the graph area has the maximum value. Indeed, this value can suggest the velocities of the best compromise to achieve the optimal Step Length Ratio and Step Cadence and guarantee an acceptable level of correct technique (see eq. 27). From the diagrams this speed varies between athletes with values between 12 and 14 km/h.

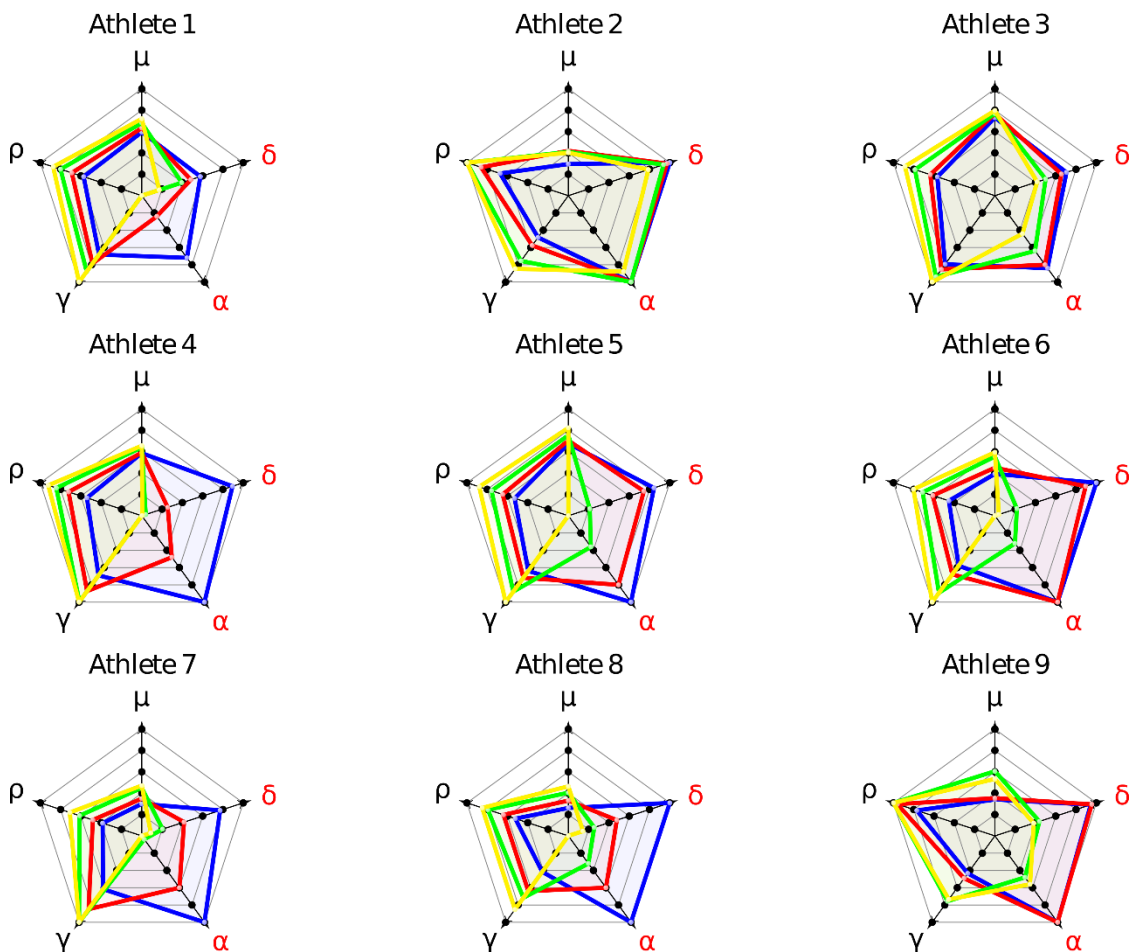


Figure 50 Radar charts for the experimental tests. The red indices are related to the infringements, the black ones to the performance. The coloured lines graphically show the trend of the indices at different speeds (blue: 12.0 km/h, red: 13.0 km/h, green: 14.0 km/h, yellow: 14.5 km/h).

We screened data: (i) for normality of distribution using the normality test of Kolmogorov-Smirnov; (ii) the homogeneity of variances through the Levene's test.

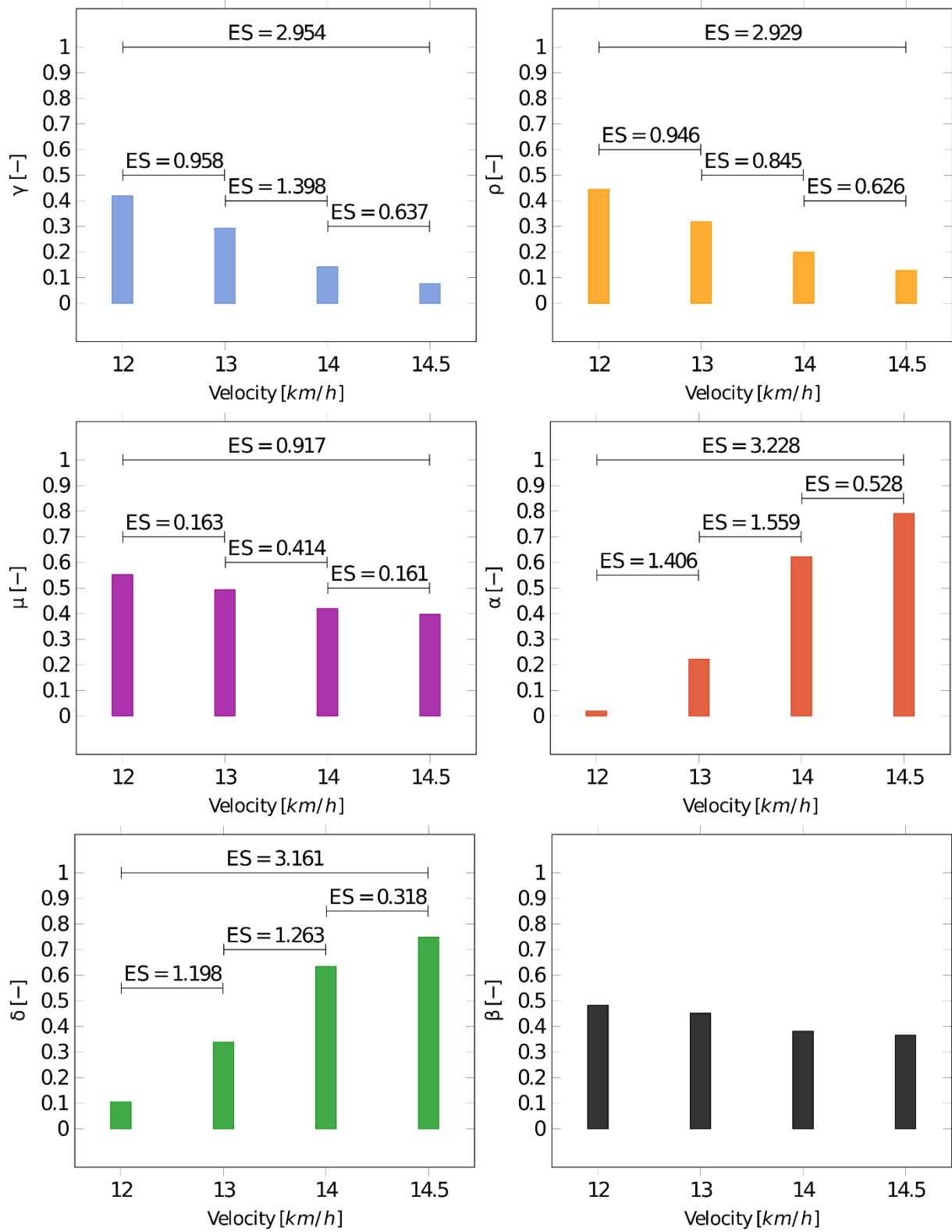


Figure 51: Performance ( $\rho$ ,  $\gamma$ ,  $\mu$ ), infringement ( $\alpha$ ,  $\delta$ ) and overall ( $\beta$ ) indices at different speeds. ES, effect sizes according to Hedges'  $g$

The magnitude of differences or effect size (ES) for each performance and infringement index between different following pair of velocities was calculated according to Hedges' g and interpreted as small ( $>0.2$  and  $<0.6$ ), moderate ( $\geq 0.6$  and  $<1.2$ ) and large ( $\geq 1.2$  and  $<2$ ) according to the scale proposed by Hopkins et al. (Hopkins, 2009). The ES analysis underlined that the performance indices  $\rho$  and  $\gamma$  always have moderate ES (except for  $\gamma$  having large ES between 13 and 14 km/h). Moreover, in Figure 50 we can notice a reduction of ES in the last pair of velocities (14.0-14.5 km/h), characterized by a fixed smaller gain of speed. The third performance index ( $\mu$ ) shows a trivial ES with a small value only between 13 and 14 km/h. Indeed, infringement indices show large ES for velocities pairs of 12.0-13.0 km/h and 13.0-14.0 km/h. While, in the last comparison (14.0-14.5 km/h), there are smaller ES (small for  $\delta$  and moderate for  $\alpha$ ). It is important to notice that the reduction of ES value in the last comparison (underlined both for infringement parameters ( $\delta$  and  $\alpha$ ) and in the performance one ( $\rho$  and  $\gamma$ ) is also related with the reduction of velocity incremental gain (from 1.0 km/h to 0.5 km/h). Finally, in order to assess the weight of the key performance indices ( $\mu$ ,  $\rho$ ,  $\delta$ ,  $\alpha$  and  $\gamma$ ) on the race-walking overall index ( $\beta$ ) we evaluated the  $\kappa$  index:

$$\kappa_i = \frac{H_i^{12,14.5}}{\sum H_i^{12,14.5}} \text{ (eq. 32)}$$

where  $H_i$  represents the Hedges'g value for a generic key performance index  $i$  evaluated between the groups at the minimum velocity (12.0 km/h) and maximum one (14.5 km/h). In concern with (eq. 32) we derived the several  $\kappa$  indices shown in Figure 52.

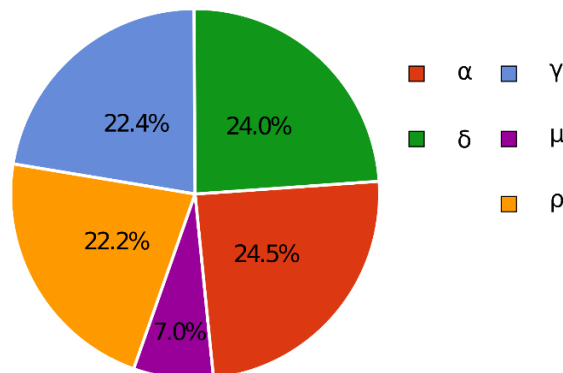


Figure 52 Pie graph showing  $\kappa$  indices

In this pie graph, we can observe how, even if the infringement indices are fewer than the performance ones (2 compared to 3, respectively), their weight represents almost the 50% of the totality. This proves their important role in the definition of the total area  $\beta$ , as well as and a good balance between performance and infringement indices contribution in the radar chart structure.

CHAPTER 5:  
TOWARDS THE EXPERIMENTAL PROOF-OF-  
CONCEPT OF A CUSTOM SYSTEM FOR  
EVALUATION OF INFRINGEMENTS AND  
PERFORMANCE IN RACE-WALKING

Basing on the optimal system architecture, obtained in Chapter 2, and on assessment methodologies for performance and infringement (starting from inertial sensor data), developed Chapter 3 and validated in Chapter 4, in this chapter we introduce the realisation process for the proof of concept. For the measuring unit, starting from the selection of a commercial device, we will expose the design and manufacturing of a customized case box. For the control unit, we will show the development of a dedicated mobile app. Figure 53 shows the design of proof of concept development.

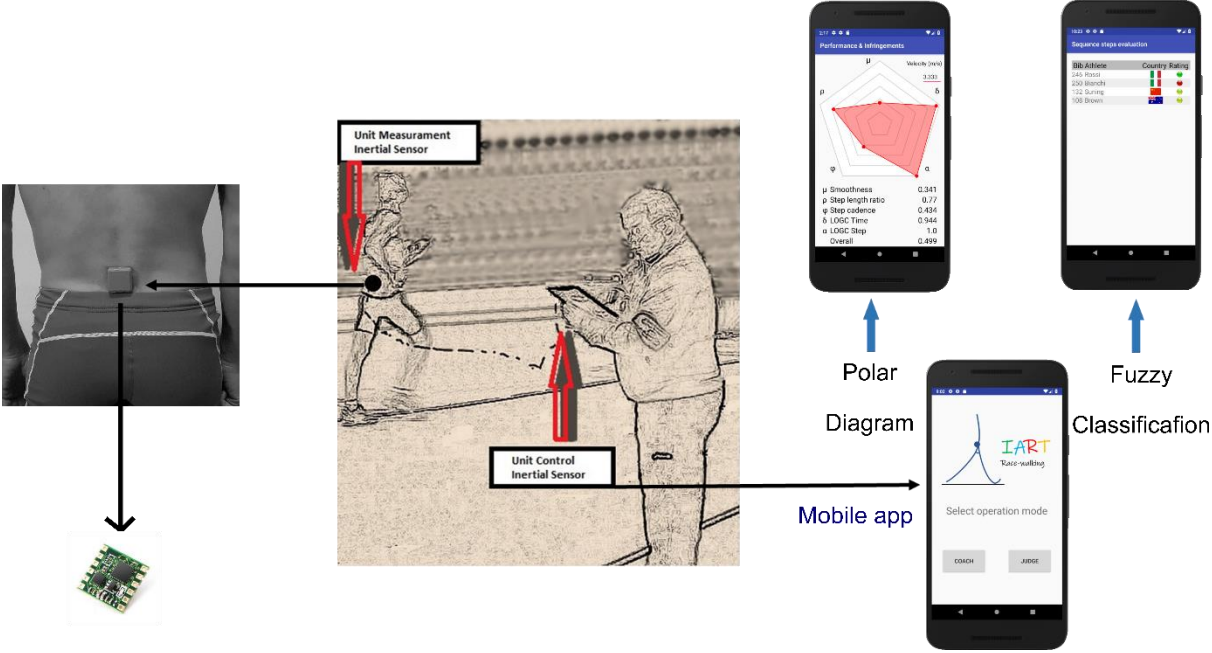


Figure 53 Architecture design proof of concept development

## 5.1 Proof of Concept: Measurement Unit

For the development of a physical prototyping of the Measurement Unit we chose a commercial inertial platform with the following features according to the user's requirement (see section 2.3):

- Sample frequency  $\geq 200$  Hz (in order to achieve a good efficiency in relationship the quality of assessment of infringement and performance parameters);
- Small volume and Lightweight (in order to obtain comfortable product).

In addition, we chose a product that allowed to transfer collected data to a mobile device and having a driver for interfacing an app (useful for the development of a dedicated mobile app).

### 5.1.1 Inertial sensor platform

The chosen inertial sensor platform (BWT901CL, WitMotion) consists of a module chip JY901 (composed by a triaxial accelerometer, a triaxial gyroscope and a triaxial magnetometer) integrated with a Bluetooth module. This system has a Baud Rate equal to 115200, its operating voltage is 3.3-5V and a mass of 4,25 g. The external dimensions of the integrated module are 34×34×7 mm. Data transmission is via Bluetooth 2.0 (with a transmission distance >10m). The battery (150mAh lithium battery, external dimensions 20x25x4 mm, weight 4,65 g) is rechargeable with an operating time of about 2h/3h hours (Consumption current: 25mA). The sampling frequency, for this study, was set to 200 Hz (*i.e.* the maximum value).

Table 40 Data sheet of the BWT901CL, WitMotion inertial platform

Technical feature	Accelerometer sensor	Gyroscope sensor
Dynamic range	$\pm 16g$	$\pm 2000^\circ/s$
Resolution	$6.1 \cdot 10^{-5}g$	$7.6 \cdot 10^{-3}^\circ/s$
Stability	0.01g	0.05°/s

The drift is solved by magnetic field. Table 40 shows the sensor's additional technical features. This system acquired the CoM Inertial acceleration.

### 5.1.2 Inertial sensor packaging

Packaging refers to how the chosen inertial sensor is housed or contained (James, 2016). This is the last stage of the design hardware lifecycle process and it aims to build a customized box for the sensor. We started from the case box proposed by the WitMotion and we developed a customized solution for race-walkers. Our design solutions include end user analysis (see section 2.3) in consideration with the available technologies.

Main improvements:

- Few openings in order to reduce water and dust intrusion;
- Establishing a port cover;
- Removing the lateral appendages, not functional to our aim;
- Increasing the slope of lateral edges in order to facilitate taping application to fix it.

So, the encapsulation is undertaken to make inertial sensor platform components resistant to shock and to make the device more user friendly (small volume).

For the physical realization of the customized box we choose the technology of 3D printing. It allows lower costs, an ease of customisation and complex designs can be printed (Bak, 2003).

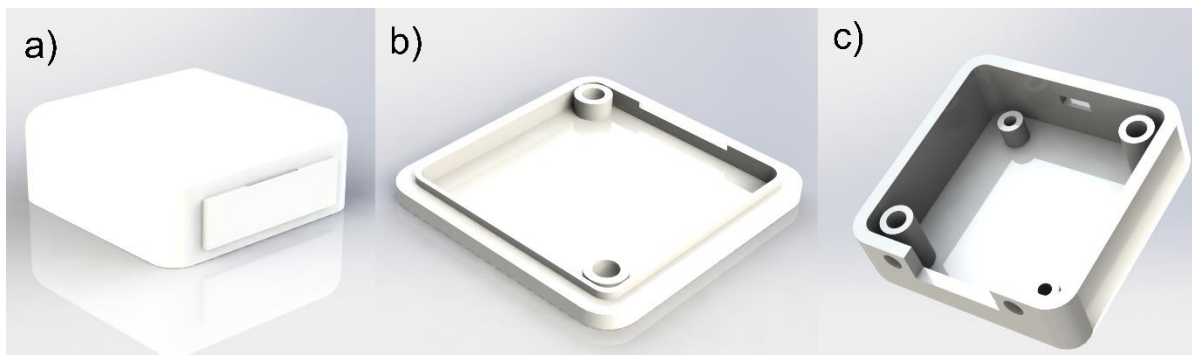


Figure 54 Rendering of the box case components: a) whole box b) upper part; c) lower part

For manufacturing a customized case box, we used Zortrax M200 (print time about 2h30'). The generation of supports was chosen in order to reduce the print time and the following removal.

For the setting of the parameter of 3D printing we defined the layer thickness (a measure of the layer height of each successive addition of material). In order to obtain better quality, we chose a thin layer (0.09mm) (Vaezi, 2011). About the parameter of the infill density, in order to guarantee the best resistance of the case box, we set this parameter equal to 100%, not having excessive weight. According to the setting parameters of 3D printing, the weight of used material was equal to 9g. Total weight, including 4 Philips screws: 2 for fixing the inertial platform and 2 for closing the case, the inertial platform and the battery was 23g.

Finally, in addition to the technical features shown in Table 40, the following Table 41 describes additional features of the complete device (with customized case and battery showed in the Figure 55).

*Table 41 Additional technical features of the inertial sensor with case*

Technical Features Inertial Sensor (with case)	
Total volume	36 X 36x15 mm
Total weight	23 g
Manual interface	On/off button
Digital interface	IART Mobile App
Colour	Grey
Material	ABS
Closing	2 screws

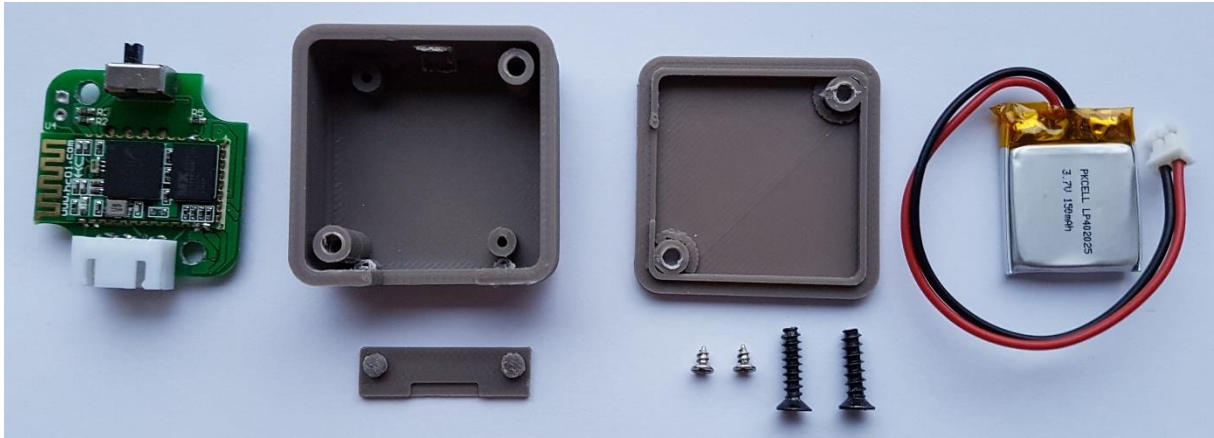


Figure 55 Picture showing the several component of measurement unit: inertial sensor, case box upper and lower part, port cover, 4 screws and battery.

## **5.2 Proof of Concept: Control Unit**

In agreement with the optimal system architecture concept achieved in paragraph 2.4, in order to answer the features of the control unit (an easy user interface), in this paragraph we will describe the script and the development of a mobile app for race-walking performance and infringements assessment. Our aim was to obtain an easy graphic interface displayable by the user on mobile devices. This app was called IART (Inertial Assistant Referee and Training for Race-walking) and had two operation modes: one for coaches and the other one for judges. These two modes used the exposed inertial sensor data processing, step classification and the development of a customized approach for elite athletes, showed in paragraph 3.1, 3.2 and 3.3.

### **5.2.1 Development of IART: a mobile app for evaluation of infringements and performance in race-walking**

The mobile app was developed in Android mobile operating system (the best-selling OS worldwide on smartphones since 2011 and on tablets since 2013). The mobile app was built using Android Studio (version 3.1.4). It is the official integrated development environment (IDE) for Google's Android operating system and designed specifically for Android development. Android Studio allows to run and debug apps through the emulator driver Android Virtual Device or directly on physical device. It supports different programming languages (i.e. IntelliJ, CLion, Java, C++; Kotlin). In our case study, we chose the Java programming language.

The app interface was defined through the structure of Activities. An Activity represents a screen of our app. It is made by a layout (.xml file text), defining its structure, and a .java class, containing the activities logic. If, in order to build an activity, we need complex elements, not available in the standard Android libraries (both as class and structure), they must be built through assembly of basic elements. An intent was used in the launching of activities. An overview of main component of the IART app is shown in Figure 56.

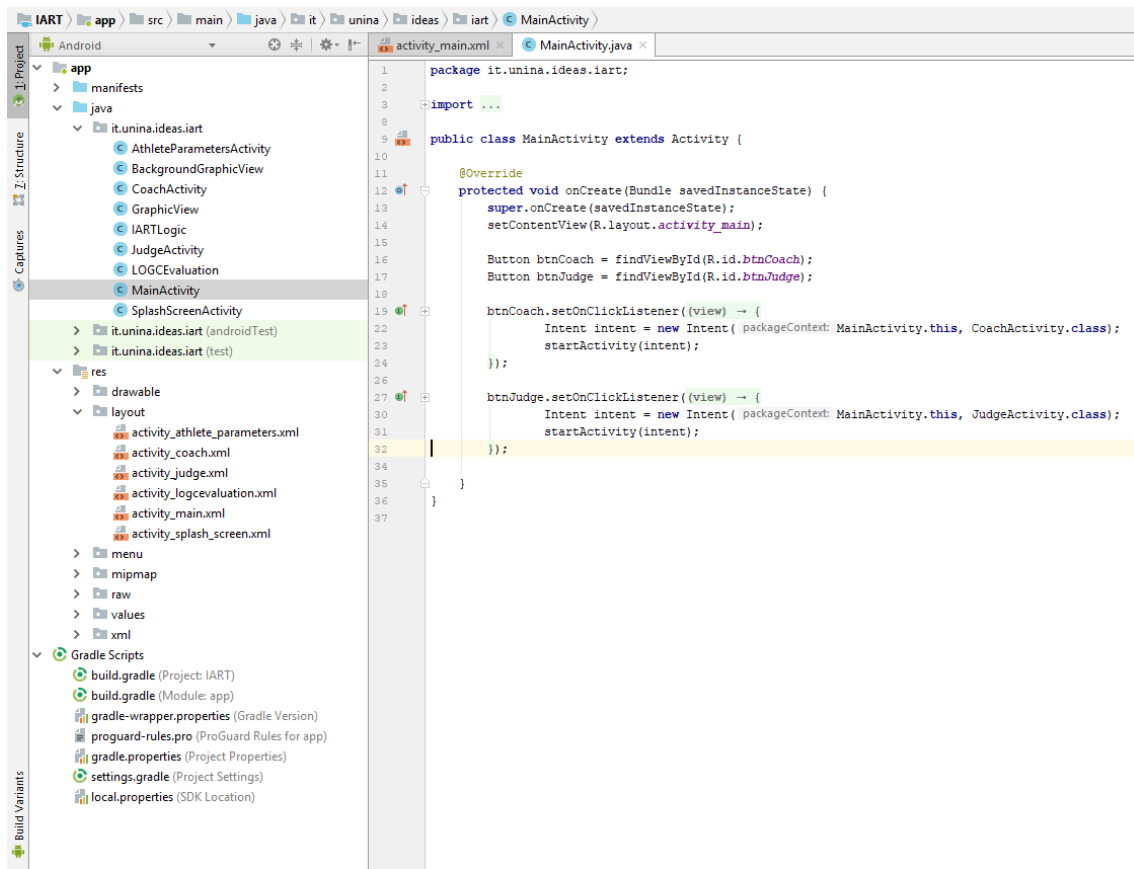


Figure 56 A screenshot of the IDE Android Studio

In the Figure 57 is shown the developed user interface execution flow. It is composed by seven screen that are described in detail below.

Splash screen: start screen. It has an introductive aim and it shows the app logo for three seconds, then automatically moving to another more functional screen.

Select operation mode: under the app logo, there are two buttons for choosing two operation modes, one for coaches and the other one for judges, leading to two different activities.

Choosing coach mode, we access the following sequence:

Athletes list: allows to view the saved athletes' names. The button downward activates another screen, that permits to create a new athlete's profile, with name, surname, sex, age, height and weight.

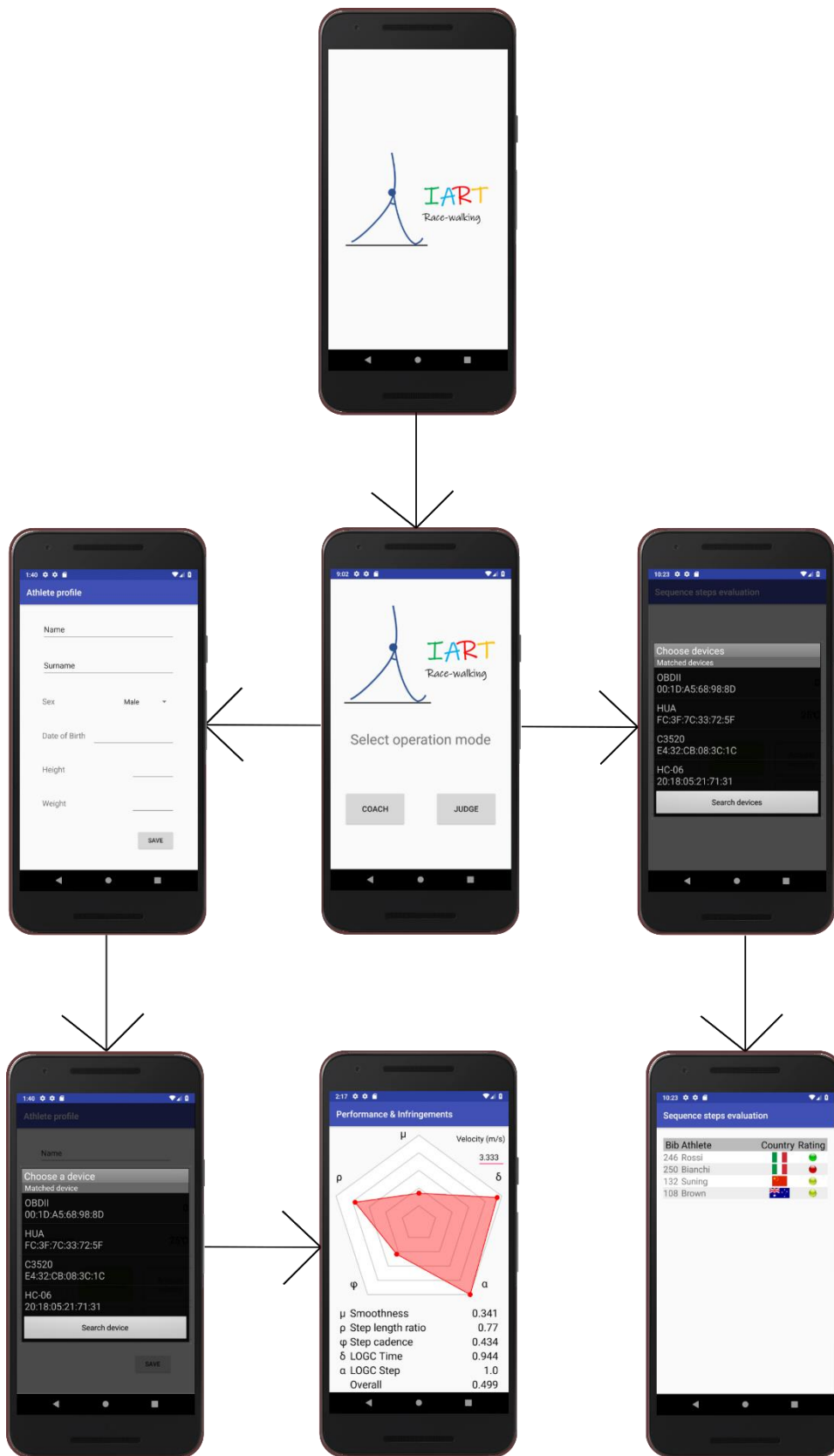


Figure 57 Flow diagram of app user interface

Pairing device: after choosing an athlete, another activity searches for Bluetooth devices. The user selects the right device. Then, a thread is launched, receiving inertial device data every 5 ms (prefixed sample frequency), through the WitMotion driver.

Radar chart: the screen shows a dynamic radar graph with 5 vertexes, plotted on a regular pentagon (background). The vertexes of the radar chart represent the athlete's performance and infringement indices. Their values are shown in a table under the radar graph. The activity automatically updates, processing data of the last 10 seconds (about 30 steps). The developed logic of the activity allows to implement the methodology shown in sections 3.1 and 3.3. For the screen building, we developed customized elements in order to make data graphically clear.

Choosing judge mode, we access the following sequence:

Pairing device: the activity acquires the list of athletes and paired devices. Then, it tries to start acquisition from all the visible devices. Then, for each device a thread is launched, receiving inertial device data every 5 ms (prefixed sample frequency), through the WitMotion driver.

Step evaluation: data from all the visible devices are elaborated using the developed logic (based on the methodology shown in the section 3.2). The screen shows the list of visible athletes with the related step sequences evaluation (through a control coloured light).

# Conclusions

In the presented work the development of biomechanical-based tools for the evaluation of infringements and performance in race-walking was presented. The user center approach for designing the tools allowed the definition of the optimal system architecture for a wearable device for real-time monitoring of performances and evaluation of infringements in race-walking. The device consists of an inertial sensor positioned close to the centre-of-mass of the athlete and an external control unit.

Laboratory experimental data showed that the proposed algorithms for measuring the performance and for step classification achieved good results compared with state-of-the-art approaches. In particular, the statistical analysis showed that the model has highest value of accuracy and the best placement in ROC graph.

The field tests showed that the inertial system with the advanced and previous model allowed to correctly identify at least the 98% of LOGC events (better performance than similar systems in the literature (Lee, 2013)). The mean difference with the Ground truth system in the assessment of loss of ground contact time, result reduced with the advanced method. In the binary classification, the accuracy values are improved with the advanced model for all the velocities and for step sequences evaluation (with values between 79% and 92%). For better understanding these values, in similar experimental tests (Knicker, 1990), with the same step classification, the judges achieved an accuracy of 65% compared to a camera evaluation. In addition, on the ROC graph, the advanced classifier had the best performance. It was close to the perfect classifier (coordinates: 0,1); therefore, the performance of the advanced model becomes very interesting. The analysis on three levels confirmed the best performance of the advanced model in relationship with the accuracy value and the Area Under Curve value on Precision-Recall graph. The third method of step classification (fuzzy classification) confirmed that the advanced method outperformed the previous one with acceptable evaluation over the 90%. The representation on the developed radar chart allows an intuitive analysis of performance and infringements. Indeed, it permits

to understand the strong and critical points that characterize the technique of the single athlete. Statistical analysis confirms a good balance between performance and infringement indices contribution in the radar chart structure.

Finally, the experimental proof-of-concept of a wearable device for race-walking was presented. The associated mobile app offers two possible setting modes: coach and judge. To date, our device can be classified in the scale of Technology Readiness Level<sup>2</sup> (that gives measuring of the maturity of a given technology) as value equal to 4. The research project has also achieved the following award: (i) selection ideas at call Federico II “Dalla ricerca all’innovazione” – Campania New Steel; (ii) finalist in the start-up competition “Start Cup Campania 2018”; (iii) 2<sup>nd</sup> place in the ISEA (International Sports Engineering Associations) Student Project Competition.

In the future development, we will consider the multi-sensor scenario, in order to explore the problems dealing with the monitoring of multiple features/signals. In this situation the main issues could be: (i) pairing with multiple control units of many devices; (ii) scalability cloud computing (the ability to adapt to the increase of users, to the increasing in data and to the diversification of the required functionalities).

---

<sup>2</sup> <https://enspire.science/trl-scale-horizon-2020-erc-explained/>

# Acknowledgments

The challenge to develop an inertial system device for assisting referee and training in race-walking was very exciting for me, a mechanical engineer but at the same a professional race-walker.

At the end of this work, it is my pleasure to acknowledge people who have been the sources of help and inspiration for this work.

First of all, I would like to gratefully thank my advisors, Professor Giuseppe Di Gironimo and Professor Antonio Lanzotti. Advisors' supports represented a fundamental element for my growth, and I will always thank them for the opportunities they gave me. Professor Giuseppe Di Gironimo has been a reference point for me since I met him in my master thesis period. He allowed me to start my studies in the ErgoS Lab that became in these years like a second house for me. Every talk with him has always been deeply supporting for me. Professor Antonio Lanzotti, who has been important for me since my master education in the exciting course of Product design and development. He also guided me during the master thesis period and then introduced me to the world of Sport Engineering. His teachings have been essential for me in developing a system-oriented perspective of Engineering. A special thank goes to PhD Stanislao Grazioso who was also important in my PhD studies. His passion in doing research, combined with his scientific rigor, is a meaningful example for me.

During this research, I had the opportunity to spend a period at the Department of Sport Equipment and Technology of University of Technology – Chemnitz, Germany. In this period, under the supervision of Prof. Stephan Odenwald, I had designed the first experimental trials of my research activities. I would like to acknowledge Prof. Stephan Odenwald and Professor Pasquale Franciosa, for the time they spent to review this manuscript, as well as for their precious comments. Many thanks go to Professor Thomas Allen, Professor Tommaso Ingrassia and Professor Adolfo Senatore to have accepted to be the members of the examination committee.

The IDEAS group of the University of Naples Federico II has been also important for me. I would like to thank my colleagues Domenico D., Domenico M., Domenico C., Stefano, Andrea, Rocco for the never boring time that we spent together.

The race-walking world has been a wonderful and fundamental environment for me. I sincerely thank the Italian Air Force that gave me the opportunity to be a professional race-walker (and supported me even during a long injury) and at the same time they gave me the opportunity to complete the PhD course.

I would like to thank my coaches Giovanni Caruso that gave me the opportunity to start my life in athletics, Roberto Sanginario that guided me in my first important steps in race-walking and Diego Perez that has been my technical guide since 2008. He has allowed me to reach important sport goals (in particular the Olympic Games) and he taught me important personal life values. I would like to thank also my race-walking friends, in particular the “Rotoballa’s friends” Luca, Mario and Sibilla.

A special thank goes to the dear friends of my first university life Antonino and Erica. Although we have been in different places, we always had the opportunity to meet and exchange support.

Nothing could express the feeling of love and gratitude towards my family without their support, this thesis would not exist. A special thanks from my brother Michele for his special support in the development of this thesis. Heartfelt thanks to all my friends, in particular the “historical” ones Francesco, Pellegrino and Antonio. My last words go to Angela. Her unconditional love and support are my daily source of energy and equilibrium.

# Appendix A

## Questionnaire “Support device to control the loss of contact with the ground-level in the race-walking”

Define five adjectives you would link to this device

---

---

---

- 1) What is your status?
  - a. Judge
  - b. Trainer
  - c. Athlete
- 2) What is your range?
  - a. National
  - b. National and international
- 3) How long have you been part of the race-walking “world”?
  - a. Less than 5 years
  - b. 5 to 10 years
  - c. 10 to 20 years
  - d. More than 20 years
- 4) According to you, is it important to introduce an electronic support device to control the loss of contact with the ground?
  - a. Yes, it is
  - b. No, it isn't
- 5) Rule 230 (IAAF Competition Rules) says that “...the walker makes contact with the ground, so that no visible (to the human eye) loss of contact occurs”. According to you the device might judge:

- a. Time of loss of contact
  - b. Maximum height from the ground
- 6) According to you, which might be the maximum price of every single device?
- a. < 100 €
  - b. 100 – 500 €
  - c. 500 – 1000 €
  - d. > 1000 €
- 7) In which competition would it be used?
- a. European Championships, World Championships, Olympic Games
  - b. The previous ones plus European and World Race-walking Cup
  - c. The previous ones plus Race-walking Challenge
  - d. From National Championships on
- 8) Where do you think it would be more comfortable the device positioning?
- a. inside the shoe
  - b. on the external part of the shoe
  - c. at pelvis height
  - d. on the quadriceps
  - e. on the shorts
  - f. elsewhere
- 9) Who should be the addressee(s) of the communication of the eventual offence?
- a. the closest judge
  - b. the closest judge and the race-walker
  - c. the closest judge, the race-walker and the chief judge
  - d. the chief judge only
  - e. the chief judge and the race-walker
  - f. everybody

## DEVICE FEATURES

Give a mark from 1 to 10 according to the importance you would assign to the following device features:

- 1) measurement accuracy and precision \_\_\_\_\_
- 2) measurement communication promptness \_\_\_\_\_
- 3) measurement understanding facility \_\_\_\_\_
- 4) measurement data recording \_\_\_\_\_
- 5) weight \_\_\_\_\_
- 6) volume \_\_\_\_\_
- 7) durability \_\_\_\_\_
- 8) usage flexibility \_\_\_\_\_
- 9) fragility \_\_\_\_\_
- 10) cheapness \_\_\_\_\_

Thank you for your kindness

# References

- Alvarez, D. S.-R. (2017). VALIDATION OF THE PHOTOELECTRIC OPTOGAIT SYSTEM TO MEASURE RACEWALKING BIOMECHANICAL PARAMETERS ON A TREADMILL. *ISBS Proceedings Archive*, 35(1), 253.
- Amigo, A. (2013). *Electronic system for loss of contact control in race walking. The victorian race walking club*. Retrieved from <http://www.vrwc.org.au>
- Awang, Z. A. (2016). The Likert scale analysis using parametric based Structural Equation Modeling (SEM). *Computational Methods in Social Sciences*, 4(1), 13.
- Bak, D. (2003). Rapid prototyping or rapid production? 3D printing processes move industry towards the latter. *Assembly Autom*, 23(4), 340–345.
- Balasubramanian, S. M.-C. (2012). A robust and sensitive metric for quantifying movement smoothness. *IEEE transactions on biomedical engineering*, 59(8), 2126-2136.
- Barreto Andrade, J. V.-A. (2017). Biomechanics of the athletic walk. Kinematic analysis of its development and comparison with normal walk. *Revista Cubana de Investigaciones Biomédicas*, 36(2), 53-69.
- Benson, R. C. (2011). "Heart Rate Training." Champaign. *Human Kinetics*, 10-12.
- Bishop, D. (2008). An applied research model for the sport sciences. *Sports Medicine*, 38(3), 253-263.
- Borg, G. A. (1982). Psychophysical bases of perceived exertion. *Medicine and science in sports and exercise*, 14(5), 377-381.
- Burgess, S. C. (1996). The design optimisation of poles for pole vaulting. *The engineering of sport (pp. 83–90)*. Rotterdam: Balkema.
- Cairns, M. A. (1986). A biomechanical analysis of racewalking gait. *Medicine and science in sports and exercise*, 18(4), 446-453.

- Caporaso, T. D. (2017). Digital human models for gait analysis: experimental validation of static force analysis tools under dynamic conditions. *n In Advances on Mechanics, Design Engineering and Manufacturing. Springer, 479-488.*
- Caporaso, T. G. (2018). Estimation of performance and infringements during race-walking field tests using a wearable inertial sensor system. *Measuring Behavior 2018.* (pp. 211-216). Manchester: Metropolitan University.
- Caporaso, T. G. (2018). User-centered design of an innovative foot stretcher for ergometers to enhance the indoor rowing training. *International Journal on Interactive Design and Manufacturing (IJIDeM), 1-11.*
- Caporaso, T. P. (2017). Towards performance indices for neuromuscular synergy in patients with intellectual disability. *Gait & Posture, 57, 25-26.*
- Caporaso, T. P. (2018). Correlation of neuromuscular synergies and performance indices in indoor rowing using a custom foot stretcher for ergometers: a preliminary study. *Proceedings of SIAMOC 2018.*
- Caporaso, T. P. (2018). Sport e tecnologia: verso un nuovo occhio elettronico per la marcia. *Rivista Scuola dello Sport 117, 31-38.*
- Cazzola, D. P. (2016). Can coordination variability identify performance factors and skill level in competitive sport? The case of race walking. *Journal of Sport and Health Science, 5(1), 35-43.*
- Chang H-C, C. H.-Y. (2014). Optimizing product form attractiveness using Taguchi method and TOPSIS algorithm: a case study involving a passenger car. *Concurr Eng Res Appl 22(2), 135–147.*
- Chen, H. T. (2011). 3D ball trajectory reconstruction from single-camera sports video for free viewpoint virtual replay. *In Visual Communications and Image Processing (VCIP), 2011 IEEE (pp. 1-4). IEEE.*

- Choi, A. J. (2014). Kinematic evaluation of movement smoothness in golf: relationship between the normalized jerk cost of body joints and the clubhead. *BioMedical Engineering OnLine*, 13(1), 20.
- Chowdhury, H. A.-F. (2009). Design and methodology for evaluating aerodynamic characteristics of sports textiles. *Sports Technology*, 2(3-4), 81-86.
- Chwała, W. K. (2014). Changes in energy cost and total external work of muscles in elite race walkers walking at different speeds. *Journal of human kinetics*, 44(1), 129-136.
- Claypool M, C. K. (2006). The Effects of Frame Rate and Resolution on Users Playing First Person Shooter Games. *Proceedings of ACM/SPIE Multimedia Computing and Networking Conference. International Society for Optical Engineering*. San José.
- Claypool, K. C. (2007). On frame rate and player performance in first person shooter games. *Multimedia Syst.* 13(1), 3–17.
- Connick, M. J. (2016). Developing tests of impaired coordination for Paralympic classification: normative values and test–retest reliability. *Sports Engineering*, 19(3), 147-154.
- Costabile, G. A. (2013). Improving passive safety of Sports equipment through experimental testing of new protection devices. *In Proceedings of the International Conference "Ingegref-Adm-Aip Primeca"*, (pp. 45-51). Madrid, Spain.
- Costabile, G. S. (2013). Toward a new approach for passive safety assessment of gymnastic equipment. *Journal of Achievements in Materials and Manufacturing Engineering*, 56(2), 59-65.
- Cronin, N. J. (2016). Mechanical and neural function of triceps surae in elite racewalking. *Journal of Applied Physiology*, 121(1), 101-105.
- D., B. (2003). Rapid prototyping or rapid production? 3D printing processes move industry towards the latter. *Assembly Autom* 23(4), 340–345.

- DeAngelis M., M. C. (1992). Times of flight, frequency and length of stride in racewalking. *Proceedings of the X International Symposium of Biomechanics in Sports*. Milan.
- Di Gironimo, G. C. (2016). Development of a new experimental protocol for analysing the Race-walking technique based on kinematic and dynamic parameters. *Procedia Engineering*, 147, 741-746.
- Di Gironimo, G. C. (2016). Outdoor tests for the validation of an inertial system able to detect illegal steps in race-walking. *Procedia engineering*, 147, 544-549.
- Di Gironimo, G. C. (2017). Towards a New Monitoring System to Detect Illegal Steps in Race-Walking. *International Journal Interactive Design and Manufacturing*, 11(2), 317-239.
- Dolenec, A. B. (2015). A comparison of ground reaction forces between barefoot and shod race walking. *In Youth of Sport*.
- Dona, G. P. (2009). Application of functional principal component analysis in race-walking: an emerging methodology. *Sports Biomechanics*, 8(4), 284-301.
- Esser, P. D. (2009). MU: inertial sensing of vertical CoM movement. *Journal of biomechanics*, 42(10), 1578-1581.
- Fawcett, T. (2006). An introduction to ROC analysis. *Pattern recognition letters*, 27(8), 861-874.
- Feizollah, A. S. (2013). Anomaly detection using cooperative fuzzy logic controller. *In FIRA RoboWorld Congress* (pp. 220-231). Berlin, Heidelberg: Springer.
- Forczek, W. M. (2016). MUSCLE ACTIVATION PATTERN OF THE LOWER LIMBS IN A FEMALE RACE WALKER—CASE STUDY. *Antropomotoryka. Journal of Kinesiology and Exercise Sciences*.
- Furlong, D. (1990). U.S. Patent No. 4,956,628. Washington, DC: U.S. Patent and Trademark Office.

- Gomez-Ezeiza, J. T.-U.-C. (2018). Race walking gait and its influence on race walking economy in world-class race walkers. *Journal of sports sciences*, 1-7.
- Gravestock, H. J. (2018). An Analysis of Lower Body Kinematics in Response to Changes in Speed in World-Class Walkers.
- Grazioso, S. S. (2016). INBODY: Instant Photogrammetric 3D Body Scanner.
- Grazioso, S. S. (2018). A digital photogrammetric method to enhance the fabrication of custom-made spinal orthoses. *JPO: Journal of Prosthetics and Orthotics*.
- Grazioso, S. S. (2018). Design and development of a novel body scanning system for healthcare applications. *International Journal on Interactive Design and Manufacturing (IJIDeM)*, 12(2), 611-620.
- Haake, S. (1999). 17th International Symposium on Biomechanics in Sports. *Sports Engineering*.
- Haake, S. J. (2009). The impact of technology on sporting performance in Olympic sports. *Journal of Sports Sciences*, 27(13), 1421-1431.
- Hanley, B. (2013). A Biomechanical Analysis of World-Class Senior and Junior Race Walkers. *New Studies in Athletics*; 28 (1/2), 75-82.
- Hanley, B. (2015). Gait alterations during constant pace treadmill racewalking. *The Journal of Strength & Conditioning Research*, 29.8, 2142-2147.
- Hanley, B. B. (2008). A. The biomechanics of elite race walking: technique analysis and the effects of fatigue. *New Studies in Athletics*; 24(3), 17-25.
- Hanley, B. B. (2011). Kinematic characteristics of elite men's and women's 20 km race walking and their variation during the race. *Sports Biomechanics*. 10(02), 110–124.
- Hanley, B. B. (2013). Analysis of lower limb internal kinetics and electromyography in elite race walking. *Journal of sports sciences*, 31(11), 1222-1232.

- Hanley, B. B. (2013). Kinematic characteristics of elite men's 50 km race-walking. *European journal of sport science*, 13(3), 272-279.
- Hanley, B. B. (2014). Technical characteristics of elite junior men and women race walkers. *J Sports Med Phys Fitness*, 54, 700-7.
- Hanley, B. B. (2015). The contribution of the flight phase in elite race walking. In *ISBS-Conference Proceedings Archive (Vol. 33, No. 1)*.
- Hanley, B. B. (2016). Ground reaction forces of Olympic and World Championship race walkers. *European journal of sport science*, 16(1), 50-56.
- Hanley, B. B. (2017). Analysis of lower limb work-energy patterns in world-class race walkers. *Journal of sports sciences*, 35(10), 960-966.
- Hanley, B. B. (2017). Gender and age-group differences in hip muscle activity patterns in elite race walkers. *Slovak Journal of Sport Science*.
- Hanley, B. T. (2017). Differences between motion analysis systems in calculating knee angle in elite race walking. In <http://ecss-congress.eu/2017/17/index.php/programme>.
- Hanley, B. T. (2018). Comparisons between systems to measure contact and flight times in elite race walking.
- Hanley, B. T. (2018). Differences between motion capture and video analysis systems in calculating knee angles in elite-standard race walking. *Journal of sports sciences*, 36(11), 1250-1255.
- Harrison, A. J. (2016). Does the McNeill Alexander model accurately predict maximum walking speed in novice and experienced race walkers? *Journal of Sport and Health Science*.
- Hoga- Miura, K. H. (2017). RECONSTRUCTION OF WALKING MOTION WITHOUT FLIGHT PHASE BY USING COMPUTER SIMULATION ON THE WORLD ELITE 20KM RACE WALKERS DURING OFFICIAL RACES.

- Hoga, K. A. (2009). A biomechanical analysis of judgement in race walking events at world major competitions from 2004 to 2007. *BASES annual conference of the British Association of Sports and Exercise Sciences*. Leeds Metropolitan University, Great Britain.
- Hopkins, W. M. (2009). Progressive statistics for studies in sports medicine and exercise science. *Medicine+ Science in Sports+ Exercise*, 41(1), 3.
- Hubbard, M. (1984). Optimal javelin trajectories. *Journal of Biomechanics*, 17, 777–787.
- IAAF. (n.d.). Retrieved from <https://www.iaaf.org/news/press-release/taicang-to-host-2018-world-race-walking-team>
- IAAF. (2014). *Race Walking A Guide to Judging and Organising. A guide for judges, officials, coaches and athletes*.
- Ito, Y. Y. (2016). THE ROLE OF JOINTS OF LOWER LIMB DURING SHOCK ABSORBING PHASE IN RACE WALKING.
- James, D. A. (2016). *Sensors and Wearable Technologies in Sport: Technologies, Trends and Approaches for Implementation*. Berlin, Germany: Springer.
- Jindo, T. H. (1997). Application studies to car interior of Kansei engineering. *International journal of industrial ergonomics*, 19(2), 105-114.
- Knicker, A. L. (1990). Race-walking technique and judging-the final report to the International Athletic Foundation research project. *New Studies in Athletics*, 5(3), 25-38.
- Lai, H. H. (2005). A robust design approach for enhancing the feeling quality of a product: a car profile case study. *International Journal of Industrial Ergonomics*, 35(5), 445-460.
- Lanzotti, A. C. (2016). Video-Analysis of Player's Kinematics in Running out of Boundaries in Association Football Fields. *Procedia engineering*, 147, 234-239.

- Lanzotti, A. T. (2008). Kansei engineering approach for total quality design and continuous innovation. *The TQM Journal*, 20(4), 324-337.
- Lee, J. M. (2013). Detection of illegal race walking: a tool to assist coaching and judging. *Sensors* 13(12), 16065–16074 .
- Li, Y. S. (2018). A posterior preference articulation approach to Kansei engineering system for product form design. *Research in Engineering Design*, 1-17.
- Little, C. L. (2013). An evaluation of inertial sensor technology in the discrimination of human gait. *Journal of sports sciences*, 31(12), 1312-1318.
- Loschky L.C., M. G. (2005). The limits of visual resolution in natural scene viewing. *Visual Cognition* 12(6), 1057-1092.
- Lukes, R. A. (2005). The understanding and development of cycling aerodynamics. *Sports engineering*, 8(2), 59-74.
- Ma M-Y, C. C.-Y.-G. (2007). A design decision-making support model for customized product color combination. *Comput Ind* 58(6), 504–518.
- Majed, L. H. (2017). Changes in movement organization and control strategies when learning a biomechanically constrained gait pattern, racewalking: a PCA study. *Experimental brain research*, 235(3), 931-940.
- Nagamachi, M. (1995). Kansei engineering: a new ergonomic consumer-oriented technology for product development. *International Journal of industrial ergonomics*, 15(1), 3-11.
- Nagamachi, M. (2002). Kansei engineering as a powerful consumer-oriented technology for product development. *Applied ergonomics*, 33(3), 289-294.
- Nagamachi, M. (2011). *Kansei/Affective Engineering*. CRC Press.
- Nagamachi, M. (2017). History of kansei engineering and application of artificial intelligence. . In *International Conference on Applied Human Factors and Ergonomics* (pp. pp. 357-368). Springer.

- Nagamachi, M. L. (2011). *Innovation of Kansei Engineering*. CRC Press.
- Newell, J. A. (2014). *Statistics for sports and exercise science: a practical approach*. Routledge.
- Norberg, J. S. (2016). Is Race Walking Lower Impact Than Running? *In ASME 2016 International Mechanical Engineering Congress and Exposition*. American Society of Mechanical Engineers.
- Norberg, J. V. (2017). KINETIC AND MUSCLE ACTIVITY COMPARISONS IN RACE WALKING AND RUNNING.
- Odenwald, S. A. (2016). Contribution to risk assessment in football by video analysis of overstepping boundary line events. *Sports Engineering, 19(2)*, 129-137.
- Otto, K. W. (2001). *Product design: techniques in reverse engineering and new product design*. Prentice-Hall.
- Owens, N. E. (2003). Hawk-eye tennis system. . *In Visual Information Engineering, 2003. VIE 2003. International Conference on (pp. 182-185)*. IET.
- Padulo, J. (2015). The effect of uphill stride manipulation on race walking gait. *Biology of sport, 32(3)*, 267.
- Padulo, J. A. (2013). Footstep analysis at different slopes and speeds in elite race walking. *The Journal of Strength & Conditioning Research, 27(1)*, 125-129.
- Padulo, J. A. (2013). Uphill racewalking at iso-efficiency speed. *The Journal of Strength & Conditioning Research, 27(7)*, 1964-1973.
- Palomba, A. C. (2018). Can be a subjective qualitative evaluation reliable to assess the perceived physical status and the level of the performance in elite sprinters with Intellectual Impairments? *GAIT AND POSTURE, 66(1)*, S30-S31.
- Pavei, G. C. (2014). The biomechanics of race walking: Literature overview and new insights. *European journal of sport science, 14(7)*, 661-670.

- Pavei, G. L. (2016). The effects of speed and performance level on race walking kinematics. *Sport Sciences for Health, 12(1)*, 35-47.
- Pavei, G. S. (2015). 3D body centre of mass trajectory in locomotion: comparison between different measurement methods. *In The 25th Congress of the International Society of Biomechanics (ISB)*, (pp. 12-16).
- Pavei, G. S. (2017). On the estimation accuracy of the 3D body center of mass trajectory during human locomotion: inverse vs. Forward dynamics. *Frontiers in physiology, 8*, 129.
- Powers, D. M. (2011). Evaluation: from precision, recall and F-measure to ROC, informedness, markedness and correlation. *Journal of Machine Learning Technologies, 2(1)*, 37.
- Preatoni, E. C. (2014). Technical skills and movement coordination in elite, national and regional level race walkers.
- Psiuk, R. S. (2014). Analysis of goal line technology from the perspective of an electromagnetic field based approach. *Procedia Engineering, 72*, 279-284.
- Rahmillah, F. I. (2017). Design of Maternity Pillow by Using Kansei and Taguchi Methods. *In IOP Conference Series: Materials Science and Engineering (Vol. 215, No. 1, p. 012043). IOP Publishing.*
- Santoso, D. R. (2013). Development of precession instrumentation system for differentiate walking from running in race walking by using piezoelectric sensor. *Sensors & Transducers, 155(8)*, 120.
- Sawamura, S. (2016). CHARACTERISTICS OF BODY MOTION IN A NOVICE RACE WALKER. *In ISBS-Conference Proceedings Archive (Vol. 34, No. 1).*
- Schiffer, J. A. (2008). Race walking. *New Studies in Athletics; 23(4)*, 7-15.
- Schwanitz, S. C. (2014). Modelling head impact safety performance of polymer-based foam protective devices. *Procedia engineering, 72*, 581-586.

- Sebastian, P. L. (2009). Decision support systems in preliminary design. *International Journal on Interactive Design and Manufacturing, Vol. 3(4)*, 223–226.
- Shimizu, K. M. (1994). Toric intraocular lenses: Correcting astigmatism while controlling axis shift. *Journal of Cataract & Refractive Surgery, 20(5)*, 523-526.
- Skublewska-Paszowska, M. L. (2018). New Automatic Algorithms for Computing Characteristics of Three Dimensional Pelvic and Lower Limb Motions in Race Walking. *In 2018 11th International Conference on Human System Interaction HSI* (pp. 375-381). IEEE.
- Smith, L. C. (2013). Comparisons between swing phase characteristics of race walkers and distance runners. *International Journal of Exercise Science, 6(4)*, 269-277.
- Song, Q. D. (2013). Biomechanics and injury risk factors during race walking. *In ISBS-Conference Proceedings Archive (Vol. 1, No. 1)*.
- Song, Q. X. (2015). Could insoles offload pressure? An evaluation of the effects of arch-supported functional insoles on plantar pressure distribution during race walking. *Research in Sports Medicine, 23(3)*, 278-288.
- Sovenko, S. P. (2014). Technical specifications of qualified sportswomen who specialize in race walking for 10 km. *Physical education of students, 18(4)*, 37-41.
- Stanhope, S. J. (1990). Kinematic-based technique for event time determination during gait. *Medical and Biological Engineering and Computing, 28(4)*, 355-360.
- Taha, Z. H. (2013). An Overview Of Sports Engineering: History, Impact And Research. *Malaysian Journal of Movement, Health & Exercise, 2*.
- Tao, W. L. (2012). Gait analysis using wearable sensors. *Sensors, 12(2)*, 2255-2283.
- Tucker, C. B. (2017). Gait variability and symmetry in world-class senior and junior race walkers. *Journal of sports sciences, 35(17)*, 1739-1744.

- Tucker, C. B. (2018). Comparisons between systems to measure contact and flight times during treadmill race walking.
- Vaezi, M. C. (2011). Effects of layer thickness and binder saturation level parameters on 3D printing process. *The International Journal of Advanced Manufacturing Technology*, 53(1-4), 275-284.
- Wang, H. H. (2016). Kinematics of the forefoot in the horizontal plane during progressive pace barefoot racewalking on a treadmill after aerobic exercise load. *Journal of physical therapy science*, 28(2), 515-518.
- Westerfield, G. A. (2007). The use of biomechanics in the judging of race walking. *In International Race Walk Forum*. Shenzhen, China.
- Winter, D. (2005). *Kinematics*. New York: Wiley.
- Wixted, A. J. (2010). Validation of trunk mounted inertial sensors for analysing running biomechanics under field conditions, using synchronously collected foot contact data. *Sports Engineering*, 12(4), 207-212.
- Zijlstra, W. &. (2003). Assessment of spatio-temporal gait parameters from trunk accelerations during human walking. *Gait & posture*, 18(2), 1-10.